



University of southern Queensland  
Faculty of Mechanical and Electrical Engineering

**Impact of Large-Scale Solar Energy Penetration on the  
Electricity Network  
With a View of Replacing Synchronous Generators**

A dissertation submitted by

**Mkululi Mpofu**

in fulfilment of the requirement of

**ENG4111 and 4112 Research Project**

towards the degree of

**Bachelor of Engineering (Honours) (Electrical & Electronic)**

Submitted October, 2019

# Abstract

This project is an investigation into the impacts of large-scale solar energy penetration on the electricity network with a view towards replacing conventional synchronous generators. The world is shifting away from use of fossil fuels for generation of electricity as these are attributed to excessive production of carbon dioxide and other gases that are widely accepted to be linked to global warming. Solar energy has become synonymous with environmentally friendly sources of energy as it is seen as a significant contributor to global warming reduction. This has led to large penetration of solar energy into electricity networks as some world governments are targeting 100% solar generated power by as early as 2030. However, there has been insufficient research on optimal solar penetration levels given the intermittent and uncontrollable nature of solar energy generation thus setting up a stage for this research project.

The project starts with an extensive research on literature relating to the impact of high solar Photovoltaic (PV) penetration on electricity networks. A simple model of an electricity network is developed to facilitate simulation of network conditions. The model consists of two parts, the solar system and the grid system. The solar section comprises of solar array with varying irradiance and/or temperature, DC-DC boost converter to facilitate Maximum Power Point Tracking (MPPT) capability, DC-AC Inverter, Point of Common Coupling (PCC), Step-up Transformer and grid system with conventional synchronous generators. The DC-DC converter is equipped with Perturb and Observe algorithm to track the maximum power point of the PV modules. This ensures that the modules are at their maximum production level all the time. The inverter controls implement reactive power injection to support the grid during disturbances. The grid side of the network is modelled with synchronous generators that are equipped with governor control for frequency regulation and they also implement a closed loop feedback system for excitation control. The grid includes two sections of transmission lines modelled in a  $\pi$ -configuration. Two loads of 2MW and 30MW are connected to the 25kV distribution network.

Disturbances were introduced into the network in two phases. The first phase comprised of the synchronous generator, the transmission lines, transformers and the two loads. The second phase consists of the solar system. Disturbances were introduced to the network for each section. Voltage and frequency recovery after a transient three phase symmetrical fault were faster for the section with synchronous generators than that for the one comprising of solar system. Total harmonic distortion was more pronounced on the solar system for all types of simulated faults than on the synchronous generator side. The third phase had the two phases interconnected and observed under the same disturbances, as in phases one and two, while increasing the PV output and reducing synchronous generation. The investigation tested PV system for Fault Ride Through Capability, voltage and frequency regulation when synchronous generation was low. The inverter system did not inject much reactive power during faults contrary to expectations. Removal of synchronous generator did not destabilise the system but re-connection of it caused significant frequency oscillations. The rest of the test results were within the requirements of standards and rules that govern network operation.

University of southern Queensland  
Faculty of Mechanical and Electrical Engineering

**ENG4111/ENG4112 Research Project 2019**

## **Limitation of Use**

The Council of the University of Southern Queensland, its Faculty of Mechanical and Electrical Engineering and the staff of the University of Queensland do not accept any responsibility for the truth, accuracy or completeness of material contained within or associated with this dissertation.

Persons using all or any part of this material do so at their own risk, and not at the risk of the council of the University of Southern Queensland, its Faculty of Mechanical and Electrical Engineering or the staff of the University of Southern Queensland.

This dissertation reports an educational exercise and has no purpose or validity beyond this exercise. The sole purpose of the course project is to contribute to the overall education within the student's chosen degree program. This document, the associated hardware, software, drawings and other material set out in the associated appendices should not be used for any other purpose: If they are used, it is entirely at the risk of the user.

## Certification

I certify that the ideas, designs and experimental work, results, analyses and conclusions set out in this dissertation are entirely my own effort, except where otherwise indicated and acknowledged.

I further certify that the work is original and has not been previously submitted for assessment in any other course or institution, except where specifically stated.

Mkululi Mpfu



Student Number: 

Date: **17 October 2019**

## **Acknowledgements**

I would like to thank the University of Southern Queensland Staff, notably Assoc Professor Tony Ahfock, Dr Chris Snook and Andrew Hewitt for their un-ending support and guidance towards completion of this Dissertation.

My thanks also go to my fellow students, workmates and friends for their motivational support. My work supervisor and work mates deserve special mention for working around my project time pressures especially the supervisor for allocating emergence study leave when needed.

Finally, I would like to thank my Wife Nontando and my two sons, Methembe and Babongile for accommodating my tight study schedule especially, balancing life between a fulltime job, study and family.

## Table of Contents

Abstract	ii
Limitation of Use	iii
Certification	iv
Acknowledgements	v
Abbreviations	ix
<b>Chapter 1</b>	<b>1</b>
<b>1 Introduction</b>	<b>1</b>
1.1 Overview	1
1.1.1 Conventional Methods of Generating Electricity	1
1.1.2 World reaction to Global Warming	2
1.2 Background to Study	3
1.2.1 World Solar Generation Statistics	3
1.2.2 World Renewable Targets	5
1.3 Project Aims	5
1.4 Project Objectives	5
1.5 Overview of Dissertation	6
1.6 Conclusion	6
<b>Chapter 2</b>	<b>6</b>
<b>2 Literature Review</b>	<b>7</b>
2.1 Introduction	7
2.2 Effects of Intermittent Generation	7-8
2.2.1 Voltage Fluctuations	9
2.2.1.1 Voltage Flicker	10
2.2.1.2 Voltage Dips and Rises	10-12
2.3 Fault Ride Through Capability	13
2.3.1 FRTC for PV Inverter Systems	13-15
2.3.2 FRTC for Synchronous Generators	15-16
2.4 Short Circuit Ratio	16
2.5 Harmonics	16-17
2.6 Frequency Variations	17
2.6.1 PV Inverters	17
2.6.2 Synchronous Generators	18
2.7 Inverter/Converter Control	19
2.7.1 Maximum Power Point Tracking	19-20
2.7.1.1 Constant Voltage Method	20
2.7.1.2 Perturb and Observe Method	21
2.7.1.3 Incremental Conductance (IC) Method	21-22
2.7.2 Active and Reactive Power Control	22-23
2.7.3 Inverter Protection and Fault Analysis	23
2.8 Synchronous Generator Control	23
2.8.1 Governor Control	24-26

2.8.2	Automatic Voltage Regulator (AVR)	26-28
2.9	Models	28-29
2.9.1	AEMO Model Guidelines	29
2.10	Conclusion	29
<b>Chapter 3</b>		<b>30</b>
<b>3</b>	<b>Methodology</b>	<b>30</b>
3.1	Introduction	30
3.2	Project Development	30
3.2.1	Aims and Objectives	30
3.2.2	Solar Panel Model	31-35
3.2.3	Boost Converter Model	35-37
3.2.4	Inverter Model	37-40
3.2.5	Synchronous Machine Model	41-42
3.2.5.1	Excitation Control	42-43
3.2.5.2	Governor Control	44-45
3.2.6	Transmission Line Model	45-46
3.2.7	Implementation of Different Network Conditions	46
3.2.7.1	Increasing PV Penetration	46-47
3.2.7.2	Introduction of Network Disturbances	47
3.2.7.3	Introduction of Faults to Network	47
3.3	Limitations	48
3.3.1	Modelling Software	48
3.3.2	Data Collection	48
<b>Chapter 4</b>		<b>49</b>
<b>4</b>	<b>Simulation and Results Analysis</b>	<b>49</b>
4.1	Introduction	49
4.2	Single Synchronous Generator Network(No PV)	49-50
4.2.1	Steady State Conditions	51
4.2.1.1	Results Analysis	52
4.2.2	Three Phase Symmetrical Fault	52
4.2.2.1	Results and Analysis	53
4.2.3	Three Phases to ground Fault	54
4.2.3.1	Results Analysis	55
4.2.4	Phase to Phase Fault	55
4.2.4.1	Results Analysis	57
4.2.5	Major Load Rejection	58
4.2.5.1	Results and Analysis	59
4.3	Grid with PV Array ( No Synchronous Machines)	59-61
4.3.1	Simulation with 0.35%	61
4.3.1.1	Simulation of Three Phase Symmetrical Fault	61
4.3.1.1.1	Results Analysis	63
4.3.1.2	Removal of Major Load (30MW)	64
4.3.1.2.1	Results Analysis	65
4.3.2	Simulation with 1% Load	65

4.3.2.1	Three Phase Symmetrical Fault Simulation	65
4.3.2.1.1	Analysis of Results	66
4.3.3	PV Supplying 11% of Load	67
4.3.3.1	Three Phase Symmetrical Fault	67
4.3.3.1.1	Analysis of Results	68
4.3.4	PV System Supplying 100% Load	69
4.3.4.1	Simulation of Three Phase Symmetrical Fault	69
4.3.4.1.1	Analysis of Results	70
4.3.4.2	Simulation of Three Phases to Ground Fault	70
4.3.4.2.1	Analysis of Results	72
4.3.4.3	Simulation of One Phase to Ground Fault	72
4.3.4.3.1	Analysis of Results	73
4.3.4.4	Simulation of Phase to Phase Fault	74
4.3.4.4.1	Analysis of Results	75
4.4	PV System Combined with Conventional Generators	76
4.4.1	PV supplying 2% of Load	77
4.4.1.1	Three Phase Symmetrical Fault Simulation	77
4.4.1.1.1	Analysis of Results	79
4.4.1.2	Three Phase Ground Fault	79
4.4.1.2.1	Result Analysis	80
4.4.1.3	Single Phase to Ground Fault	80
4.4.1.3.1	Analysis of Results	81
4.4.1.4	Removal of Large Load	81
4.4.1.4.1	Analysis of Results	83
4.4.2	PV Supplying 10% Load	83
4.4.2.1	Three Phase Symmetrical Fault	83
4.4.2.1.1	Results Analysis	84
4.4.2.2	Phase to Ground Fault	84
4.4.2.2.1	Results Analysis	86
4.4.2.3	Removal of large load	86
4.4.2.3.1	Analysis of Results	87
4.4.3	PV supplying 50% Load	87
4.4.3.1	Three Phase Symmetrical Fault	88
4.4.3.1.1	Analysis of Results	89
4.4.3.2	Phase to Phase to Ground Fault	89
4.4.3.2.1	Analysis of Results	90
4.4.3.3	Removal of “Large Load”	91
4.4.3.3.1	Analysis of Results	92
4.4.3.4	Disconnection and Reconnection of Generator	92
4.4.3.4.1	Results Analysis	93
<b>Chapter 5</b>		94
<b>5. Conclusions and Recommendations</b>		94
5.1	Introduction	94
5.2	Summary of Results and Conclusions	94
5.2.1	Model of Synchronous Machine(without PV)	94
5.2.2	Model with PV Array (without Synchronous Machine)	95

5.2.3	Combined PV and Two Synchronous Generators	96
5.2.4	Summary	97
5.2.5	Recommendations	97
5.2.6	Further Work	97
<b>Chapter 6</b>		<b>98</b>
<b>6. References</b>		<b>98-101</b>
<b>Appendix A</b>		<b>102</b>
Appendix B		103-109
Appendix C		110
<b>Abbreviations</b>		
AEMO	Australian Energy Market Operator	
AC	Alternating Current	
AGC	Automatic Governor Control	
AVR	Automatic Voltage Control	
DTRMP	Daily Task Risk Management Plan	
FRTC	fault ride Through Capability	
IEC	International Electrotechnical Commission	
IGBT	Insulated Gate Bipolar Transistor	
IEEE	Institute of Electrical and Electronic Engineers	
MPPT	Maximum Power Point Tracking	
MW	Mega Watts	
NEM	National Electricity Market	
PFC	Personal Fatigue Calculator	
P & O	Perturb and Observe algorithm used in MPPT	
PWM	Pulse Width Modulation	
PV	Photovoltaic	
RES	Renewable Energy Sources	
ROCOF	rate of Change of Frequency	
SCADA	Supervisory Control and Data Acquisition	
SCR	Short Circuit Ratio	
UNFCCC	United Nations Framework Convention on Climate Change	
USQ	University of Southern Queensland	
<b>Figures</b>		
Figure 1.1	Total Renewable Energy Generation Capacity	3
Figure 1.2	Kamuthi Solar India	4
Figure 1.3	Australia PV Output by State	4
Figure 2.1	Structure of PV, EDLC FC Dispersed System	9
Figure 2.2	Voltage Profile per day	10
Figure 2.3	Voltage Dip	11

Figure 2.4	Typical Solar Irradiance Per Day	11
Figure 2.5	Network Structure	12
Figure 2.6	Impact of PV on Voltage Profile	13
Figure 2.7	Crowbar Protection to Give FRTC	14
Figure 2.8	FRTC Schemes of Several Energy Markets	15
Figure 2.9	Harmonic Content	17
Figure 2.10	PV Cell Characteristics	20
Figure 2.11	Overall Control of Grid Connected PV System	23
Figure 2.12	Basic Elements of a Governing System	24
Figure 2.13	Frequency Control for Normal Contingency	25
Figure 2.14	Frequency control with Dead Band and Droop	26
Figure 2.15	Buck Converter for Generator Excitation	27
Figure 2.16	FPGA Controlled Interleaved Buck Converter	27
Figure 2.17	Excitation Structure with dual Control	28
Figure 3.1	Solar Module	31
Figure 3.2	Solar Cell Equivalent Circuit	31
Figure 3.3	PV Module Curves for Constant Temperature	33
Figure 3.4	PV Module for constant irradiance	33
Figure 3.5	Irradiance and Temperature Inputs	34
Figure 3.6	PV Model Outputs	34
Figure 3.7	Boost Converter Equivalent Circuit	35
Figure 3.8	PV Array Model with Boost Converter	36
Figure 3.9	Parameters for Perturb and Observe	37
Figure 3.10	Inverter Circuit Diagram	37
Figure 3.11	120° conduction for 0° to 60°	38
Figure 3.12	Inverter Control Blocks	40
Figure 3.13	Grid Connected PV Array	40
Figure 3.14	Automatic Voltage Control for Synchronous Machine	41
Figure 3.15	Governor Control	44
Figure 3.16	Synchronous Generator Model	45
Figure 3.17	Transmission Line Model	46
Figure 4.1	Single Synchronous Generator Combined Network	49
Figure 4.2	Generator Portion of Network	50
Figure 4.3	Transmission line System and load	50
Figure 4.4	Steady State Voltage and Amps	51
Figure 4.5	Frequency Under Steady State	51
Figure 4.6	Voltage Response to 3 Phase Symmetrical fault	52
Figure 4.7	Frequency Response to three phase symmetrical fault	53
Figure 4.8	Volts and Amps after three-phase to ground fault	54
Figure 4.9	Frequency Response to three-phase to ground fault	55
Figure 4.10	Voltage Recovery After a Phase to phase Fault	56
Figure 4.11	Frequency Response after Phase to Phase fault	56
Figure 4.12	Load Rejection using CB 3	57
Figure 4.13	Voltage Recovery After Load Rejection	58
Figure 4.14	Frequency Recovery After Load Rejection	58
Figure 4.15	Inverter Frequency Measurement	59
Figure 4.16	PV System Model	60
Figure 4.17	Grid Portion of PV System	61

Figure 4.18 Voltage and Current Waveforms – 0.35% PV	62
Figure 4.19 Frequency Response after three phase fault	62
Figure 4.20 Active and Reactive Energy Injection	63
Figure 4.21 Frequency Fluctuation After Removal of big Load	64
Figure 4.22 Frequency Response	64
Figure 4.23 Voltage Recovery	65
Figure 4.24 Active and Reactive Power Injection	66
Figure 4.25 Voltage and Current Response	67
Figure 4.26 Frequency Recovery Times	67
Figure 4.27 Reactive and Active Power Injection	68
Figure 4.28 Voltage Recovery	69
Figure 4.29 Frequency Recovery	69
Figure 4.30 Voltage recovery for three-phase to ground fault	70
Figure 4.31 Frequency Recovery from three phases to ground	71
Figure 4.32 Active and Reactive Power Injection	71
Figure 4.33 Voltage Recovery after a single phase to ground	72
Figure 4.34 Frequency Recovery	72
Figure 4.35 Active and Reactive Power Injection	73
Figure 4.36 Voltage Response	74
Figure 4.37 Frequency Response	74
Figure 4.38 Active and Reactive Power Injection	75
Figure 4.39 Combined PV and Synchronous Generators	76
Figure 4.40 Generator Portion for Combined Network	77
Figure 4.41 Voltage Response	78
Figure 4.42 Frequency Response	78
Figure 4.43 Voltage Response for Three phase to ground fault	79
Figure 4.44 Frequency Response	80
Figure 4.45 Voltage Response	80
Figure 4.46 Frequency Response	81
Figure 4.47 Voltage Response	82
Figure 4.48 Frequency Response after load removal	82
Figure 4.49 Voltage Response	83
Figure 4.50 Frequency Response after a three-phase symmetrical fault	84
Figure 4.51 Voltage Response after a single phase to ground fault	85
Figure 4.52 Frequency Response after a single phase to ground	85
Figure 4.53 Voltage response after removal of load	86
Figure 4.54 Frequency Response after removal of large load	87
Figure 4.55 Voltage Response after symmetrical fault	88
Figure 4.56 Frequency Response after three phase symmetrical fault	88
Figure 4.57 Voltage Response after a phase to phase to ground	89
Figure 4.58 Frequency Response after a phase to phase to ground fault	90
Figure 4.59 Voltage Response after load removal	91
Figure 4.60 Frequency Response load removal	91
Figure 4.61 Generator Disconnection CB1	92
Figure 4.62 Frequency Response after generator off and on	93
Figure 5.1 Voltage recovery times for Various PV levels	95

**Tables**

Table 2.1	General Comparison among PV, Wind and Conventional	7
Table 2.2	ROCOF Requirements for Some Regions	18
Table 3.1	Summary of Hardware Requirements	32
Table 3.2	Transmission Line Parameters	45
Table 5.1	Voltage and frequency response for synch gen model	94
Table 5.2	Voltage and Frequency Response for PV Array Model	95
Table 5.3	Voltage and Frequency for Combined Network	96
Table 3.6	Hazard Identification and Control	51

# Chapter 1

## 1. Introduction

### 1.1 Overview

The global community is worried about the effects of global warming. Unpredictable weather patterns have been experienced worldwide with some parts of the globe registering world record heatwaves and cold spells year after year. Droughts have become common in most parts of the world. The effects of global warming are too many to enumerate as they are outside the scope of this research project. These climatic changes have been attributed to high production of carbon dioxide (CO<sub>2</sub>) mainly from human related processes and activities. The contribution of CO<sub>2</sub> to global warming has been supported observationally by spatial and seasonal characteristics of global temperatures variations (Jian-Bin et al. 2012). High up in the list of sources of CO<sub>2</sub> pollution are the conventional methods of generating electricity through burning of fossil fuels. The world has had to re-think on the use of fossil fuels and device means of mitigating the rising atmospheric pollution.

#### 1.1.1 Conventional Methods of Generating Electricity

Historically, generation of electricity for base load has been mostly through coal fired power stations. In this form of generation, coal is pulverised and fed into boilers where it is ignited using propane or butene gas. This process generates high temperatures inside the boiler. Water pipes that form the inside structure of boiler receive the heat through conduction and the water in the pipes is superheated to steam under very high pressure. The high-pressure steam is directed onto the turbine blades thereby subsequently producing a rotational motion on the turbine shaft. The turbine shaft is mechanically coupled to the generator shaft that carries the excitation electro-magnet. As the generator shaft rotates with the turbine shaft, the magnetic flux from the excited rotor magnet cuts the windings of the generator stator winding inducing a voltage on the stator windings and generating electricity.

However, during the burning of coal there are a lot of gases that are produced as by-products of the combustion process inside the boiler. One of these gases is the dreaded carbon dioxide (CO<sub>2</sub>) gas. Unfortunately, this gas is associated with negative effects on the ozone layer which lead to global warming. Global warming has adverse effects to the globe to an extent that there are fears that it might lead to human extinction if corrective action is not taken. This has prompted global leaders to throw their shoulders on the wheels and harness every available resource to mitigate the effects of global warming.

### **1.1.2 World's reactions to Global Warming**

World governments have come together to form agreements towards embracing sustainable and environmentally friendly processes and technology. An example of such agreements is the Kyoto Protocol that was adopted on 11 December 1997 as result of the United Nations Framework Convention on Climate Change (UNFCCC) (Kuriyama and Abe 2018).

The conventions and protocols have seen individual governments implementing incentive schemes for their citizens to aid in embracing the use of cleaner sources of energy. Perhaps the most outstanding agreement on climate change was the Paris agreement adopted after the Paris Conference on Climate Change in 2015. The agreement was endorsed by world powerhouses. China is one of the powerhouses that endorsed the agreement and pledged to reduce the emissions of CO<sub>2</sub> per unit of GDP by 60% to 65% by 2030 and pledged to increase the share of non-fossil fuels in primary energy consumption by 20% (Yun 2016). The world's awareness of the impact of climate change and relevant mitigatory steps have led into switching from fossil fuels to renewable sources of energy like solar energy and wind power.

Inclusive and collaborative efforts from world leaders, coupled with increased public awareness of the consequences of environmental harm, have subsequently led to a widespread use of solar energy, one of the cleanest and renewable sources of energy. Solar energy has taken the entire world by storm, becoming a perceived solution to climatic problems of planet earth and thus leading to oversubscription of solar generation, sometimes with less consideration of the negative consequences derived therefrom. The world has seen a proliferation of solar panels from small roof-top-mounted Photovoltaic cells to large scale solar farms. Solar innovation technology has become a topical item in renewable energy discussions. Researchers are busy on the designs of solar roofs, using solar technology to harness electricity even from rain drops and some such innovations to ensure maximum utilisation of the energy from the sun.

There are some places where solar farms have been built to replace coal fired thermal power stations. A typical example is found in Collinsville in Queensland where solar farms have been established around the area where the defunct Collinsville thermal power station used to be. Unfortunately, in some instances these solar farms are located at significant distances away from load centres where existing electricity networks may not have been designed to handle the additional generated capacity.

However, large-scale generation of solar energy has come with a price tag as it is understood to negatively impact the electricity grid network. Reliability, stability and dependability of power supply is grossly affected by intermittency of solar generation. These hypotheses and other network weaknesses brought about by high penetration of solar generation call for a research. This research

project seeks to investigate the effects of large-scale solar penetration to, mainly, network voltage and frequency especially given the intermittent solar generation, with a view of establishing if solar generation can eventually replace synchronous generators.

## 1.2 Background to study

### 1.2.1 World Solar Generation Statistics

Figure 1.1 below shows the growth of renewable energy use, in Gigawatts, over the years.

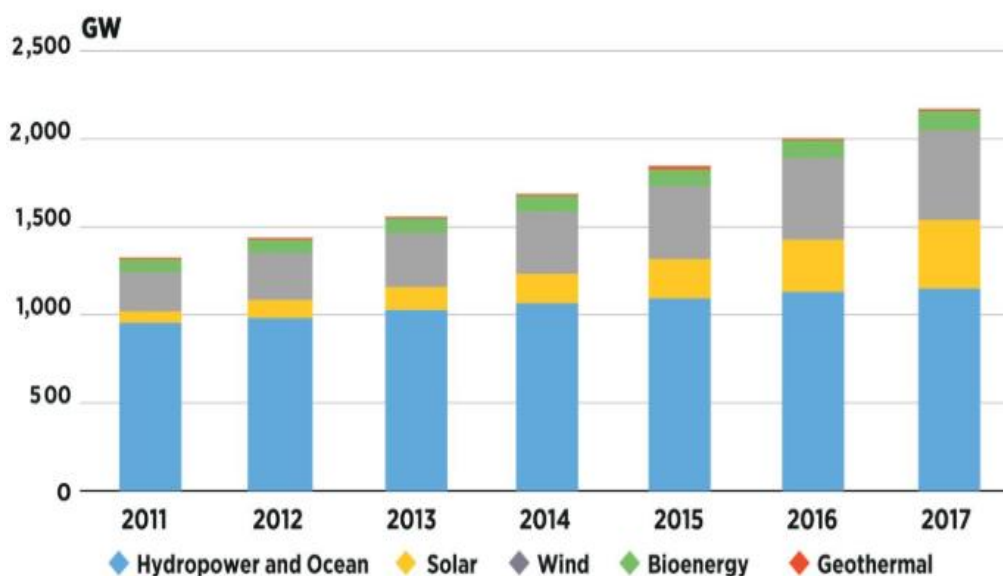


**Figure 1.1:** Total Renewable Power Generation Capacity 2011-2017 (IRENA 2018)

Solar generation has become synonymous with phrases like green energy, ozone friendly, environmentally caring and many such phrases that seek to emphasise the importance of protecting the environment through use of renewable energy sources. Large solar farms have been established around the world. India ranks top among world countries with the biggest solar farms. Kamuthi Solar Power Station in Nadu has a total generation capacity of 648MW. Kurnool Ultra Park, India has a capacity of 1000MW. Pavagada Solar Park, India has a capacity of 2000MW while Bhadla Industrial Park, India is intended to produce 2255MW.

Mexico has Enel Villanuela PV Plant that has a capacity of 750MW. China has two big solar farms namely Longyang Dam Solar Park and Tengger Desert Solar Park with capacities of 850MW and 1547MW, respectively. The United Arab Emirates (UAE) has what promises to be the biggest solar farm called Mohammed Bin Rashid Al Maktoum Solar park with a capacity of 1000MW by 2020 and 5000MW by 2030

The figure below shows a picture of one of India's Solar Power Stations.



**Figure 1.2:** Kamuthi Solar Power Station, India (Posilock 2018)

Australia has seen a boom in solar generation with the establishment of solar farms with Queensland leading the pack. Solar generation in Australia reached 11 Gigawatts in 2018. The figure below shows the monthly PV output for each state of Australia.

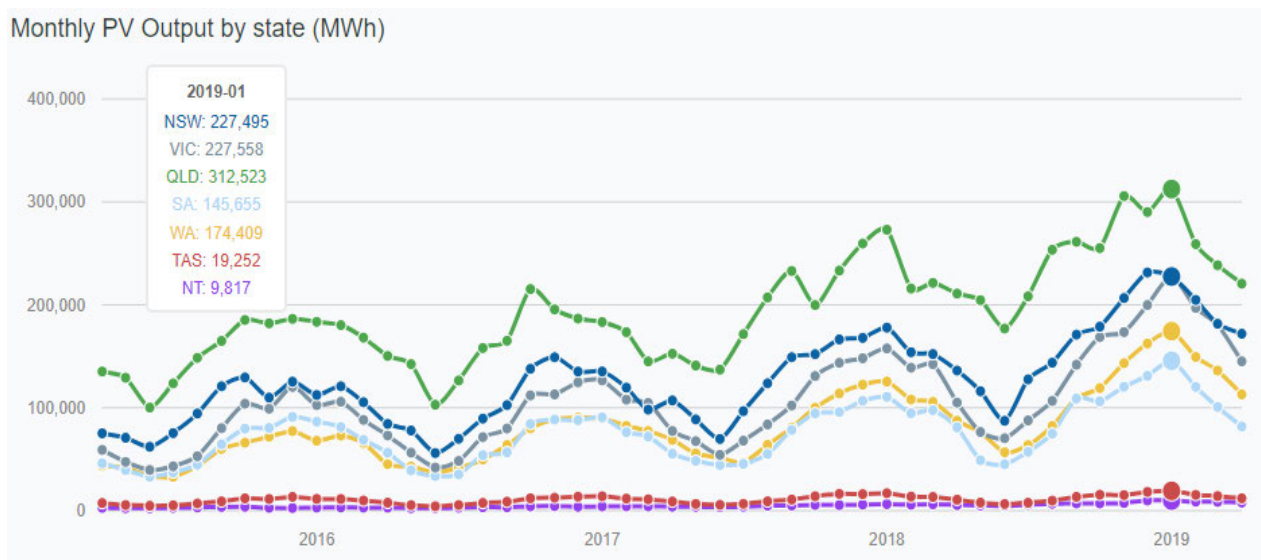


**Figure 1.3:** Australia PV Output by state a Jan 2019 (Australian PV Institute 2019)

### **1.2.2 World Renewable Energy Targets**

The world's green energy policies have seen most governments positively adhering to the Paris agreement through setting of Renewable Energy Targets (RET). These targets are part of the 2030 Agenda for Sustainable Development derived from the Durban Platform for Enhanced Action. Each of the 175 states that signed the Paris agreement formulated their own strategies and action plans to curb negative effects of climate change. The action plans included setting up of goals or targets towards renewable energy usage.

Australia have set their solar generation target to 50% of total electricity generation by 2030. New York wants all power plants to be coal-free by 2020 and shift to 100% clean electricity by 2040. North America has a target of 100% renewable energy use for its 53 cities and towns by 2050 (Jacobson et al 2018). Germany are targeting a 100% renewable energy usage by 2050, an upward move from an initial target of 50% and later 65% (Hansen et al 2018). Turkey aims to achieve 100% renewable-energy-powered-electricity by 2050 (Kilickaplan et al 2017). South Africa is targeting about 46% PV generation by 2030 (Aliyu et al 2017).

### **1.3 Project Aims**

The aim of the project is to investigate the impact of large-scale penetration of solar generation using simple models. The project seeks to establish how electricity networks respond to random and sudden variations of supply caused by intermittent power generation from PV cells. The investigations will include simulation of weak networks, monitoring of voltage and frequency variations and response to steady state and transient disturbances.

### **1.4 Project Objectives**

- Research literature on the effects of large-scale solar generation systems on power network dynamic behavior.
- Develop suitable models using Simscape/Simulink software for the analysis of power system dynamic responses for varying levels of solar generation penetration.
- Using the developed network models, analyze the dynamic response of a simplified power network with differing levels of solar generation penetration. These studies will be based on various practical situations such as fault recovery and load variations.
- Time permitting, other impacts of large solar penetration like harmonics and effects of solar connection to a weak network among others, will be investigated.

## 1.5 Overview of the Dissertation

The dissertation is organized in the following manner:

### a) Chapter 2

- The chapter involves extensive research on the effects of high penetration of PV generation. Solar intermittency, Fault Ride Through Capabilities of inverter systems, voltage and frequency variations in networks with high penetration of solar are discussed in the chapter.
- AEMO guidelines on models are also discussed.

### b) Chapter 3

- The chapter outlines the methodology used in implementing the research. A simple model is developed consisting of PV system, synchronous generator, distribution line, transmission line and two loads totaling 32MW.

### c) Chapter 4

- In this chapter the models developed in chapter 3 are simulated and results analyzed at every step. The simulation mainly focusses on the voltage and frequency responses under different PV penetration levels and different disturbances

### d) Chapter 5

- Results from chapter 4 are summarized and conclusions drawn therefrom. The chapter discusses weaknesses of the tests and makes recommendations for better tests including further works.

### e) References

- This section has a list of references in alphabetical order arranged by name of first author.

### f) Appendices

- The last part contains appendices

## 1.6 Conclusion

The world is targeting high percentages of solar energy by the year 2050. This is a very positive move towards environmental sustainability through the reduction of greenhouse emissions and control of the causes of adverse effects of climate change. However, it is not yet clear if the electricity networks will maintain stability, security and dependability of supply if there is 100% penetration of solar generation. This must be confirmed through network modelling and simulation using expected and projected network parameters.

# Chapter 2

## 2. Literature Review

### 2.1 Introduction

The following literature review provides an insight to current research into the effects of largescale PV penetration on network operation.

Current literature does not talk much about the possibility of eventually having electricity grids running on non-synchronous generation given ever rising penetration of PV and some of their alleged shortcomings compared to synchronous generation. In this section the researcher talks about how other researchers have viewed the impact of large-scale PV penetration on electricity networks with a view of replacing synchronous generators. The literature review in the sections below seeks to explore how networks respond to large scale solar penetration through journal articles and other some such published papers.

### 2.2 Effects of Intermittent generation from large scale PV penetration

PV installations are known for intermittent generation of electricity and this poses power security risks as these may not adequately meet power demand. Development of more accurate solar forecasting is required to better prepare the power system operator to manage the fluctuations in the solar PV power output (Sivaneasan et al. 2017).

**Table 2.1:** A general comparison among PV, wind and conventional powerplants. (Sivaneasan et al. 2017)

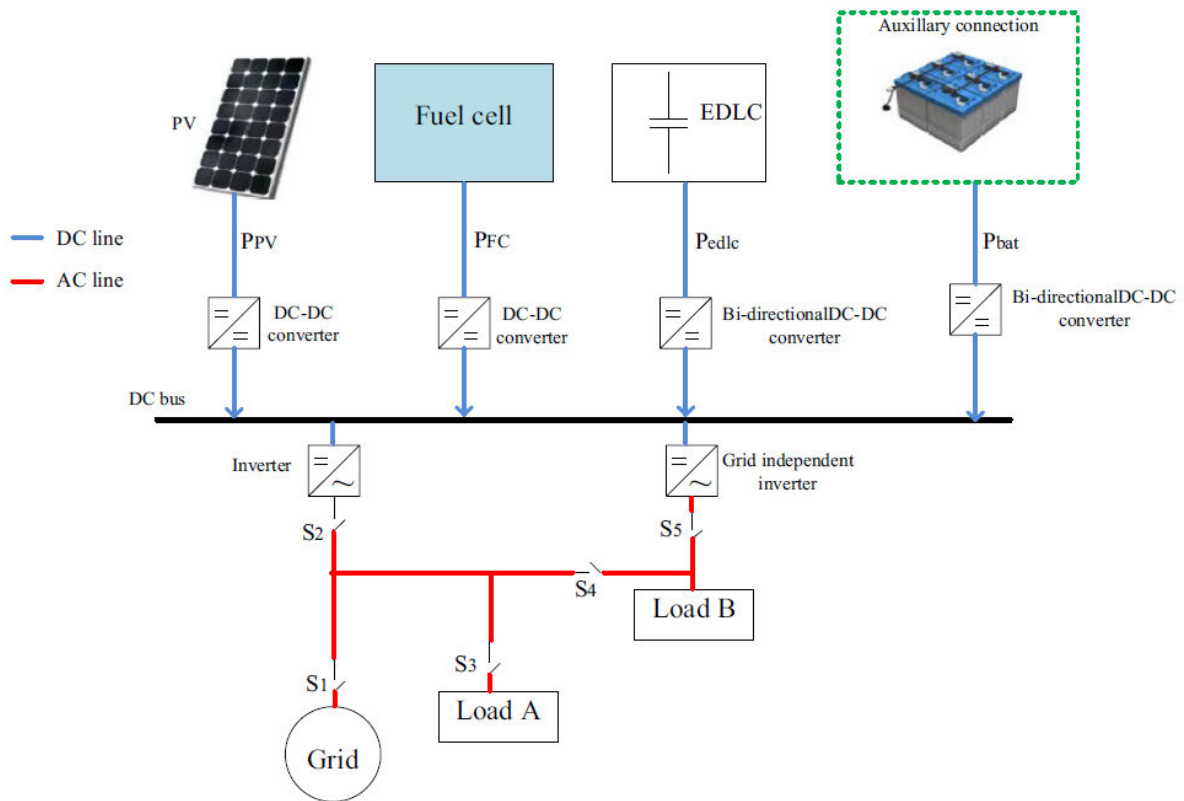
Characteristics	PV	Wind	Conventional generator
Fluctuation	High	Low	No
Cost for large-scale	High	Moderate	Low to moderate
Maintenance cost	Minimal	High	Moderate
Inertia	No inertia	Low inertia	Large inertia
Capacity factor	Very low	Low to moderate	High
Annual growth in electric power sector	Very high	High	High

Table 2.1 above confirms that PV generation is indeed characterised by higher fluctuations compared to conventional generation. The future power system must deal with not only the uncontrollable demand but also uncontrollable generation (Sivaneasan et al. 2017). The fluctuations or intermittency in PV generation is attributed to changing weather patterns for example cloud cover. Sivaneasan (2017, p.1426) says: "For example, sharp change of PV output due to the moving clouds is one of the major problems in secondary distribution system". While efforts can be made to forecast solar generation levels, there are times when these fluctuations come outside the forecast periods and this calls for urgent start-up of alternative generators and these do not start instantaneously. The deviations between forecasted and actual production must be balanced on short notice, which is costly (Notton et al 2018).

This research aims to use system models that will incorporate simulation of these unexpected deviations to establish whether power networks can remain operating within technical specifications under the given conditions.

Literature reviewed so far suggests that Solar generation cannot stand alone without backup from conventional generators. Talking about the situation in India, Chattopadhyay (2014, p.3) says: "Put differently, every MW of wind and to some extent solar, would need somewhere between 0.7 to 0.9 MW of back-up peaking capacity, failing which the system is exposed to significant risk of outage, particularly during the pre/post-monsoon months". This is caused by the fact that PV generation start after the morning peak demand and stops before the evening peak demand (Obi & Bass 2016). It is important to note that intermittency in generation also brings about voltage variations which may go outside tolerance levels if generation/demand equilibrium is not attained quickly. Utility managers, system operators and government experts believe that the intermittency of renewable energy sources is a serious obstacle to their wider use in the United States of America (Sovacool 2008). The ability of solar generators to provide base load is debatable and most authors suggest that renewable energy sources in general cannot supply base load. Solar generation is not only a bad choice for base load but also for peak load demand (Sovacool 2008). This is because peak times for most electricity users happen either before solar PV cells start to generate or after sunset when PV cells are no longer generating.

However, the fluctuations in solar generation can be smoothed by geographical dispersion (Shivashankar et al 2016). Spacing of solar cells over a large area ensures that not all solar cells are exposed to the same weather conditions at the same time. This tends to average out the effects of intermittency. Another method of smoothing solar generation intermittency is by using Electric Double Layer Capacitors (EDLCs) as shown in figure 2.1. The capacitors absorb the power difference between inverters and the PV system (Shivashankar et al 2016). Storage devices, for example batteries and pumped water storage systems also play a role in smoothing the effects of intermittency. However, storage devices are not yet extensively available and are still considered an expensive solution as reported by Szabo et al (2018).



**Figure 2.1:** Structure of PV, EDLC, FC dispersed system (Shivashankar et al 2016)

### 2.2.1 Voltage Fluctuations

Solar irradiance variations due to, for example, cloud cover cause the system voltage to change in magnitude (Jamal et al. 2017). Literature reviewed around this topic shows that intermittency in generation from solar causes grid voltage fluctuations. Figure 2.2 below shows voltage fluctuations with and without PV generation. The pattern shows that voltage rises to above 1 p.u around midday when there is maximum solar irradiance resulting in more solar generation. Otherwise the voltage drops steadily to about 0.95 p.u without solar generation due to generally increased load between midday and 6pm. The voltage fluctuations must conform to stipulated grid codes. The proposed models for this research are expected to show how these fluctuations change with increased percentage of solar energy penetration.

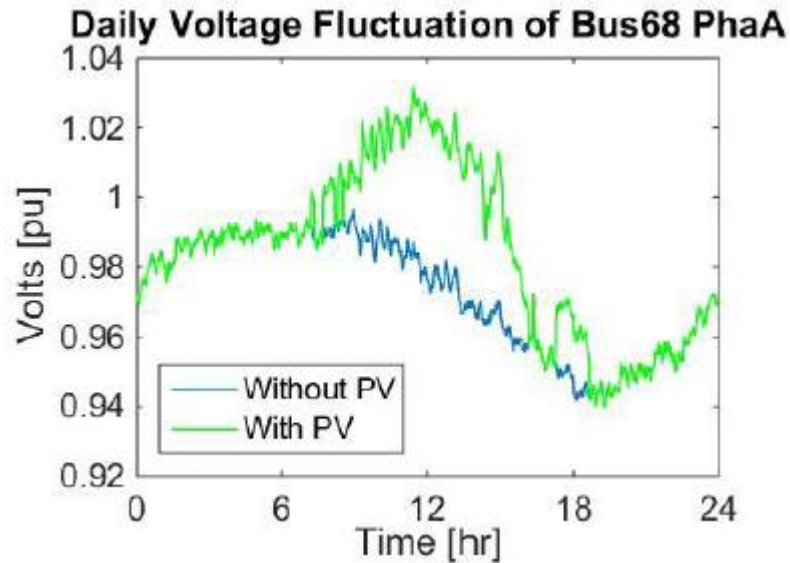


Figure 2.2: Voltage profile for a day (Zhu et al 2017)

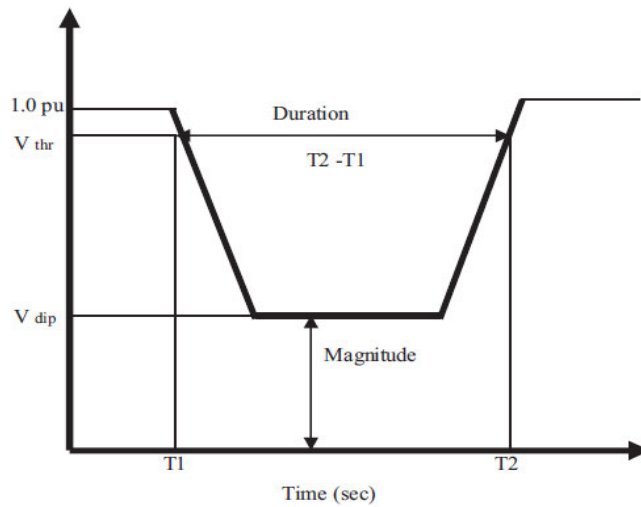
#### 2.2.1.1 Voltage Flicker

A passing cloud causes the output of PV cells to vary which in turn causes system voltage peaks to vary in rhythm with PV output variations (Shivashankar et al 2016). Apart from harmful technical effects, voltage flicker has negative impact on the physiological side of the operational environment as it affects the ergonomics of operators (Bouchakour et al 2017).

#### 2.2.1.2 Voltage Dips and Rises

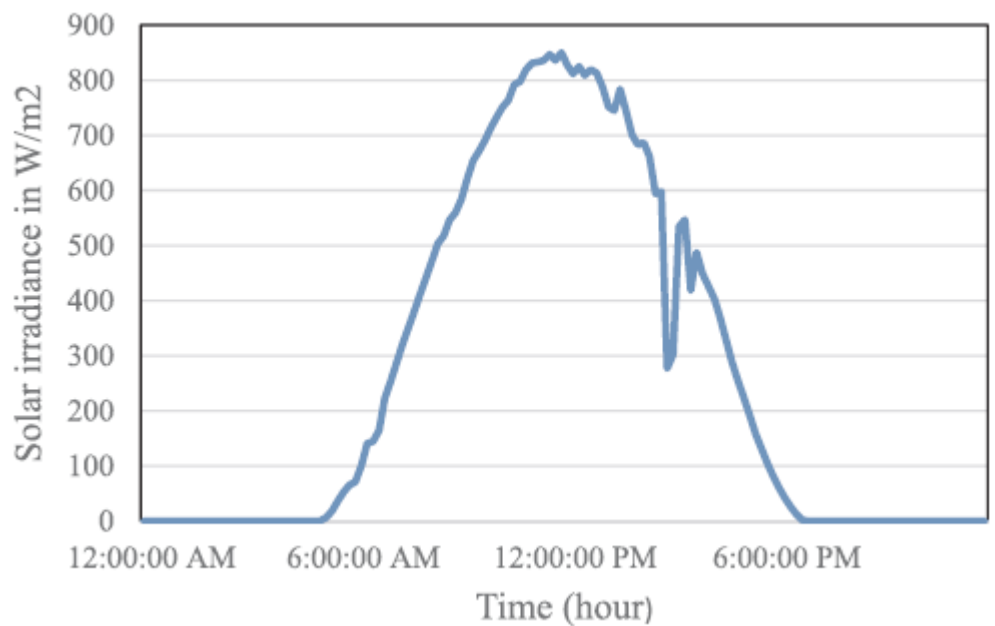
When penetration of solar generation increases so does the voltage at the substation (Shivashankar et al). Normally, capacitor banks or voltage regulators are installed at substations and voltage rise from PV cells might cause the system voltage to go beyond what the electricity regulator prescribes for the distribution or transmission utility company. The intermittent nature of PV generation can lead to voltage dips where the voltage falls below a permitted threshold, typically 0.9 p.u for most power utilities.

Figure 2.3 below shows a typical example of voltage dip.



**Figure 2.3:** Voltage dip (*Jamal et al. 2017*)

Large scale PV penetration can also lead to voltage rises especially during peak solar irradiance which may coincide with low power demand especially in winter in some parts of the world. Figure 2.4 below confirms this assertion.



**Figure 2.4:** Typical solar irradiance for a day (*Chaudhary & Rizwan 2018*)

Figure 2.5 below shows a general network structure from which voltage drop calculations can be evaluated.

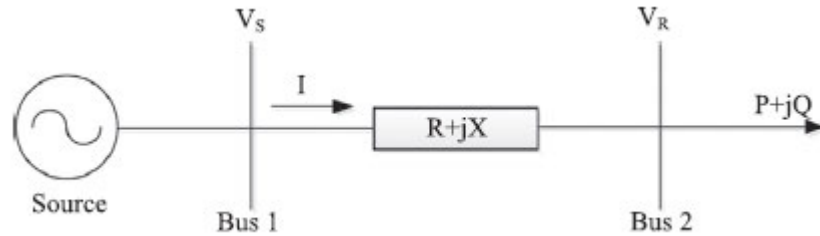


**Figure 2.5:** Network Structure (Chaudhary & Rizwan 2018)

Voltage drop across the line is represented by:

$$\begin{aligned} \Delta V &= I(R+jX) = \frac{(P+jQ)}{V_R} (R+jX) \\ &= \frac{(PR+QX)}{V_R} + j \frac{(PX-QR)}{V_R} \end{aligned}$$

Imaginary part can be ignored (if  $|I(R+jX)| \ll |V_R|$  then  $|V_s| - |V_R| \approx \frac{R}{V_R} dP + \frac{X}{V_R} dQ$ )

$$|\Delta V| = \frac{(PR+QX)}{V_R}$$

Using power transfer principle gives:

$$|\Delta V| = \frac{R}{V_R} dP + \frac{X}{V_R} dQ$$

This equation shows that an increase in active power increases the voltage difference while an increase in reactive power reduces the voltage difference. High PV penetration often leads to high generation of active energy during afternoons when load demand might be low, and this subsequently leads to an increase in voltage difference. The above discussion illustrates the complications associated with high PV penetration on voltage variation (Chaudhary & Rizwan 2018).

Figure 2.6 below shows the effects of PV penetration on voltage profile for LV network. As shown, voltage rises with increase in penetration.

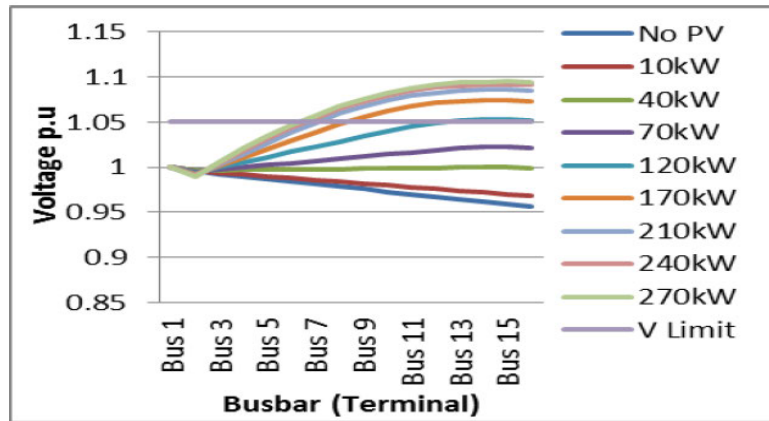


Figure 2.6: Impact of PV penetration on voltage profile (Kenneth & Folly 2014)

## 2.3 Fault Ride Through Capability (FRTC)

### 2.3.1 FRTC for PV Inverter Systems

Fault Ride Through Capability (FRTC) is the characteristic of a generator to return to its pre-fault state after a disturbance thereby re-establishing its generation, within a prescribed timeframe. Large scale penetration of PV generation implies that the Solar generators must remain connected to the grid during faults as their disconnection would lead to a major disturbance likely to cause blackouts. Wide-spread deployment of Renewable Energy Sources (RES) has seen international organisations and electricity markets introducing regulations and standards to ensure their safe integration to existing grid networks (Perpinias et al. 2015). The revised IEEE standard and the AS/NZS 4777.2:2015 are some of the standards requiring PV generators to remain connected to the grid during fault conditions, only disconnecting from the grid during loss of grid supply. This anti-islanding protection is a safety measure meant to protect field workers while re-establishing supply.

Haidar & Julai (2019) report that the current grid codes require that solar PV inverters remain connected to the grid during fault conditions for specific values of voltage sag and duration to participate in grid functions like voltage regulation. The authors go on to propose a Low Voltage Ride Through Capability (LRTC) strategy that uses a crowbar protection as shown in figure 2.7.

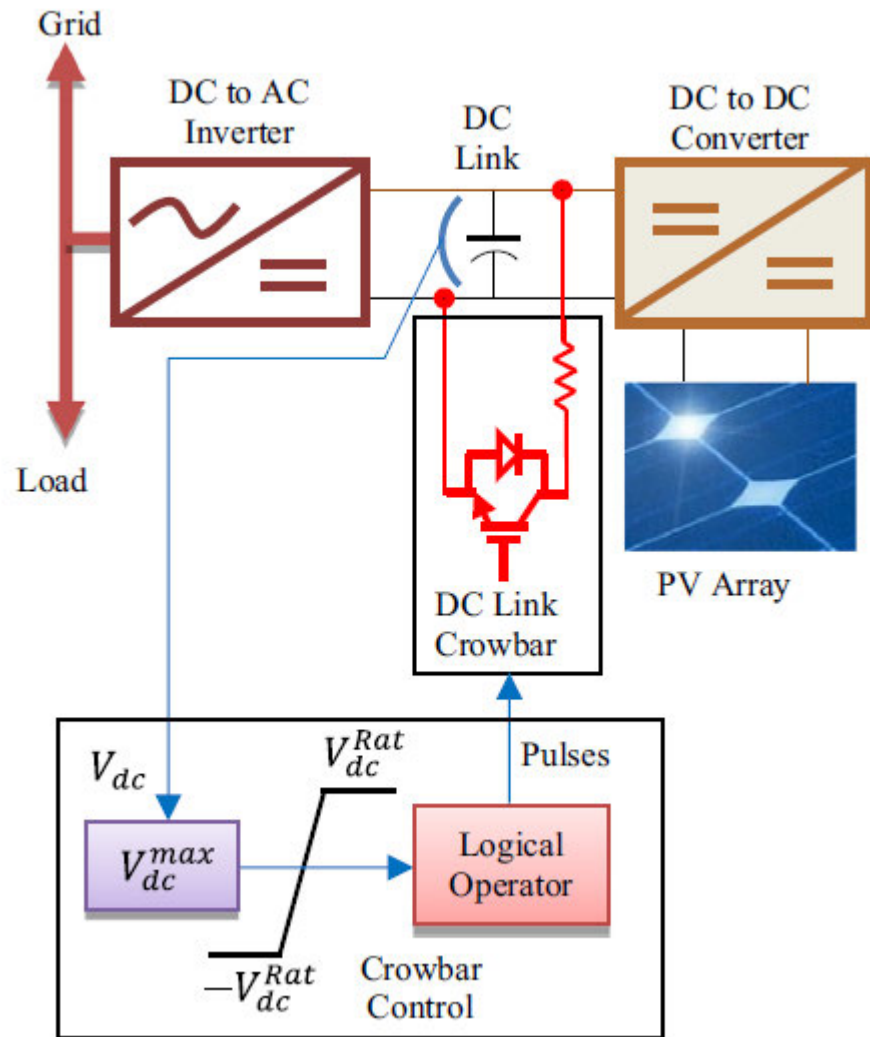


**Figure 2.7:** Crowbar protection to give LVRT

Figure 2.7 above shows one of the methods used to achieve LVRTC. The resistor in the DC Link Crowbar (parallel to the DC link) is used to absorb excess energy due to overcurrent. The DC Link Crowbar circuit gets connected through a signal coming from a voltage sensor located in the DC link circuit. The signal triggers the Insulated Gate Bipolar Transistor.

Naderi et al (2016) propose another strategy of FRTC using Adjustable Resistive type Fault Current Limiter. This achieves required FRTC by charging and discharging a DC inductor through a large resistor. The inductor, by its nature, limits  $di/dt$ . Therefore, any rise in current caused by a fault is countered by the inductor characteristic that reduce the change of current. Excess energy is absorbed by this inductor through an adjustable resistor which helps to discharge the absorbed energy.

There is no common FRTC standard for large-scale solar generation and as such, the behaviour of these under abnormal conditions is still open for research (Perpinias et al. 2015). Figure 2.8 below shows FRTC for various nations.

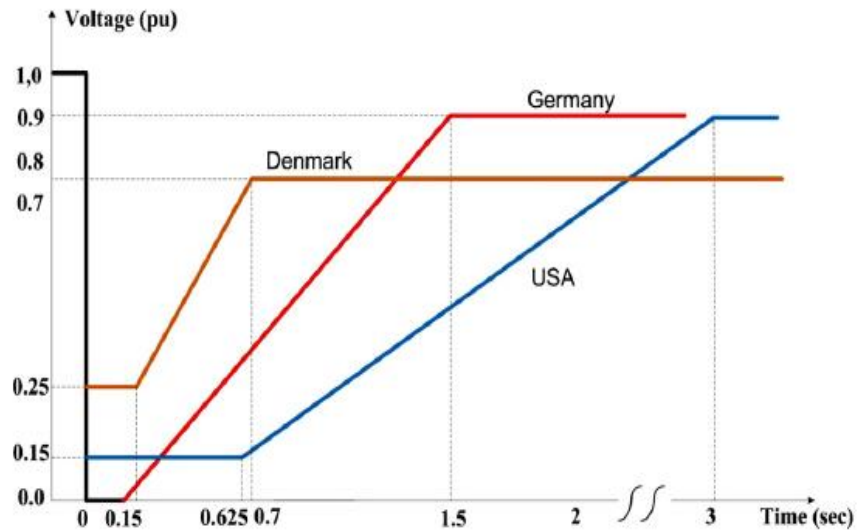


**Figure 2.8:** FRTC schemes of several energy markets: (Perpinias et al. 2015)

Unfortunately, some literature on this subject points to the effect that PVs do not offer the required FRTC like their conventional counterparts as they behave like constant current sources. However, Perpinias et al (2015) reports that PV inverters can be controlled such that they have improved FRTC capabilities by making them behave like a voltage source in series with a reactance.

Literature reviews indicate that a survey conducted by International Council on Large Electric Systems (CIGRÉ) has pointed out that there are not enough studies regarding the changing nature of a grid-connected PV power system with higher penetration of asynchronous generation (Kirtley cited in Jaalam et al. 2017). In order to meet the FRTC standards, PVs must be able to inject reactive power at required levels during disturbances so that voltage can recover (Carrasco et al. 2013).

### 2.3.2 FRTC for Synchronous Generators

The International Electrotechnical Commission (IEC) and the Institute of Electrical and Electronics Engineering Standards are two major bodies governing the technical requirements for synchronous generators. Synchronous generators, like all other generators connected to the grid, are required to remain connected to the network after a disturbance for as long as the voltage at the connection point remains above a defined value (Maroto et al. 2016). This, therefore, implies that the synchronous generator must have good fault ride through capability as required by relevant grid codes. A good FRTC means an ability by the generator control system to re-adjust active and reactive power generation to counter any system variations that deviate from the normal set levels.

Grid codes specify the fault duration in milliseconds and the percentage of retained voltage. According to the British grid code, a synchronous generator must remain connected to the grid for a fault that lasts for 340ms with 30% retained voltage or 710ms for 50% retained voltage.

Maroto et al. (2016) report that “A key parameter that affects synchronous machine transient stability is rotor inertia.” The synchronous generator rotor opposes change to speed which in turn implies an opposition to frequency variation. Solar PV intermittency is known to increase the frequency of system disturbances. In that case it stands to be proved through models and simulations if synchronous generators will maintain their FRTC levels with increasing solar PV penetration.

## 2.4 Short Circuit Ratio (SCR)

The short circuit ratio is a measure of the strength of the network. A low SRC means a weak network. System strength reflects power system sensitivity to disturbances (Australian Energy Market Operator 2017). A robust network is less sensitive to minor disturbances. North American Electric Reliability Corporation reports that: “The short-circuit ratio (SCR) is used in order to develop an understanding of the reliability implications and to quantify the risks associated with high-level integration and penetration of inverters”. A high SCR is a measure of the strength of the response to faults. Unfortunately, there is limited literature on this topic. This parameter is a vital component in determining system robustness and measure of immunity to sporadic disturbances. Given the limited research on the subject might entail a knowledge gap towards successful implementation of large-scale PV penetration without compromising on power supply security. The hypothesis is that PV systems have a low SCR and therefore, bring with them a complication of network weakness. This research seeks to confirm or disapprove this hypothesis through network simulation results. The general formula for SCR is given by:

$$SCR = \frac{S_{scMVA}}{P_{RMW}} \text{ where } S_{scMVA} \text{ is short circuit capacity at the bus and } P_{RMW} \text{ is the rated power in MW of the generator to be connected.}$$

## 2.5 Harmonics

Contradicting literature was found with regards to harmonics associated with PV penetration due to switching nature of associated inverters. While Karim et al (2016) allege that voltage and current harmonic distortions are becoming an issue due to penetration of PV onto distribution networks, Hernandez et al (2011) observe that most new inverter designs are based on Insulated Gate Bipolar Transistors (IGBTs) that use Pulse Width Modulation (PWM) technology and can generate clean output that satisfies the IEEE/IEC requirements for harmonics. However, distribution and transmission companies stipulate the levels of harmonic content introduced by PV generator as part of the conditions for connection to the grid implying that harmonics are still an issue. This research will endeavour to investigate these allegations through modelling and simulation of the electricity network with variable PV penetration. Figure 2.9 illustrates the current harmonic contribution due to PV penetration over a period of one day.

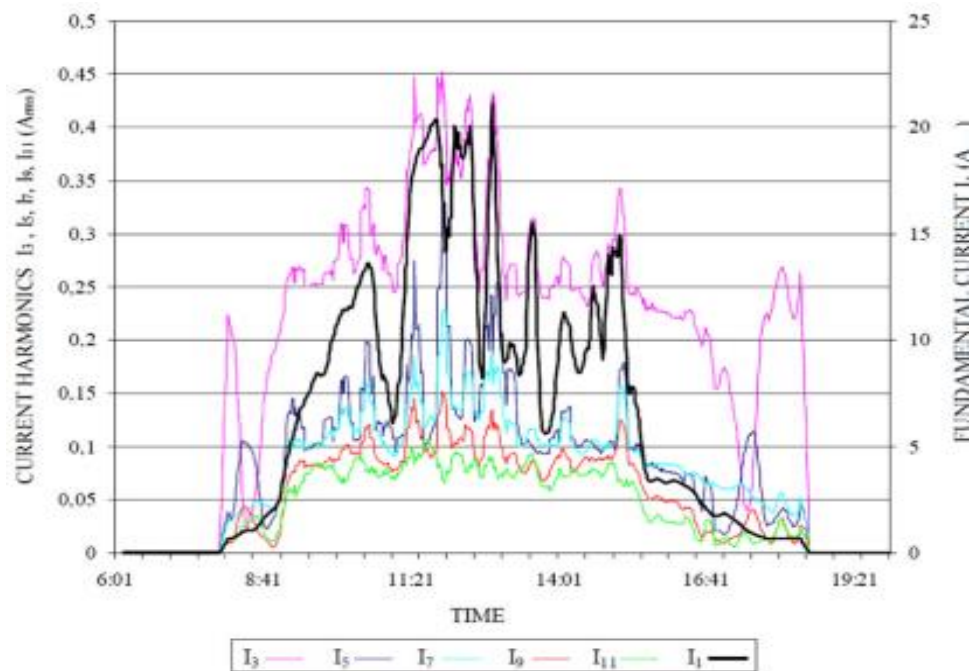


**Figure 2.9:** Fundamental, 3rd, 5th, 7th, 9th and 11th order of current harmonic within a day (Karimi et al. 2016)

## 2.6 Frequency Variations

### 2.6.1 PV Inverters

Electricity network systems are designed to maintain a constant frequency in compliance with national and international standards. Frequency variations and the rate of change of these variations (Hz/sec) are important parameters in network system monitoring as they determine the stability of a system. PV generators, like conventional synchronous generators, are required to supply power at a frequency that is within acceptable limits. Literature indicates a perceived weakness on PV generators with regards to timeous response to, and correction of, frequency variations.

According to a paper by Deidy et al (2017), the inability of PV generators to provide inertia has created technical issues for network planners and operators as this shortfall makes the network vulnerable to frequency variations. The paper goes on to say, "The more the percentage increase of installed renewable Energy Sources (RES) the more the Rate of Change of Frequency (ROCOF) increases even for minor imbalances in the system." However, current control algorithms for PV inverters do incorporate active power control to cater for frequency variations. The Inverter frequency control uses power electronic interfaces, and these may not naturally respond to changes in system variables (Ye et al. 2019). The rate of change of frequency is directly proportional to change of active power. PV generators'

outputs fluctuate in tandem with fluctuating irradiances, therefore, implying higher ROCOF in networks with a high penetration of PV energy.

### 2.6.2 Synchronous Generators

Synchronous machines, on the other hand, have inertia to stabilise frequency in cases of disturbances. Synchronous generators release or absorb kinetic energy onto or from the grid to oppose the frequency deviation (Tielens & Van Hertem 2016). This energy is vital in synchronous generators as it offers compensation during disturbances like loss of generation caused by PV intermittent generation. This helps in bringing the grid frequency to required levels. When system frequency falls, a synchronous generator releases kinetic energy and speed of rotation changes to cater for frequency drop (DIGSILENT 2017 p.25). According to (DIGSILENT 2017 p.25): “Large thermal power stations tend to have high inertia and at the other extreme, inverter-based generators like solar photovoltaic (PV) generators do not contribute at all to system inertia”. The paper adds that a lower inertia leads to a higher rate of change of frequency. Etxegaria et al (2014) report that frequency regulation in synchronous generators is governed by the swing equation as follows:

$$2.H \cdot \frac{d^2\delta}{dt^2} = P_m - P_e - K_D \cdot \frac{d\delta}{dt}$$

where H is the inertia constant,  $\delta$  is the load angle,  $P_m$  is the mechanical power,  $P_e$  is the electromagnetic power and  $K_D$  is the damping factor. The rate of change of frequency is given by

$$\text{ROCOF} = \frac{\Delta P}{2.H}$$

where  $\Delta P$  is the active power mismatch between the load demand and supply, H is the constant of inertia. This equation illustrates that the rate of change of frequency is proportional to power mismatch and the inertia constant. Table 2.2 below shows ROCOF values for different countries.

**Table 2.2:** ROCOF Requirements for some regions

Region	ROCOF
Republic of Ireland	$\pm 0.5$ Hz/s
Northern Ireland	$\pm 0.5$ Hz/s
Spain SEIE	$\pm 2$ Hz/s
Tasmania	$\pm 4$ Hz/s (AAS), $\pm 1$ Hz/s (MAS)

A sharp rise or fall in frequency might imply a loss of the grid therefore, under normal operating conditions, ROCOF should not be too high to an extent that it leads to under frequency load shedding.

The literature in this section shows that PV cells may not be able to provide a quick enough response to frequency variations.

## **2.7 Inverter/Converter Control**

The inverter models used in this project incorporate controls to enable appropriate integration of solar PV inverters into electricity networks. Close control of inverter parameters in this case is very imperative especially if the PV system is to remain connected to the grid under fault conditions. Kim (2015) elaborates this position by saying “When the generated electrical energy from renewable energy resources is delivered to grid through the grid-connected inverter, the inverter should provide fast response, zero steady-state error, and robustness to disturbance.” However, it stands to be confirmed through simulations in this project whether the intended inverter control strategies provide a fast-enough response to sustain network stability. The control approach must be in line with the requirements for FRTC as stipulated in relevant grid codes.

### **2.7.1 Maximum Power Point Tracking (MPPT)**

Solar PV output is affected by weather conditions. Cloud cover reduces solar irradiance and consequently affects the current that can be drawn from the cell. High temperatures reduce the maximum power point voltage of PV cells. Not all solar cell output voltages will coincide with maximum power point of the solar cell. In view of these uncontrollable factors, it stands to reason that there is a need to constantly monitor the solar cell output and match it with the load to maintain maximum power transfer between solar cells and the load. This is achieved by electronically tracking the voltage and current that correspond to maximum power transfer between solar cells and load using DC to DC converters.

Faranda and Leva (2008) submit that due to abrupt daily variations in solar irradiance, the Maximum Power Point (MPP) of PV array changes continuously hence the need to change the PV system’s operating point to maximise the energy produced. Cheng et al (2015) add on to this by saying that “the characteristic curves of a solar cell are nonlinear and depend on the irradiance level and ambient temperature, resulting in a unique current-voltage (I-V) curve.” They go on to add that “consequently, the operating point (OP) of a photovoltaic generating system must be adjusted to the extent in which the maximum efficiency of the solar cells can be achieved, and this technique is called maximum power point tracking.” MPPT forms an integral part when modelling grid connected PV inverter system as it helps to represent a solar cell in its most efficient state when investigating the impact of large solar energy penetration on network operations. According to Kamran et al (2018), MPPT is used to let the photovoltaic cell function at its maximum power point by properly adjusting the duty cycle of the converter.

Figure 2.10 below shows the nonlinear characteristic curves of a solar cell.

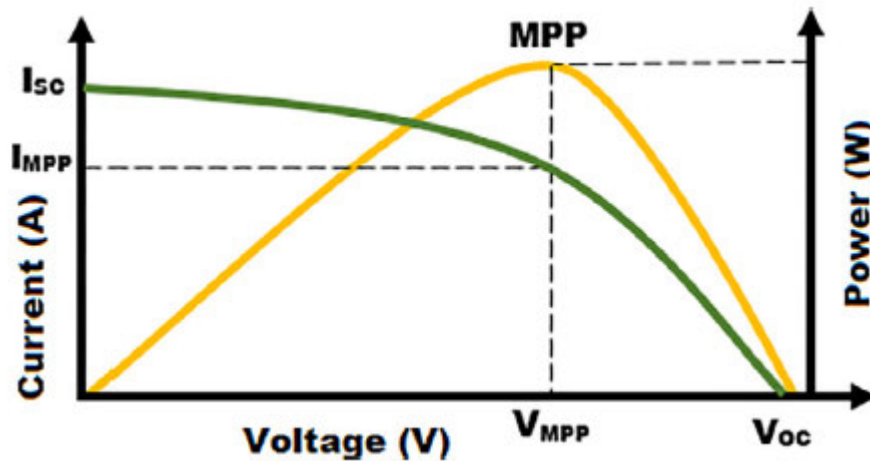


**Figure 2.10:** I-V and P-V characteristics of solar PV cell (Kamran et al, 2018)

Most authors concur that MPPT techniques must be instituted in order to realise maximum efficiency from solar cells even when given their exposure to uncontrollable weather conditions.

Various algorithms are used in implementing MPPT technique and some of them have been explored by researchers as given below.

#### 2.7.1.1 Constant Voltage Method

The constant voltage method is reportedly the simplest algorithm in MPPT techniques according to Faranda and Leva (2008). The PV array voltage is regulated to near the maximum power point voltage ( $V_{MPP}$ ) of the module as given by the module manufacturer's test certificate. This is achieved by matching the PV output voltage to this fixed reference voltage ( $V_{MPP}$ ) using a DC-DC converter by adjusting the duty cycle of the converter. However, it must be noted that with varying irradiance and temperature, the PV array voltage corresponding to maximum power may not necessarily be equal to this reference voltage all the time. Critiquing the constant voltage method, Lasheen et al (2016) postulate that the method suffers from low accuracy and requires more than one sensor to improve its accuracy.

### 2.7.1.2 Perturb and Observe (P & O) Method

This algorithm is the most extensively used method as opined by Kamran et al (2018). The method is implemented by varying (perturbing) the duty cycle of a DC-DC converter and noting the calculated power output. A small change in duty cycle is added to the converter duty cycle to make it  $D + \Delta D$  and power ( $V \times I$ ) is noted. A second perturbation is applied with  $D_{NEW} = D + 2\Delta D$  and the new power is noted. If the new power is greater than the old power, the iterations are continued by adding a small positive change to the duty cycle. Whenever the new power is found to be smaller than the old one, a negative step change is applied to the duty cycle. The algorithm keeps repeating the iterations as a means of tracking the maximum operating point on the PV power characteristic curve. Farand & Leva (2008) define the algorithm as one that operates “by periodically perturbing (ie incrementing or decrementing) the array terminal voltage or current and comparing the PV output power with that of the previous perturbation cycle”. Talking about the effect of the size of the voltage perturbation, Kamran et al (2018) observed that a small perturbation increases the response time while a large perturbation improves response time but increases oscillations on the PV output.

### 2.7.1.3 Incremental conductance (IC) Method

In its basic form, conductance is the inverse of resistance given by  $\frac{I}{V}$ . The incremental conductance algorithm uses the slope of current to voltage ( $dI/dV$ ) relationship in tracking the maximum operating point. According to Saravanana & Babu (2016), “The incremental conductance algorithm operates using the slope from PV array power curve to compute the sign of derivative of power and voltage.” They go on to say: “The slope is zero at MPP, positive when the optimum point is left to the MPP, and negative when the optimum point is right to the MPP. The maximum power is obtained by differentiating the power with respect to voltage and equate to zero.” Putri et al (2015) transform the  $\frac{dI}{dV}$  relationship to  $\frac{dP}{dV}$  and develop an equation for IC method as follows:

$$\begin{aligned} \frac{dP}{dV} &= \frac{d(V \cdot I)}{dV} = I \frac{dV}{dV} + V \frac{dI}{dV} \text{ (Product Rule)} \\ &= I + \frac{V dI}{dV} \end{aligned}$$

$$\text{MPP is reached when } \frac{dP}{dV} = 0$$

$$\frac{dI}{dV} = \frac{-I}{V}$$

When  $\frac{dP}{dV} > 0$  then  $V_p < V_{MPP}$

When  $\frac{dP}{dV} = 0$  then  $V_p = V_{MPP}$

When  $\frac{dP}{dV} < 0$  then  $V_p > V_{MPP}$

The authors express that this method was developed in 1993 to address the drawbacks of the Perturb and Observe algorithm.

### 2.7.2 Active and Reactive Power Control

PV generation systems must have active and reactive power control capability in order to support power quality of the grid and for them to remain connected to the grid under abnormal conditions. Literature on the subject reveals that a high penetration of Photovoltaic generators is associated with voltage problems on the Low Voltage (LV) side of the grid. Hamrouni et al (2019) mention that the problems attributed to high PV penetration include amplitude drop, frequency deviations and high harmonic components. The authors go on to state that: "The impact of those problems cannot be ignored on the LV level grid because they affect the grid stability and the safety, as well as the power quality." In view of these problems, control measures must be instituted on the grid connected inverters for them to ride through faults.

The control strategies must have a feedback system that monitors the grid voltage and current at the Point of Common Coupling (PCC) and supply such feedback to the control parameters of the inverter control system. Solar PV systems normally use Maximum Power Point Tracking (MPPT) to achieve maximum efficiency from the solar cells. However, during abnormal/faulty situations, the control system must temporarily disable MPPT using reference inverter currents and voltages.

Figure 13 shows an example of a control system used in a double staged inverter system. The DC-DC boost converter helps in keeping the PV voltage at an acceptable range for the PV inverter and aids in the control algorithm for MPPT. The DC capacitor  $C_{DC}$  is placed between the DC-DC converter and the inverter to limit ripple in the DC input to the inverter and to limit di/dt. An LCL filter is used to filter away and bar harmonic components from passing on from the inverter to the grid. When the monitoring system detects a voltage dip it switches to non-MPPT mode to avoid tripping inverter over current protection and the inverter should inject reactive power in proportion to the voltage sag (Hamrouni et al 2019). However, Gandhi et al (2018) observe that using PV inverters for local reactive power compensation reduces the life span of inverters as it increases the current flowing through the inverter subsequently increasing the inverter losses and temperature of its components.

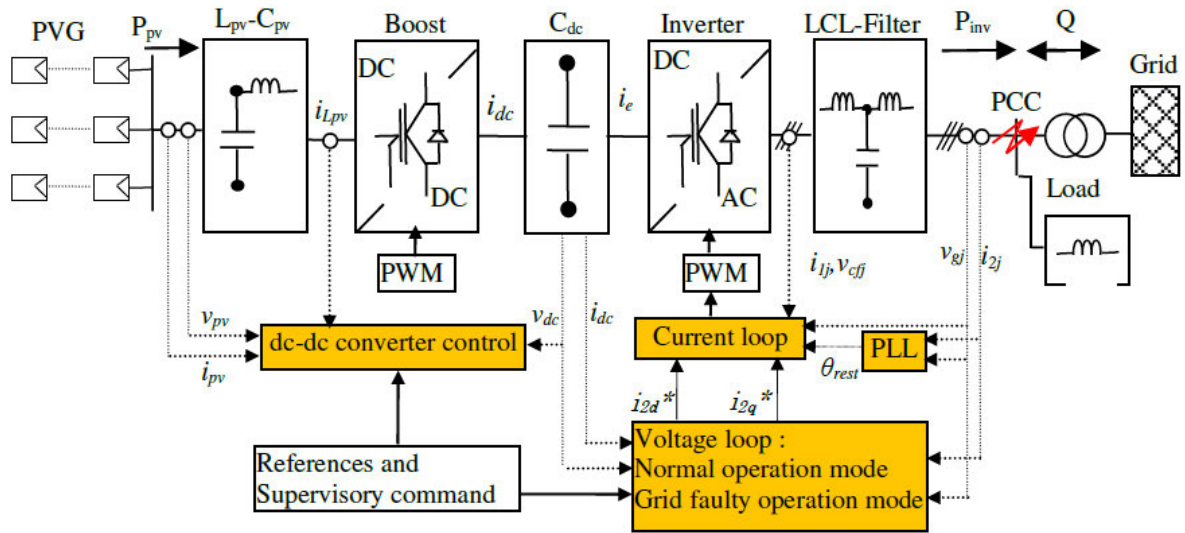


Figure 2.11: Overall Control of Grid Connected PV System (Hamrouni et al 2019)

### 2.7.3 Inverter Protection and Fault Analysis

An inverter is an integral part of a solar PV system and as such requires efficient and effective protection from overloads, overvoltage, over current and some such abnormal conditions that may damage the electronic devices that make up the inverters. This project is mainly concerned with overcurrent protection of the inverter as this type of protection is greatly affected by faults occurring on the grid side during reactive energy injection.

According to Cooper Bussmann paper (2015), the NEC 690.9(A) requires that inverter output circuit be protected from overcurrent. Talking about inverter overcurrent protection, Koutroulis et al (2003) point out that “The most common form of overcurrent protection is fusing.” They go on to say, “but this method is not always effective because fuses have relatively slow response time”. Bui et al (2017), suggest that digital relays with different protection principles will be an effective protection solution for the DC/AC inverters. In order to avoid component damage and self-blocking, the working current of an inverter should be no more than twice the rated current (Lin et al, 2014). It is imperative to ensure that this condition is considered when using the inverter to inject reactive power for grid support as excess current may isolate the inverter from the grid and cause instability. Australian Standard AS/NZS 5033:2014 stipulates that the DC isolator for inverters must be equal to  $I_{sc} \times 1.25$  and AC circuit breaker must be rated above the inverter maximum AC current output rating. Where  $I_{sc}$  stands for the inverter short circuit current as specified by the manufacturer.

With regards to inverter short circuit fault analysis, Turcotte & Katiraei (2015) report that when dealing with short circuits, the two decision-making mechanisms for disconnection of inverter from the grid are under-voltage and over-current measurements. The fast response of the semiconductor devices calls for control of voltage dip and over current flow to avoid any damage to the devices during faults (Hota et al, 2016).

## 2.8 Synchronous Generator Control

Most literature in this subject is centred around the requirements of the Australian Energy Market Operator (AEMO) and the National Electricity Market (NEM) as all grid connected generators must conform to the requirements of these bodies among others. The main control devices in synchronous generators are the Automatic Voltage Regulator (AVR) and the governor. The two devices control the generator reactive and active power outputs respectively.

### 2.8.1 Governor control

The governor is used to vary the active power output of the generator which subsequently affects the system frequency. Xavier & Muthukumar (2010), emphasise that the Governor is an important controller in a power plant as it regulates turbine speed, power and participate in grid frequency regulation. They further point out that the governing system is essential since load on the turbo generator does not remain constant but varies as per consumer demand requirements. Large penetration of solar PV generation coupled with intermittency further necessitate the need for a faster and more accurate governing system. The governor control uses the steam valve to regulate steam into the turbine thereby subsequently increasing or decreasing the rotor speed. Figure 14 below shows the basic elements of a governing system.

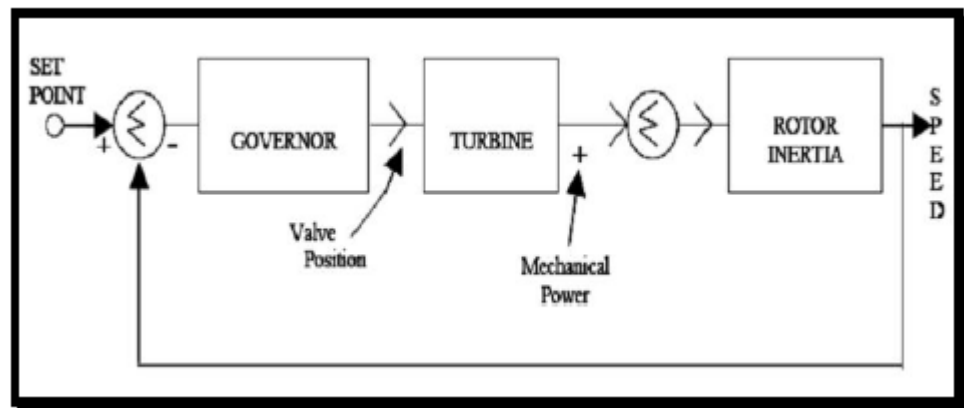


**Figure 2.12:** Basic Elements of a governing System (Xavier & Muthukumar, 2010)

Short et al. (2007) report that, “A generator connected to the grid is designed to respond to drop in grid frequency by increasing its output.” They further observe that generator governors are typically designed with approximately 4% droop meaning that a 4% drop in frequency will cause a 100% increase in generator output. This method of frequency control is called primary frequency control.

Figure 2.13 below shows different frequency control mechanism for normal and contingency conditions of a power system.

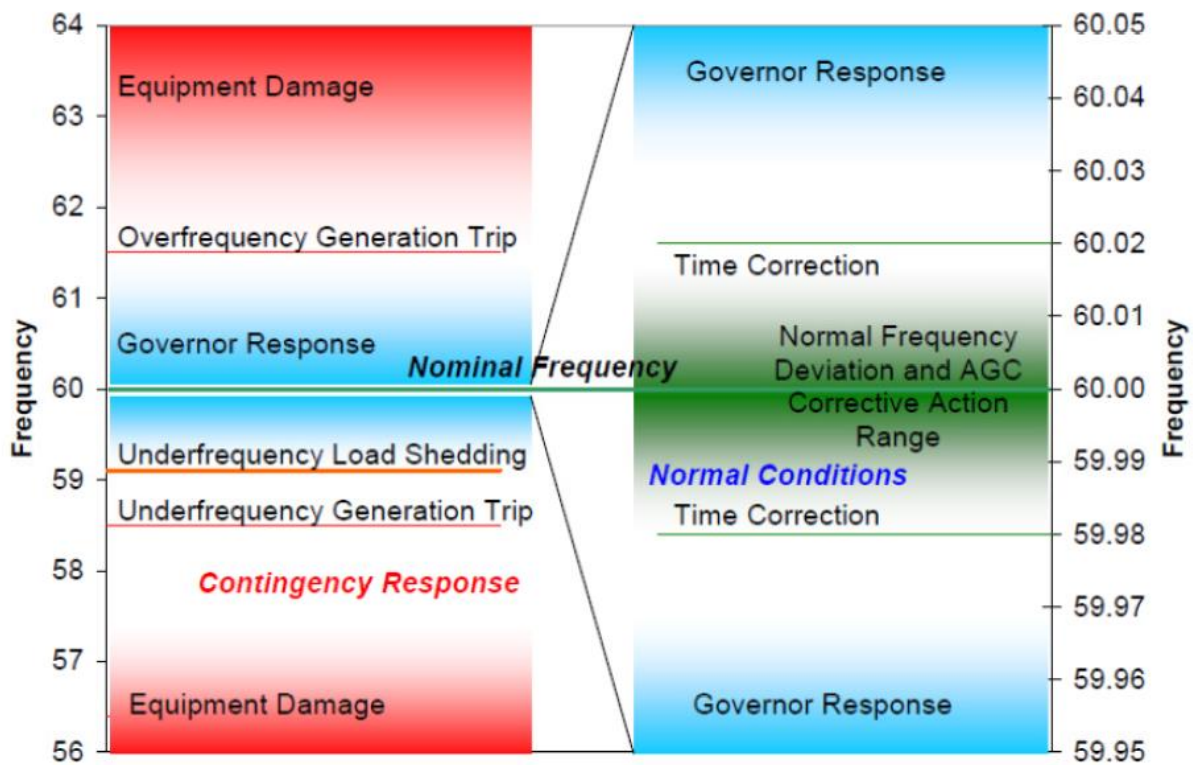


**Figure 2.13:** Frequency Control for Normal and Contingency Conditions for a 60Hz system (Peydaesh & Baldick, 2012)

An improvement in frequency regulation has seen an introduction of Automatic Governor Control (AGC) in power system control. However, the Australia Energy Market Operator through DigSILENT (2017) reports that AGC is not suitable to manage fast changes to frequency oscillations in normal power system operating frequency band. It is meant to work in parallel with primary frequency control provided by governor response. AGCs perform better when providing load-following regulation.

Most synchronous machines have governors that are equipped with frequency droop control DigSILENT (2017). The National Electricity Market stipulates droop of 4-5% and a dead band of 0.15Hz. Droop control takes effect outside the dead band. Some international standards, for example, the IEEE standard 446-1995 and BS EN50160:1995 state a maximum frequency variation of  $\pm 0.5\text{Hz}$ . Figure 16 shows Megawatt/Frequency graph with droop control and dead band. Seneviratne & Ozansoy (2016), point out that governor response time is an important parameter in frequency control. They add to this by mentioning that system frequency response is affected by Head Room (HR) which they define as the 'hot spinning available for dispatch for governor control'. Governor setting must be such that frequency deviations are arrested quick enough before customer loads are shed off due to under frequency protection especially after loss of a large generator.

AEMO through DigSILENT (2017), reports that frequency regulation has become challenging due to large penetration of low-inertia generators given that there is a correlation between frequency excursion size and inertia. This research seeks to investigate the extent to which frequency is affected by large solar generation as most literature concur that frequency variations seem to have increased with an increase in solar PV penetration. However, the literature does not dwell on the optimum level of penetration beyond which the network becomes unstable and uncontrollable.

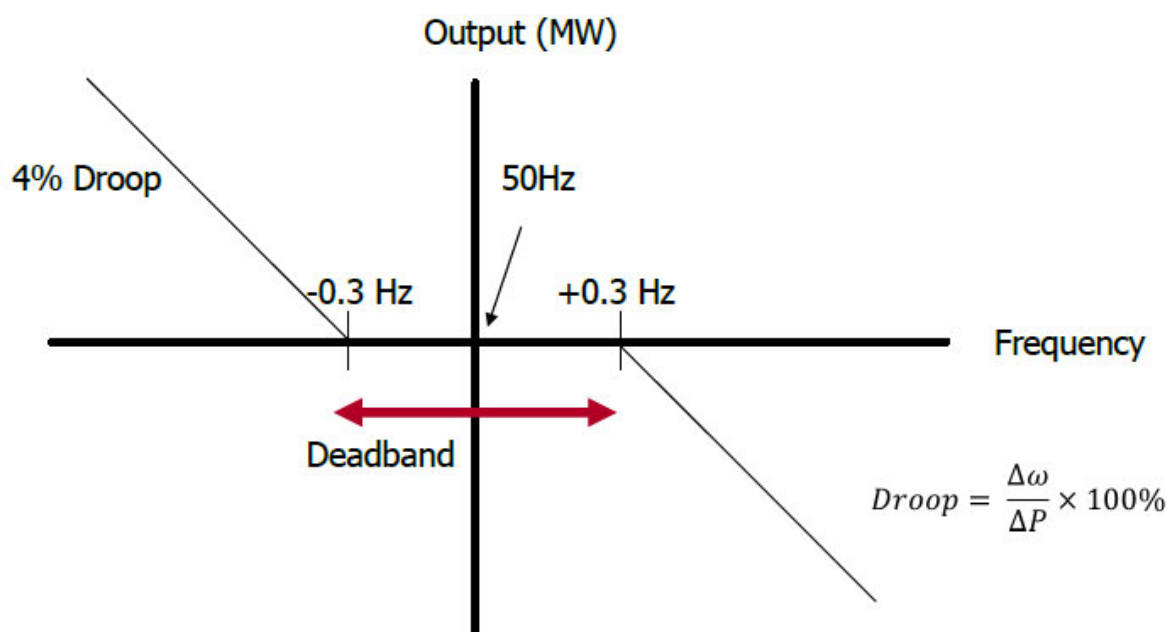
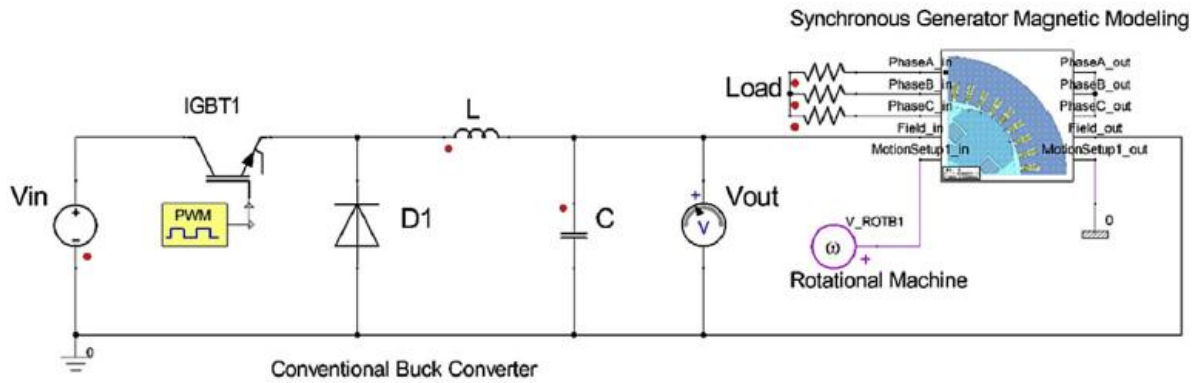


Figure 2.14: Frequency Characteristic showing dead band and droop (DigSILENT,2017)

### 2.8.2 Automatic Voltage Regulator (AVR)

Synchronous generators are equipped with voltage regulation capabilities to aid in supporting the grid during voltage dips caused by disturbances in the network. The terminal voltage of a synchronous generator varies with the load even though the infinite busbar tries to keep the system voltage constant. The AVR adjusts the excitation voltage, consequently increasing or decreasing the generator reactive power, an important parameter in voltage stabilisation. Bayram et al (2017), elaborate the function of the AVR by stating that the AVR uses the terminal voltage error as a control input in the excitation control loop. The excitation current is varied until the error is zero. In most cases a buck converter is used to control the excitation voltage and current as shown in figures 2.15.



**Figure 2.15:** Buck Converter for generator excitation system (Bayram et al, 2017)

The duty cycle of the buck converter is varied in relation to the generator terminal voltage variations. The voltage output of the converter is related to the output as follows:

$V_{out} = V_{in} \times D$  where  $D$  is the duty cycle of the converter. Varying  $D$  varies the output of the converter and this in turn varies the excitation voltage. An example of a control system with Field Programmable Gate Array (FPGA) for a converter used in excitation voltage control is shown in figure 2.16 below.

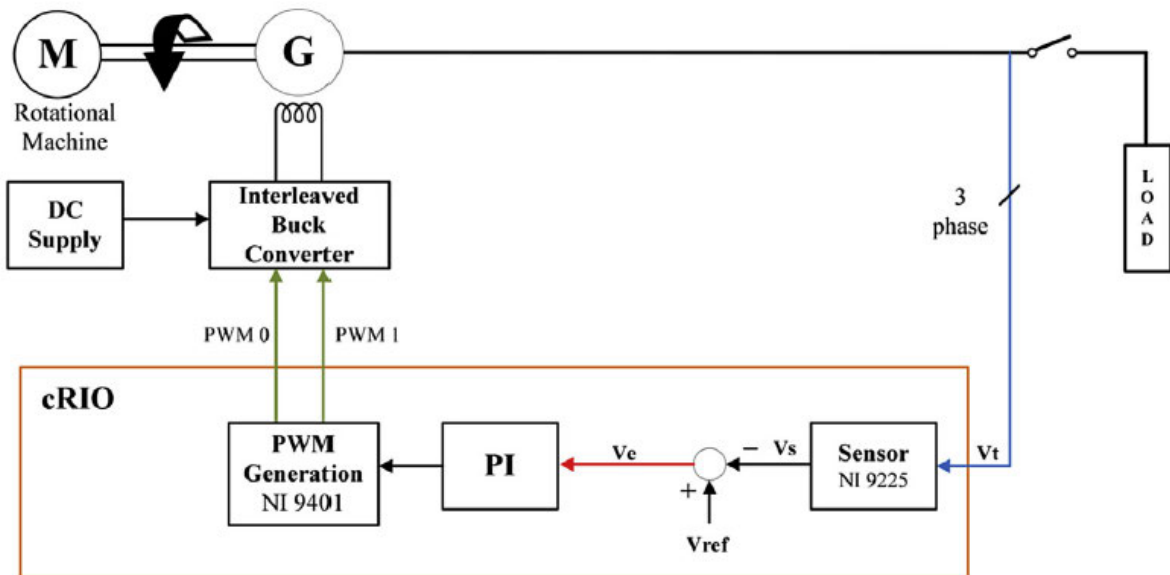


**Figure 2.16:** FPGA controlled interleaved buck converter for synchronous generator excitation system (Bayram et al, 2017)

Li & Zhang (2011), highlight the importance of synchronous generator excitation control in ensuring a 'safe and stable operation of power system and improve power system dynamic quality'. They further emphasise that excitation controller is the core part of regulating the generator voltage and reactive power. Kennedy et al (1995), concur by stating that the excitation controller must ensure that good voltage tracking is achieved at all operating points of the system and must be effective during both major disturbances and small changes in load.

The excitation structure is a major factor in influencing the dynamic behaviour of synchronous generators, Bensmaine et al (2012). Most literature reveal that a very robust and accurate automatic voltage control system is essential in maintaining system stability and requires careful planning and implementation. Figure 2.17 below shows dual control excitation structure where SG stands for synchronous generator and EM is an exciter machine mounted on the shaft of the main machine.

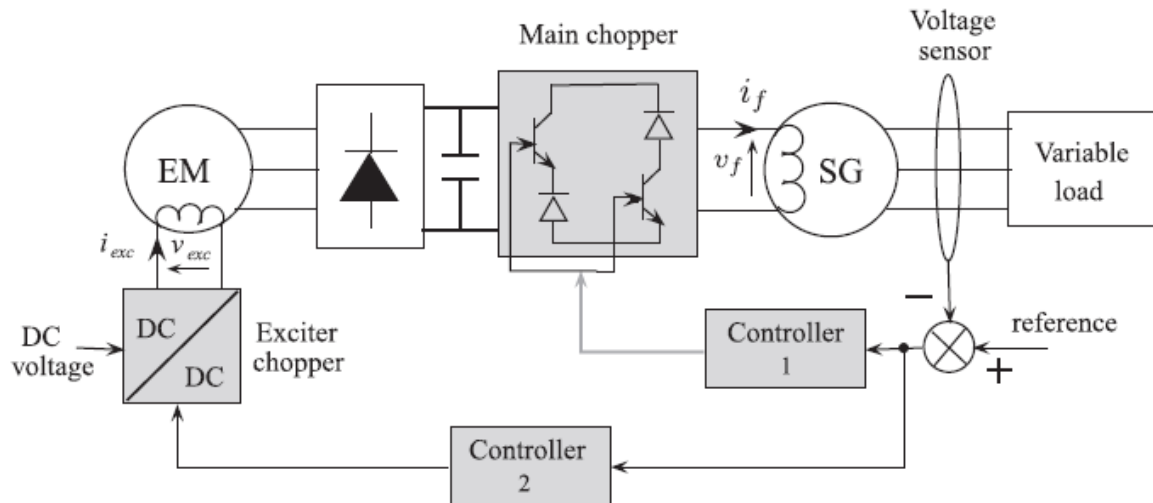


**Figure 2.17:** Excitation Structure with dual control (Bensmaine et al, 2012)

## 2.9 Models

This project is an investigative research that uses models of power system components and simulation of various dynamic conditions experienced by electricity networks. Therefore, literature on models has been explored to establish the most effective modelling techniques used worldwide and in Australia in particular as prescribed by the Australian Energy Market Operator (AEMO). Lammert et al. (2017), report that the increasing penetration of inverter-based generation has seen a rise in the development of inverter-based models of power system dynamics studies.

Discussing the level of models used for all types of equipment, Lammert et al. (2017) comment that, 'At one end of the spectrum are stability models, sometimes also referred to as positive sequence or Root Mean Square (RMS) models. At the other end of the spectrum are very detailed equipment level Electro-Magnetic Transient (EMT) based models.' The electromagnet transient models are reported to cater for instantaneous values of voltage and currents and therefore, are suitable for investigating high frequency disturbances like lightning strikes. Abourida et al. (2016) suggest that the existence of fast electronic models in renewable energy systems calls for a hybrid simulation tool where some parts of the grid system are simulated using EMT and others use RMS if better simulation accuracy is expected. However, the hybrid system may be affected by different time steps in the two methods.

AbdelHady (2017), writes that a grid-connected system comprises of solar panels, DC-DC converter, MPPT, inverter and point of common coupling. The author goes on say that Matlab/Simulink is selected as the modelling software due its 'flexibility, reusability and extendibility in such systems.'

### **2.9.1 Australian Energy Market Operator (AEMO) Model Guidelines**

Applicants who intend to connect generators to the grid must conform to pre connection models and simulations as outlined in the AEMO guidelines. The guidelines play an important role in this research project as all models and simulations must be as close as practically possible to the prescribed limits. The Australian Energy Council (2018) reports that the guidelines are prescriptive in terms of model types, model requirements and accuracy. Senvion in AEMO (2018) complain that the EMT model is cost and labour intensive. Supporting this position, DlgSILENT in AEMO (2018) add that 'the EMT model is an additional and, arguably, unnecessary cost on synchronous generating systems.'

AEMO's clause 7.1 of the generating system model guidelines requires that models for such systems must demonstrate the dynamic performance for a combination of disturbances. The National Electricity Rules (NER) of Australia require that PV generation sources be modelled with variable irradiance as will be the case in a practical situation.

### **2.10 Conclusion**

Literature on the research topic has revealed that high penetration of PV generation has an ability to cause voltage and frequency variations in the electricity network. While modern PV inverters are equipped with both active and reactive power control, the controls may not be fast enough to meet network requirements especially as penetration keeps increasing. Synchronous generators have added advantage in controlling frequency due to their inertia provided by rotating parts. Harmonics are reported to be more pronounced in networks with higher penetration of PV generation. However, literature does not specify the level or extent of PV penetration that leads to network instability. The next sections of this project aim to establish that cut-off point.

# Chapter 3

## 3. Methodology

### 3.1 Introduction

This chapter of the project looks at how the research is going to be executed. A whole power system network comprising of PV solar panels, DC-DC converter with MPPT, DC-AC inverter, a power transformer, and a grid with synchronous generators is modelled and simulated in Simscape electrical under MATLAB/Simulink. Each section is initially modelled as a separate block before being integrated into the final network model with the rest of the components. Each sub-block is modelled with automatic control of active and reactive power to aid in grid support especially during and after disturbances. The complete network model is simulated under different practical network operating conditions, both steady state and transient conditions.

The simulation process involves varying the irradiance of the solar panels and implementing Maximum Power Point Tracking, providing a closed loop control of the inverter for active and reactive power control and ensuring that the synchronous machines have automatic voltage and governor control. The percentage penetration of solar PV generation will be varied from zero up until the network is supplied solely by solar (100% penetration). Disturbance scenarios are created at each percentage level of penetration and effects on network voltage and frequency are recorded. The recorded values include the maximum and minimum values of each parameter including the duration of the disturbance and network recovery time from a disturbance. The magnitudes of network parameters and their times frames must conform to network requirements as specified in National Electricity Rules, AEMO guidelines and Grid Codes and any relevant standards or legislation.

### 3.2 Project development

#### 3.2.1 Aims and objectives

The main aim of the project is to come up with verified facts about the impact of large-scale solar PV generation on network stability through simulation, recording and analysis of simulation results. The research project further aims at ensuring that the benefits of using clean and renewable solar energy do not lead to premature discarding of synchronous generators before ensuring that their desirable characteristics are incorporated into inverter systems where possible. It is hoped that the outcomes of this research will assist in averting disasters like the one that happened in South Australia in September 2016.

### 3.2.2 Solar Panel (Cell) Model

The solar cell plays an important role in this project as the research is about the impact of large-scale solar penetration on the network. Therefore, it goes without saying that a solar cell model is essential in giving an understanding of how the components of a complete model will interact to give the outcomes of the intended investigations during simulation. The solar cell is modelled as shown below:

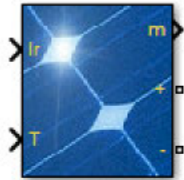


Figure 3.1

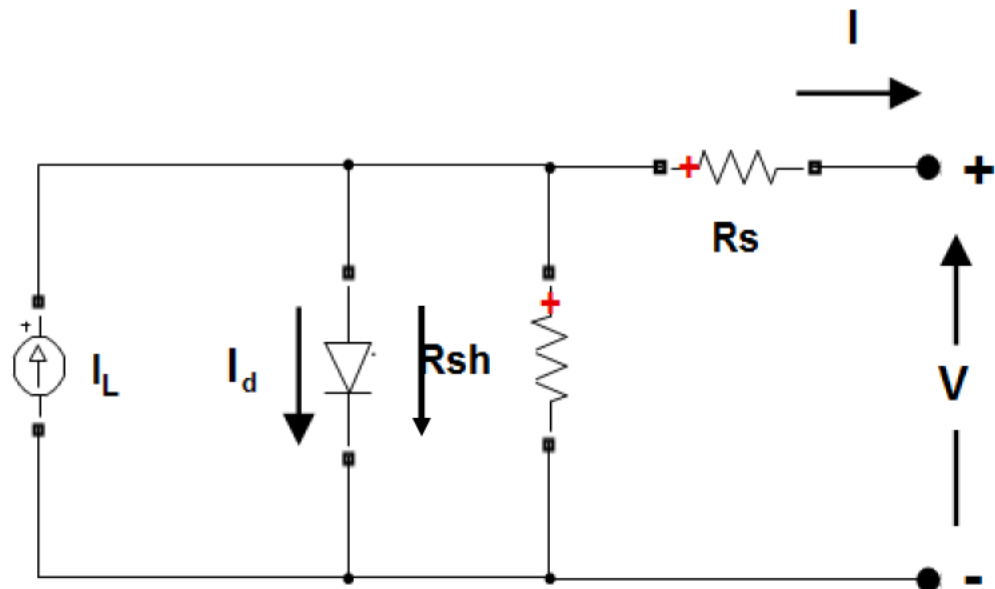


Figure 3.2 Solar Cell Equivalent Circuit

A solar cell is modelled as a current source driving current  $I_L$  with shunt branches comprising of a diode and a shunt resistance  $R_{sh}$  and a series resistor  $R_s$ . The output current is given as  $I$ .

The model equations can be derived as follows:

$$I = I_L - I_d - I_{sh} \quad (1)$$

$$V_{sh} = V + IR_s \quad (2)$$

$$I_{sh} = \frac{V_{sh}}{R_{sh}} = \frac{V + IR_s}{R_{sh}} \quad (3)$$

$$I_d = I_0 \left[ \frac{V_{sh}}{e^{nVT}} - 1 \right] \quad (4)$$

Substituting  $I_{sh}$  and  $I_d$  with values given in equations (3) and (4) into (1) gives:

$$I = I_L - I_0 \left[ \frac{V_{sh}}{e^{nVT}} - 1 \right] - \frac{V+IR_s}{R_{sh}} \quad (5)$$

The open circuit conditions can be derived using  $I = 0$  and those of short circuit conditions are obtained by putting  $v = 0$  in equation (5).

$$I_{sc} = I_L - I_0 \left[ \frac{V_{sh}}{e^{nVT}} - 1 \right] - \frac{I_{sc}R_s}{R_{sh}} \quad (6)$$

The solar array that is used in this research project is the 1Soltech 1STH-215-P with the following characteristics.

**Table 3.1: PV Module Parameters**

	Parameter Description	Value
1	Maximum Power (W)	213.15
2	Open Voltage Voc (V)	36.3
3	Voltage at Max Power Point Vmp (V)	29
4	Temperature coefficient of Voc (%/deg.C)	-0.36099
5	Cells per Module	60
6	Short circuit current Isc (A)	7.84
7	Current at Maximum power point Imp (A)	7.35
8	Temperature coefficient of Isc (%/deg.C)	0.102
9	Light generated current IL (A)	7.8649
10	Diode saturation current I <sub>0</sub> (A)	2.93E-10
11	Diode Ideality factor	0.98117
12	Shunt resistance Rsh (ohms)	313.3991
13	Series resistance Rs (ohms)	0.39383

The solar module characteristics are shown in figure 3.3 below. In the figure, the module temperature is fixed at 25°C while the irradiance is varied from a vector of [1000 800 500 300 100] kW/m<sup>2</sup>. The power versus voltage characteristic curve shows that the output power and voltage relationship is non-linear implying that there is only one point where power output is at maximum and the rest of the curve points do not correspond to maximum power. This maximum power point is tracked using MPPT Perturb and Observe algorithm.

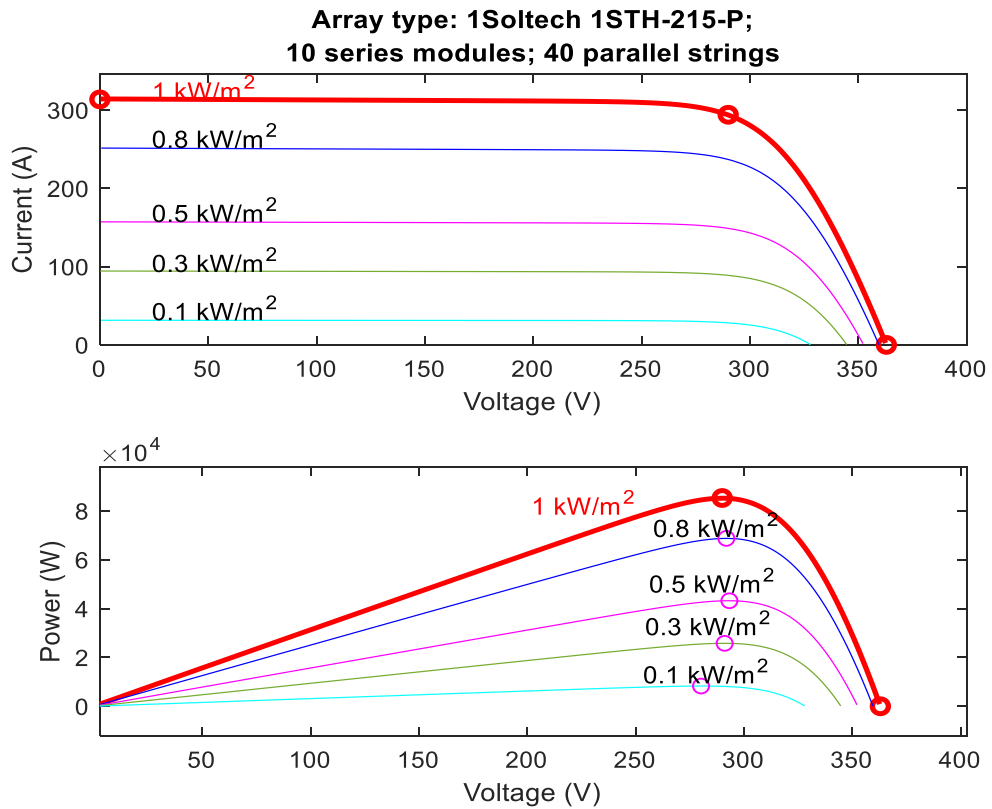


**Figure 3.3:** PV Module Curves for constant temperature(25°C) and varying Irradiance.

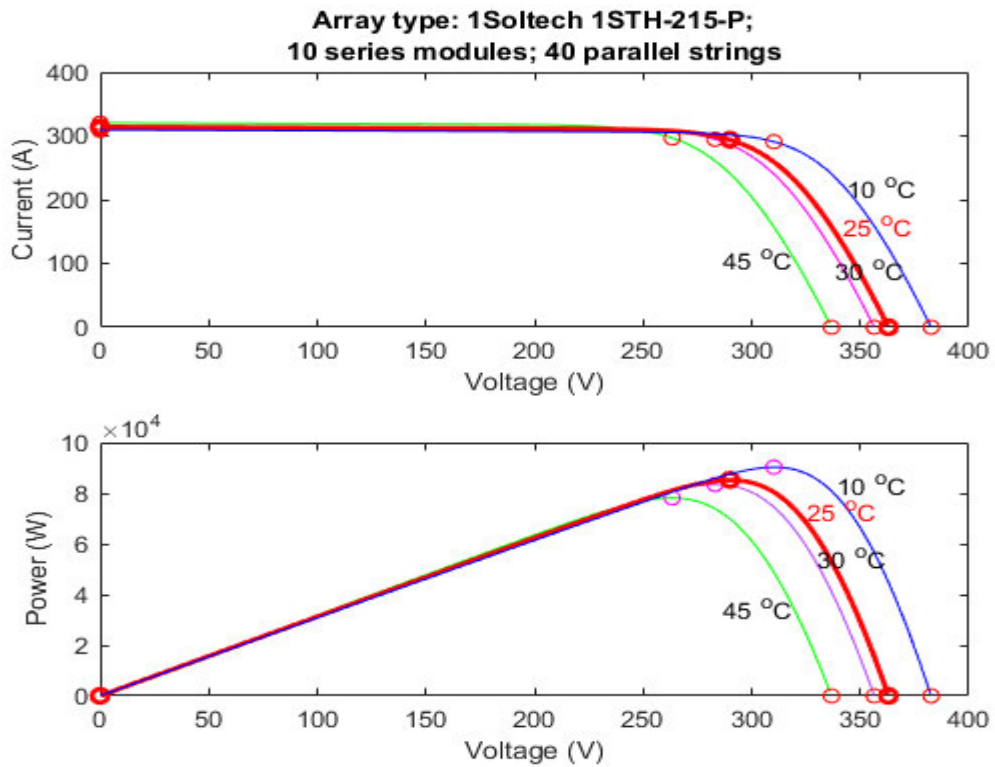


**Figure 3.4:** PV module Curves for constant irradiance(1000W/m<sup>2</sup>) and varying temperature.

However, in a practical environment both irradiance and temperature vary simultaneously. In order to cater for these variations, the temperature and irradiance are varied at the inputs of the PV array using a ramp up/down signals as shown in figure 3.5 below.

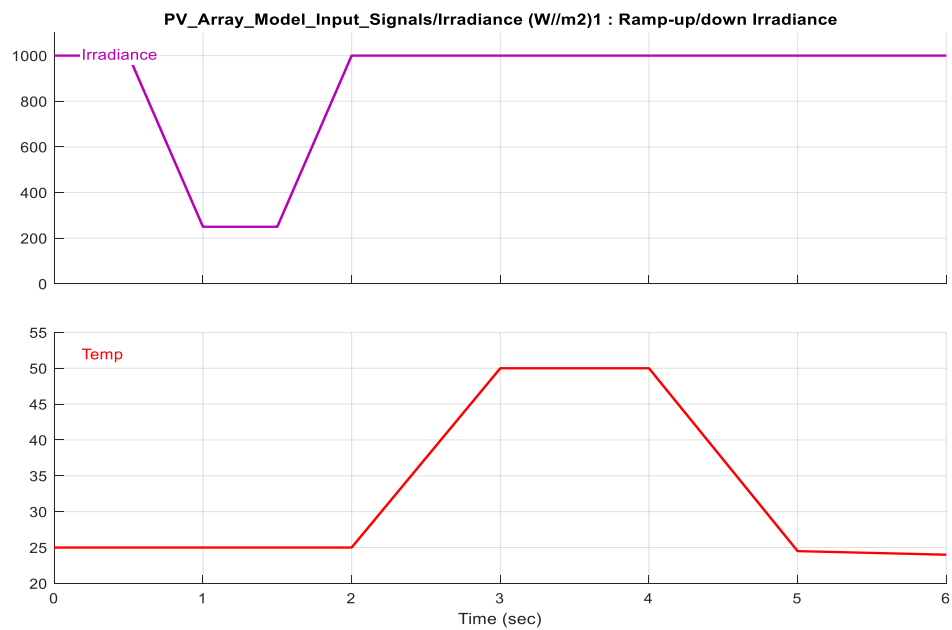


**Figure 3.5:** Irradiance and temperature inputs to PV Model

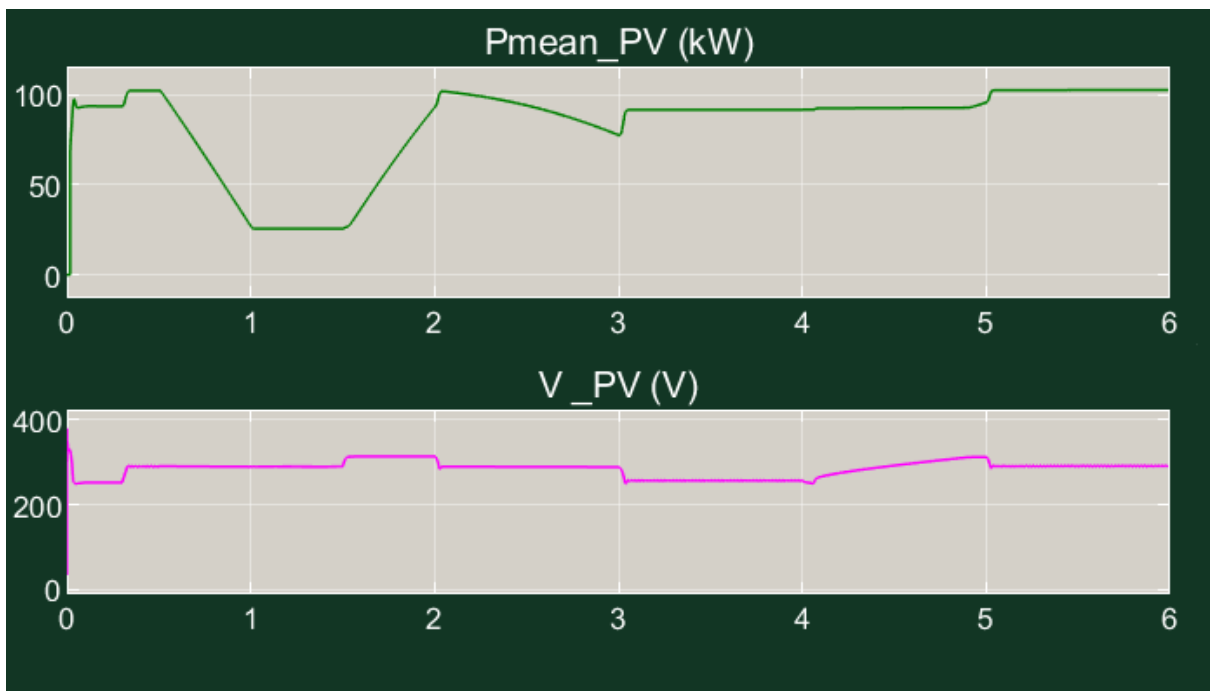


**Figure 3.6:** PV Model Outputs

The voltage output of the PV Model is not smooth and needs to be moderated. The boost converter regulates the output voltage of the PV array and tracks the point of maximum power using the Perturb and Observe algorithm as stated in preceding sections.

### 3.2.3 Boost Converter Model

The boost converter is included in the model to help implement MPPT algorithm for the solar panel modules. This will ensure the solar modules operate at their maximum capacity as would be the case in a practical situation. The buck boost converter is modelled as shown below: The duty cycle of the converter is varied using the switch. The power curve of a PV cell is non-linear therefore, an algorithm is necessary to track the point of maximum power. In this project Perturb and Observe algorithm is used to track the point of maximum power from the solar module.

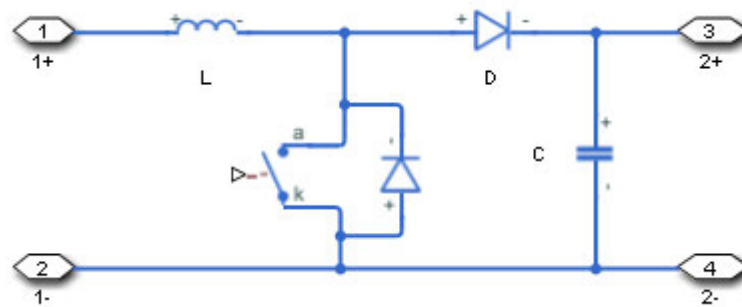


**Figure 3.7:** Boost converter Equivalent Circuit

During the on state of the switch, the inductor L charges up and diode D is reverse biased and the capacitor discharges to the load if has charge already. In the off state, the inductor dissipates stored energy to the capacitor and the load.

Output voltage is measured across terminals 3 and 4. The equation for  $V_{OUT}$  is given by:

$V_{OUT} = V_{IN} + V_L$  where  $V_{IN}$  is measured across terminals 1 and 2 And  $V_L$  is the voltage across the inductor.

The duty cycle is given by:

$$D = \frac{t_{on}}{t_{on} + t_{off}} \quad (7)$$

The duty cycle is the ratio of the switch's on time ( $t_{on}$ ) to that of the total time of the period ( $T = t_{on} + t_{off}$ ).

Switching the electronic device for different on times varies the duty cycle of the converter and therefore changes the output voltage of the converter. Small changes of the duty cycle are implemented in the Perturb and Observe algorithm.

The output of the algorithm control system is fed into the gate control circuit of the electronic switch that is made up of an Insulated Gate Bipolar Transistor.

When a small change in the duty cycle leads to an increase in the output Power of the PV module, the perturbation is maintained in that positive direction until power output remains constant, in which case the current duty cycle is maintained but tested periodically. However, if the output power decreases then a negative change in the duty cycle is implemented. The algorithm tracks the maximum power point in that way.

$$V_{OUT} = V_{IN} \times \left(1 + \frac{t_{on}}{t_{off}}\right) \quad (8)$$

$$V_{OUT} = V_{IN}/(1-D) \quad (9)$$

The boost converter model used in this project is one from Simulink/Simscape Electrical as shown in figure 3.8. The “D” input into the converter is coming from the Perturb and Observe algorithm and it controls the duty cycle of the converter during implementation of MPPT.

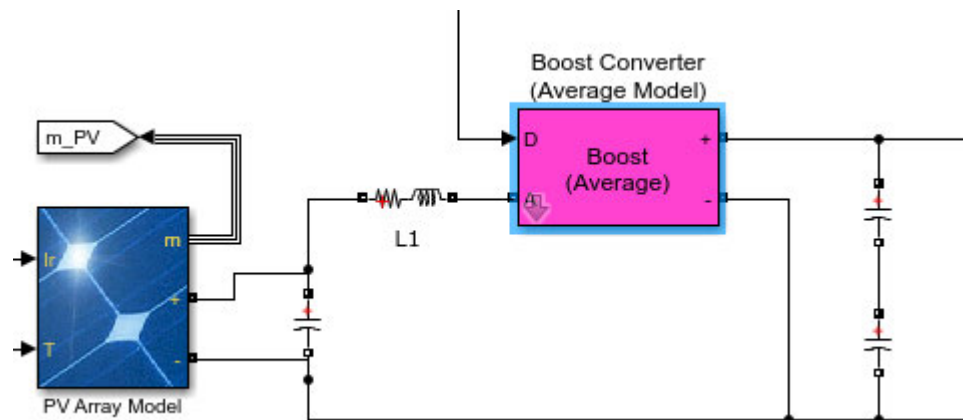


**Figure 3.8:** PV Array model with Boost Converter

### Parameters for Perturb and Observe Algorithm:

(D = Boost converter duty cycle)

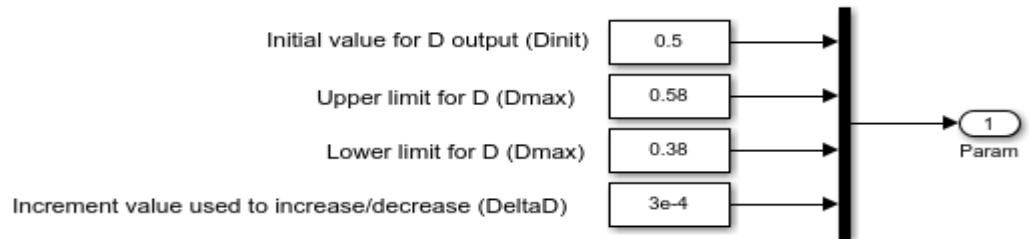


Figure 3.9: Parameters used for Perturb and Observe algorithm.

### 3.2.4 Inverter Model

The inverter plays an important role in this project as it is the interface between the DC supply from the solar modules and the AC grid. The DC input is converted to an AC supply using electronic switching devices. The electronic devices, in this case Insulated Gate Bipolar Transistors, are used as switches. The devices are fired at different times or angles to produce three symmetrical phases that are displaced by 120 degrees. A simple model of the inverter is shown below where Insulated Gate Bipolar Transistors (IGBTs) are used for switching.

The IGBTs switches are fired such that a three phase AC output comes out of the inverter with sinusoidal waveforms displaced by 120 degrees. Three phase inverters use 120°, 150° and 180° conduction. In a 180° conduction, three switches conduct at the same time and they conduct for half a cycle.

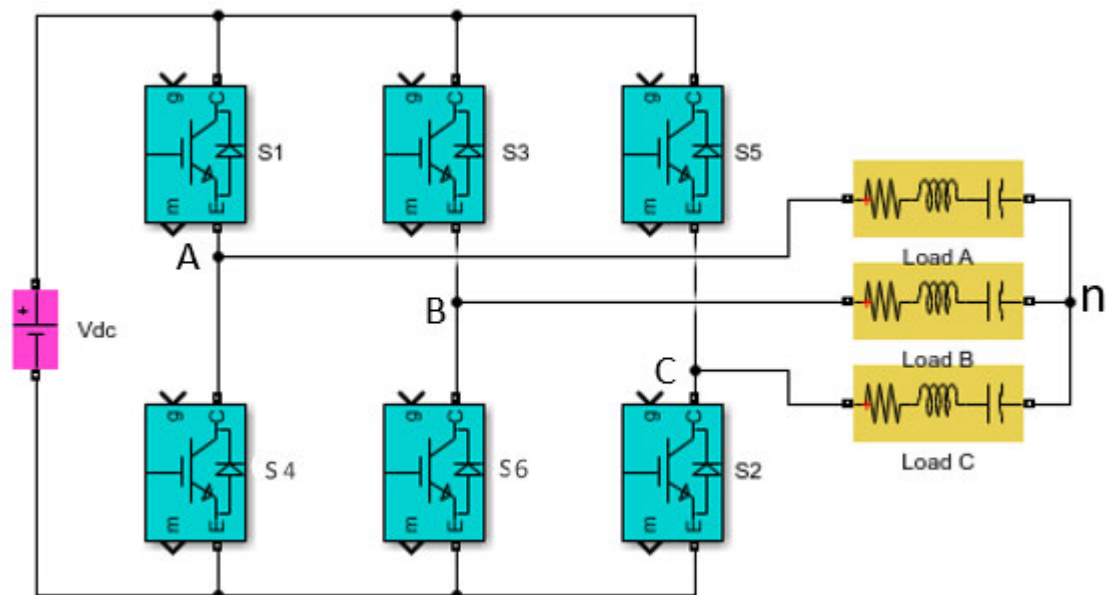
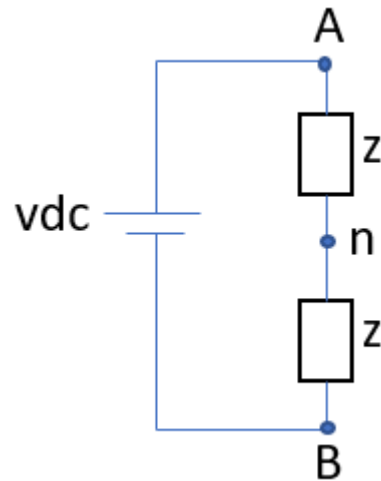


Figure 3.10: Inverter circuit diagram

In the 120° conduction, only two switches conduct at any given time. Each switch conducts for 120°. From 0° to 60°, S1 and S6 conduct. If the phase loads are represented by impedance Z, the equivalent circuit is as shown below:



**Figure 3.11:** 120° conduction 0° to 60°

Using the voltage divider principle, the voltage across phase 'A' load is given by:

$$\begin{aligned} V_{An} &= V_{dc} * \frac{Z}{2Z} \\ &= \frac{V_{dc}}{2} \end{aligned}$$

$$V_{nB} = \frac{V_{dc}}{2} \quad (10)$$

$$V_{Bn} = -\frac{V_{dc}}{2} \quad (11)$$

$$V_{Cn} = 0 \quad (12)$$

Similarly, from 60° to 120° S1 and S2 conduct resulting in the following equations:

$$V_{An} = \frac{V_{dc}}{2} \quad (13)$$

$$V_{Cn} = -\frac{V_{dc}}{2} \quad (14)$$

$$V_{Bn} = 0 \quad (15)$$

During the conduction cycle from 120° to 180°, Switches S2 and S3 conduct leading to the below equations:

$$V_{Bn} = \frac{V_{dc}}{2} \quad (16)$$

$$V_{Cn} = -\frac{V_{dc}}{2} \quad (17)$$

$$V_{An} = 0 \quad (18)$$

The process continues to the next half cycle until it re-starts again at 0°. The waveforms for both half cycles are used to evaluate the root-mean-square value (r.m.s) of phase voltage as given below:

$$V_{p_{rms}} = \sqrt{\left(\frac{1}{\pi} * \frac{V_{dc}^2}{4} * \frac{2\pi}{3}\right)} \quad (19)$$

$$V_{L_{rms}} = \frac{V_{dc}}{\sqrt{2}} = \sqrt{3}V_{p_{rms}} \quad (20)$$

At any given instant of conduction, there are two impedances in series and if these are represented by resistors, the RMS current is then given by:

$$I_{rms} = \frac{V_{dc}}{2R} * \sqrt{\frac{120}{360}} = \frac{V_{dc}}{2R} * \frac{1}{\sqrt{3}} \quad (21)$$

Normally, the 120° conduction is preferred to the 180° one because the latter has both odd and triplen harmonics while the former only has odd harmonics. Triplen harmonics are multiples of the 3<sup>rd</sup> harmonic and are zero sequence harmonics hence are additive. This makes them the most harmful to electrical system components and machines hence they are not desirable in the system.

The inverter model used in this project ensures that the output is a clean sinusoidal waveform by using a voltage regulator, a current regulator and a Phase Locked Loop (PLL) as shown in figure 31. Voltages and currents are measured at the point of common coupling and compared with reference parameters. This closed loop control strategy helps in supporting the grid during both minor and major disturbances. Simulation results are expected to confirm or disapprove the effective functionality of the control strategy.

### VSC Main Controller

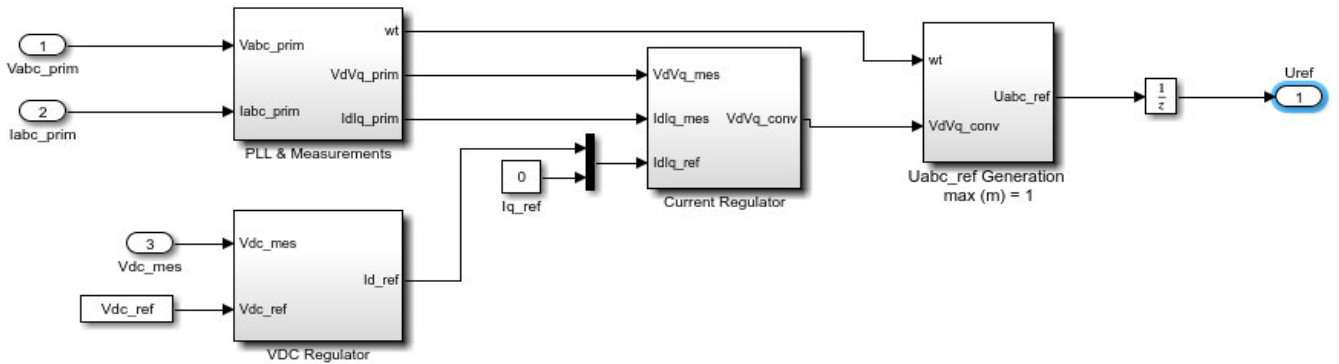


**Figure 3.12:** Inverter control blocks

The voltage regulator block compares the reference DC voltage and the measured value. The error is fed into the current regulator block for comparison with a reference component of current. The measurement block implements a Phase Lock Loop that extracts frequency and phase angle from input three phase voltages and currents. The output of the Voltage Source Controller is the control input to the Universal bridge that is used as an inverter. The complete Solar Generation model including a series RL circuit, a reactor, a step-up transformer and point of common coupling are shown in figure 32 below.

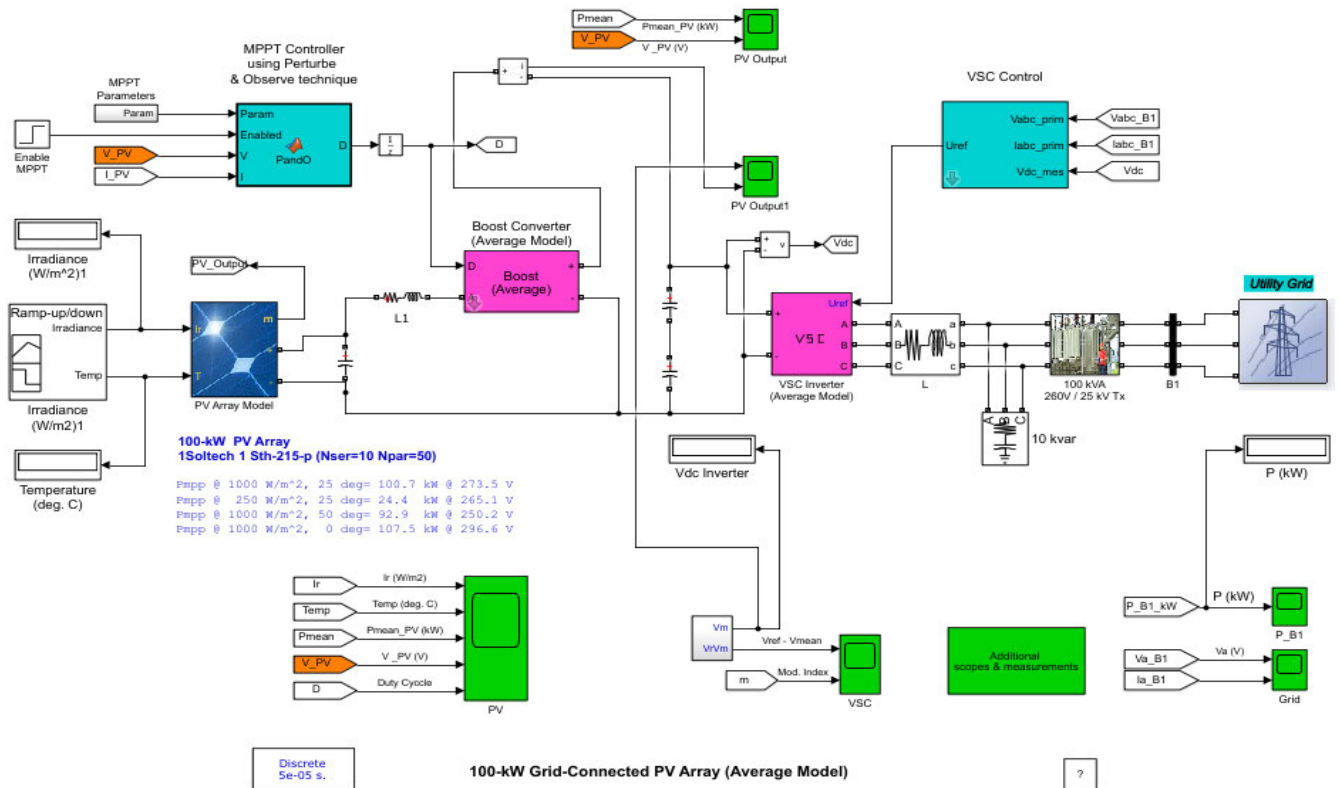


**Figure 3.13:** Grid connected PV array

### 3.2.5 Synchronous Machine Model

The synchronous machine model used in this project comprises of the synchronous machine, the governor control and excitation system control (Automatic Voltage Regulator). The model has these controls to ensure that the machine supports the grid during minor and major disturbances in the system. The excitation system controls the reactive power generated by varying the excitation current. The terminal voltage of the generator is compared with a reference voltage and the difference is fed into the excitation closed loop feedback system.

The governor control regulates the grid frequency by controlling active power generated. The adjustment is achieved by controlling the valve that controls the steam to the turbine. When the generator load increases, the speed of the generator rotor decreases, and this affects frequency since frequency and speed are related by the equation:

$$f = \frac{pN}{120}$$
 where  $f$  is frequency in Hz,  $p$  is pole pairs and  $N$  is the speed of the rotor in revolutions per minute. When speed goes up due to light loading, frequency also goes up. These variations must be regulated. The model must accommodate this automatic control system.

A simplified synchronous machine model is shown in Figure 32 below. The model diagram illustrates how frequency error between reference frequency and measured frequency is used to control the steam valve. More steam through the valve means more mechanical energy into the generator. The rotor speed increases but is kept constant by infinite busbar. This results in more active power output from the generator. On the other hand, a voltage error between the measured terminal voltage of the generator and a reference voltage is fed into the excitation controller to either increase or decrease the excitation voltage depending on the polarity of the error.

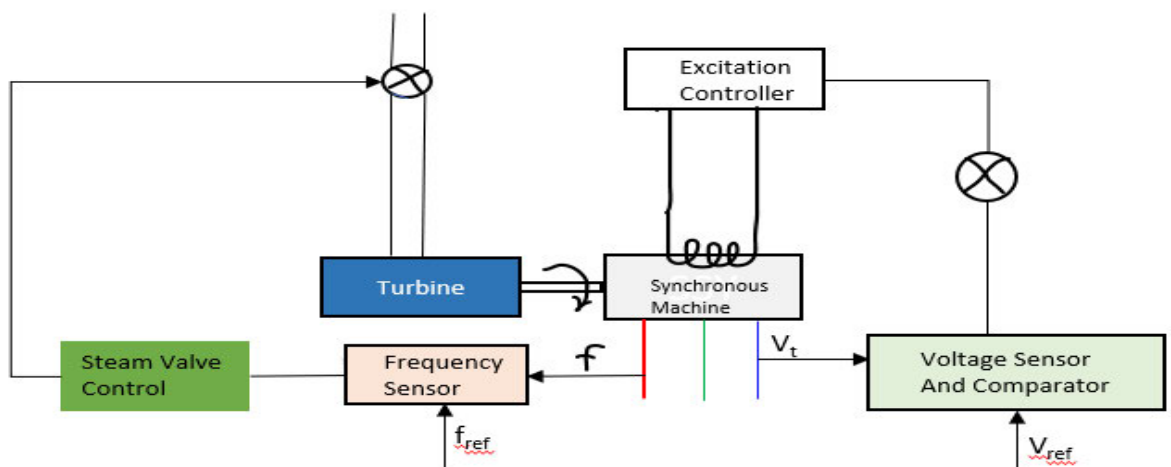
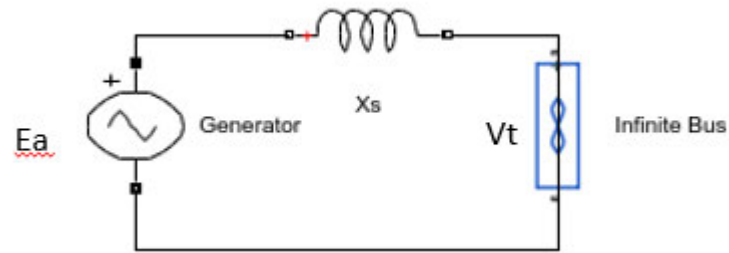


**Figure 3.14:** Automatic voltage and frequency control for a synchronous generator.

Synchronous generator equations can be derived using the circuit diagram as shown below:



### 3.2.5.1 Excitation control

At the point of synchronisation, the generator is not delivering active power. Therefore, the terminal voltage at the infinite bus is equal to the generated voltage since there is no voltage drop across the reactance for zero current ( $I_a$ ) from the generator.

The phasor diagram is as follows:



$E_a$  and  $V_t$  are equal and in phase. The generator is said to be floating,  $E_x$  and  $I_a$  are equal to zero.

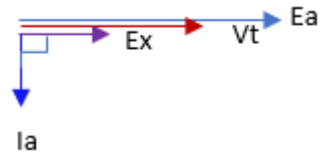
$$|I_a| = \frac{E_a - V_t}{|X_s|} = \frac{E_x}{X_s}$$

$$E_x = E_a - V_t$$

$$P_{gen} = \frac{E_a * V_t \sin \delta}{X_s} \text{ where } \delta \text{ is the rotor angle.}$$

$$E_a = k\Phi\omega$$

When the field current is increased beyond its value at synchronization, the generator is over-excited. An increase in field current implies an increase in flux  $\Phi$  which in turn means an increase in  $E_a$ . However,  $V_t$  is fixed by the infinite busbar and cannot increase. In this case  $E_a$  is greater than  $V_t$  and  $E_x$ , the voltage across the generator reactance, is positive. Current  $I_a$ , lags voltage  $E_a$ . The generator sees the infinity bus as an inductive load therefore, the generator supplies reactive energy to the infinity busbar. The phasor diagram is as shown below:



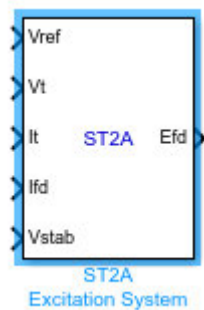
In this case  $E_a > V_t$  and  $I_a$  lags  $E_a$  by  $90^\circ$

On the other hand, when the generator is under excited,  $E_a$  is less than  $V_t$ . The voltage across the generator inductance becomes negative and  $I_a$  leads the generated voltage. In this case the generator behaves like an inductive load. The generator field has weakened hence the infinite busbar supplies reactive power to the generator to compensate for lost magnetic field. The phasor diagram is as shown below:



In this case  $E_a < V_t$ ,  $I_a$  leads  $E_a$  by  $90^\circ$  and  $E_x$  is negative since  $E_x = E_a - V_t$ . The above equations confirm that variation of excitation leads to variation in the amount of reactive power delivered by the generator. If the voltage at the infinite bus were to change, then the generator excitation must either increase or decrease depending on whether the bus voltage drops or rises. In that way, excitation control regulates the voltage.

The excitation system for this project is controlled by an Excitation System Block (ST2A) from Simscape library.



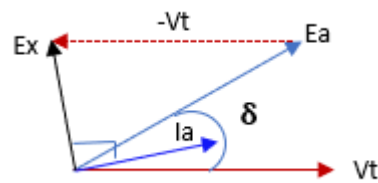
The output of the block is a field voltage to be applied to the input of the synchronous generator block.

### 3.2.5.2 Governor Control

The generator starts to deliver active power to the infinite busbar only after more mechanical torque is applied to the rotor beyond that which is required for synchronisation speed. As the mechanical torque is increased, by letting in more steam to the turbine, the rotor axis changes position from zero until it steadies at an angle  $\delta$ . During this transient state, active power generated increases with an increase in the rotor angle as given in the equation:

$$P_{\text{gen}} = \frac{E_a * V_t \sin \delta}{X_s}$$

The rotor locks at the steady state angle and can no longer accelerate further since the speed of the generator is fixed by the infinite busbar. Energy can neither be created nor destroyed, therefore, the extra mechanical energy derived from increasing mechanical torque is supplied to the infinite bus as electrical energy. If the rotor accelerates, then frequency increases. The applied torque must match the induced torque for the machine to remain in synchronism. A phasor diagram below illustrates the voltage, current and rotor angle relationships.



The governor control is implemented using a Steam Turbine and Governor block from Simulink/Simscape library. The block components are shown in figure 33 below:

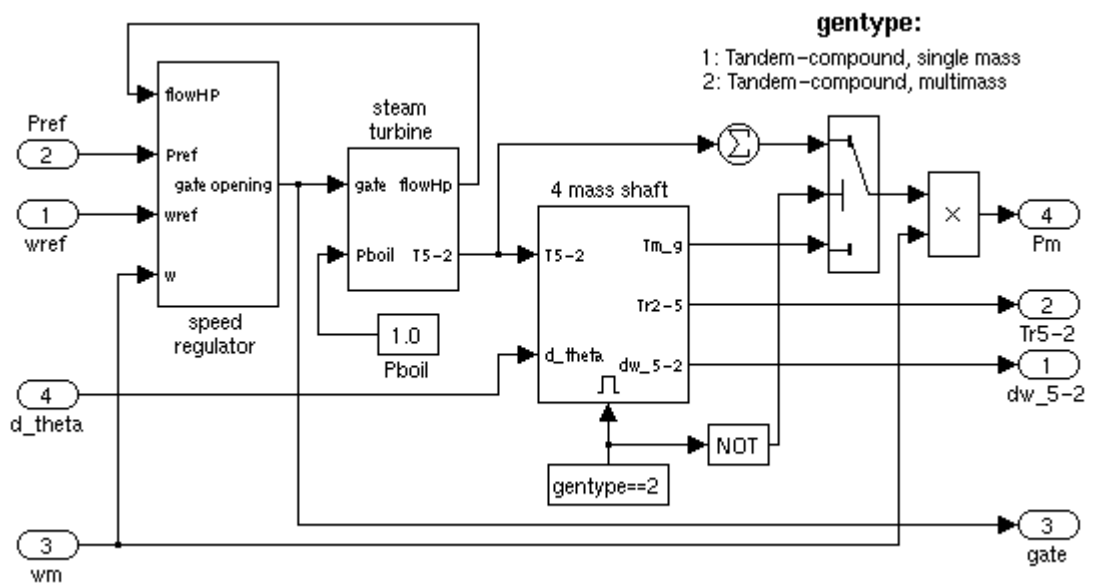
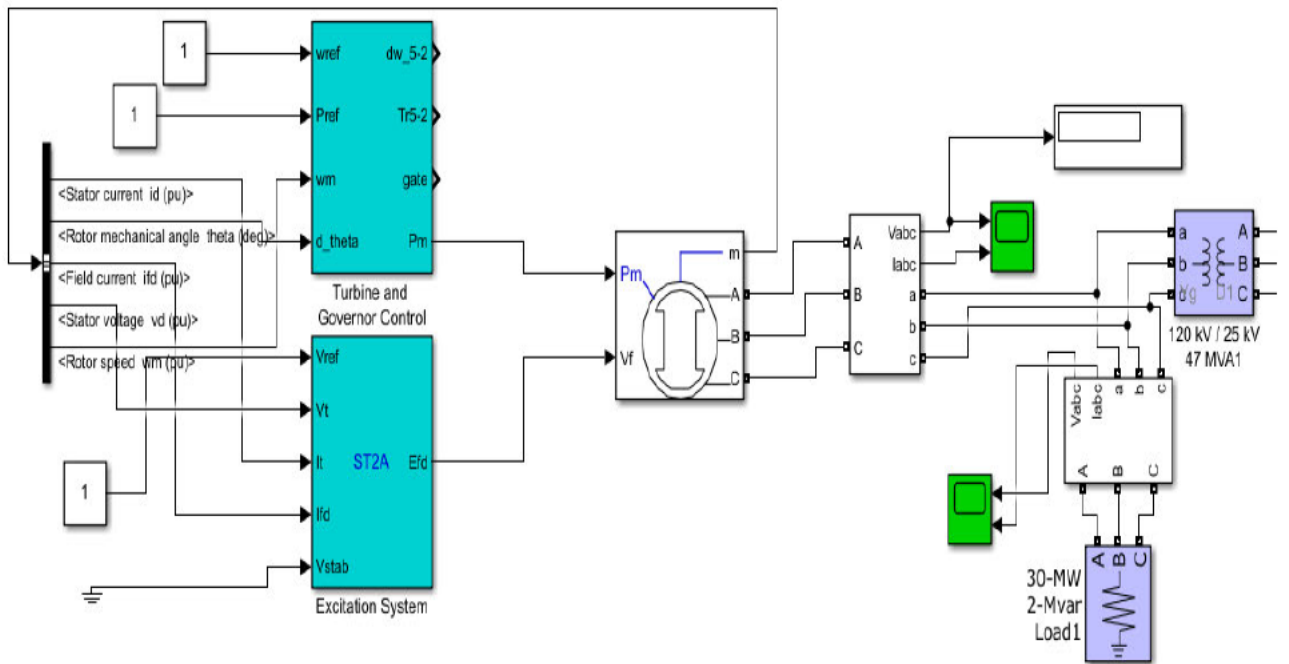


Figure 3.15: Governor Control System



**Figure 3.16 Synchronous Generator Model**

The figure above shows a single synchronous generator with excitation and governor control. The model is connected to a micro grid that contains solar system

### 3.2.6 Transmission Lines

The transmission lines are modelled as balanced three phase lines with their parameters lumped in a  $\pi$ -network configuration. The model used is taken from the Simulink library together with parameter values.

**Table 3.2: Transmission Line Parameters**

Transmission Line Parameters/km		
Parameter	Positive Sequence	Zero Sequence
Resistance ( $\Omega$ /km)	0.0153	0.413
Inductance (H/km)	1.05E-03	3.32E-03
Capacitance (F/km)	1.13E-08	5.01E-09

The model is shown in figure 3.17 below:

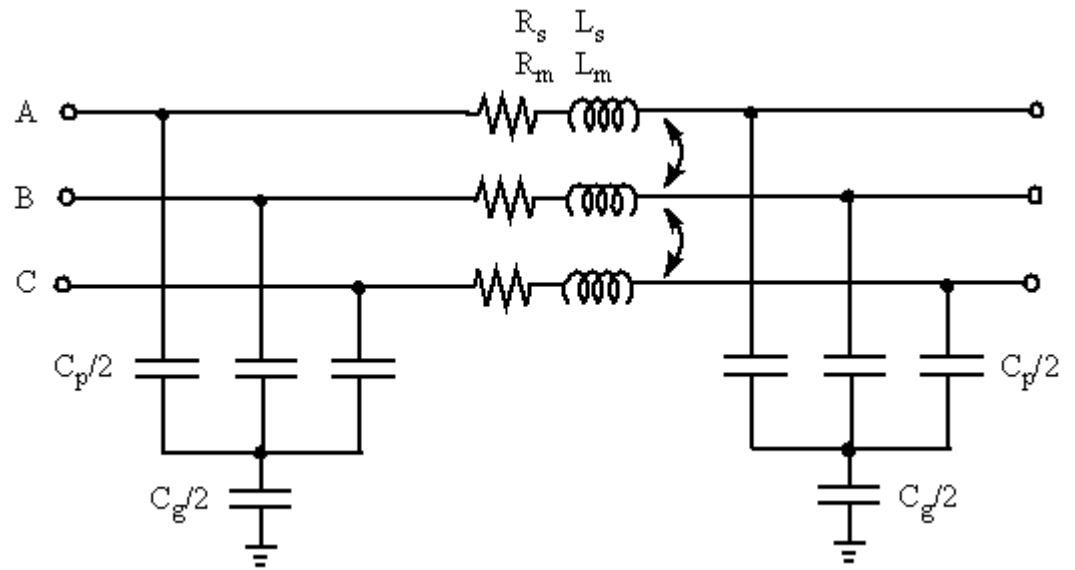


**Figure 3.17:** Model of a transmission line

The model implements a long line that is more than 50km in length. In shorter lines, capacitance is usually ignored.

### 3.2.7 Implementation of different Network Conditions for Simulation

Various network conditions and scenarios are created on the network to assist in investigating the impact of large-scale PV penetration. The conditions created include steady state running of the network, varying the PV penetration, introducing faults on the network and disconnecting a major synchronous generator or load. All these induced conditions are meant to test the stability of the network under different practical conditions.

#### 3.2.7.1 Implementation of Increasing PV Penetration

An investigation of the impact of large-scale PV penetration on the network starts with a PV penetration of as little as 100kW maximum. Irradiance of the PV array is varied between 250 W/m<sup>2</sup> and 1000 using an input vector to the array. This variation is maintained for the rest of the investigation. PV penetration is slowly increased by adding parallel strings and arrays to the model.

The increase in PV penetration must be matched by an equivalent reduction in active power generated by synchronous generators in order to maintain a supply and demand balance on the network. These steps are repeated until the PV array supplies between 90% and 100% of the connected load.

The model is simulated, and measurements of network parameters taken for every new step for both steady state and transient conditions. The main

parameter readings recorded are those for frequency, voltage, currents and reactive power. Parameter magnitudes, rate of change and phase angles will be recorded and kept for analysis. The analysed data will be benchmarked with the standards and regulation requirements. Network parameter measurements are taken at the point of common coupling and at the synchronous generator terminals.

### **3.2.7.2 Introducing Disturbances to the Network**

The modelled network is subjected to various disturbances that include the loss of one of the synchronous generators or energy sources. This test allows for an investigation of system voltage recovery times when there is a supply and demand mismatch. Ideally, the network should quickly recover from the disturbance within expected time frames as stipulated in the grid codes. Frequency range and duration of disturbance must conform to Clause 8.8.3(a)(1) of the rules and section 38 of the National Electricity Market (NEM).

Disturbances will include a disconnection of one of the loads. Under normal autonomous network operation, the synchronous generators must self-adjust their output power in response to load reduction. Parameter measurements are recorded for analysis later. The disturbances are implemented using circuit breakers that open and close at times that are pre-set in the model.

### **3.2.7.3 Introducing Faults**

Transient electrical faults are introduced into the network using circuit breakers with relevant faults simulated on the load side of the circuit breaker. The following faults are simulated:

- (1) Three phase symmetrical fault
- (2) Phase to earth faults
- (3) Phase to phase faults

The above faults are introduced at different parts of the transmission system to test the weaknesses and strength of the network. The network model is simulated at for each fault conditions and network parameter values are recorded for analysis.

### **3.3 Limitations**

Some of the resources that were meant to be used in implementing the methodology could not be sourced for the project. The limitations are outlined in the next sections below.

#### **3.3.1 Modelling Software**

The original plan was to source the model and simulation software from the organisation that the researcher works for. Due to limited licences within the organisation, the researcher could not be accorded extra financial resources to obtain the licence as the organisation felt the researcher's current job activities did not involve use of the relevant software package (PowerFactory).

The university of Southern Queensland have an alternative software package but unfortunately the software package is not yet available online for students. The researcher used Simscape/Simulink in MATLAB. Unfortunately, the student licence has limitations on the number of blocks that can be contained in a single simulation model. Due to these limitations, a complete network model could not be simulated as a complete assembly but had to be split into two halves.

One half comprises of the solar panels with irradiance and temperature control, DC-DC Converter with MPPT control using Perturb and Observe algorithm, Inverter with active and reactive power control, parallel load, power transformer, Point of Common Coupling, utility grid comprising of two sections of a 25kV transmission line, two load totalling 32MW a power transformer and a three phase source. The other half comprises of the utility grid and synchronous generator equipped with excitation system control and turbine and governor control. The two systems are simulated separately, and their outcomes are compared to establish how the network behaves under different PV penetration levels. The second half of the model has zero PV penetration. The third stage of the model was simulated at University of Southern Queensland(USQ) during Residential school under limited timeframes. There were compatibility issues between blocks created with latest version of MATLAB and an older version on the USQ laptop.

#### **3.3.2 Data Collection**

Data from specific solar farms and respective energy meters and transmission line parameters could not be used in this research as such data is protected by relevant data agents under the overall control of AEMO. The Power of Choice has brought up ring fencing rules on data transfer between regulated and unregulated distribution and transmission utility companies making it difficult to obtain solar farm data.

# Chapter 4

## 4 Simulation and Results Analysis

### 4.1 Introduction

This section of the project covers the simulation stage. Three stages of models were created in Simulink to test conditions that are expected in practical network situations. The first stage model comprises of a single synchronous generator with generator transformer to step up generator voltage to transmission voltage of 120kV, governor control and excitation control, two transmission lines and two loads. The second stage model consists of PV and associated inverter system supplying the same load as in first stage model. The third stage model is a combination of PV system and synchronous generator system. The individual stages are subjected to network disturbances as outlined in Chapter 3. Frequency and voltage behaviour are analysed before, during and after the disturbances.

### 4.2 Single Synchronous Generator Network (no PV)

A Simscape/Simulink block diagram is as shown in the figure 4.1 below.

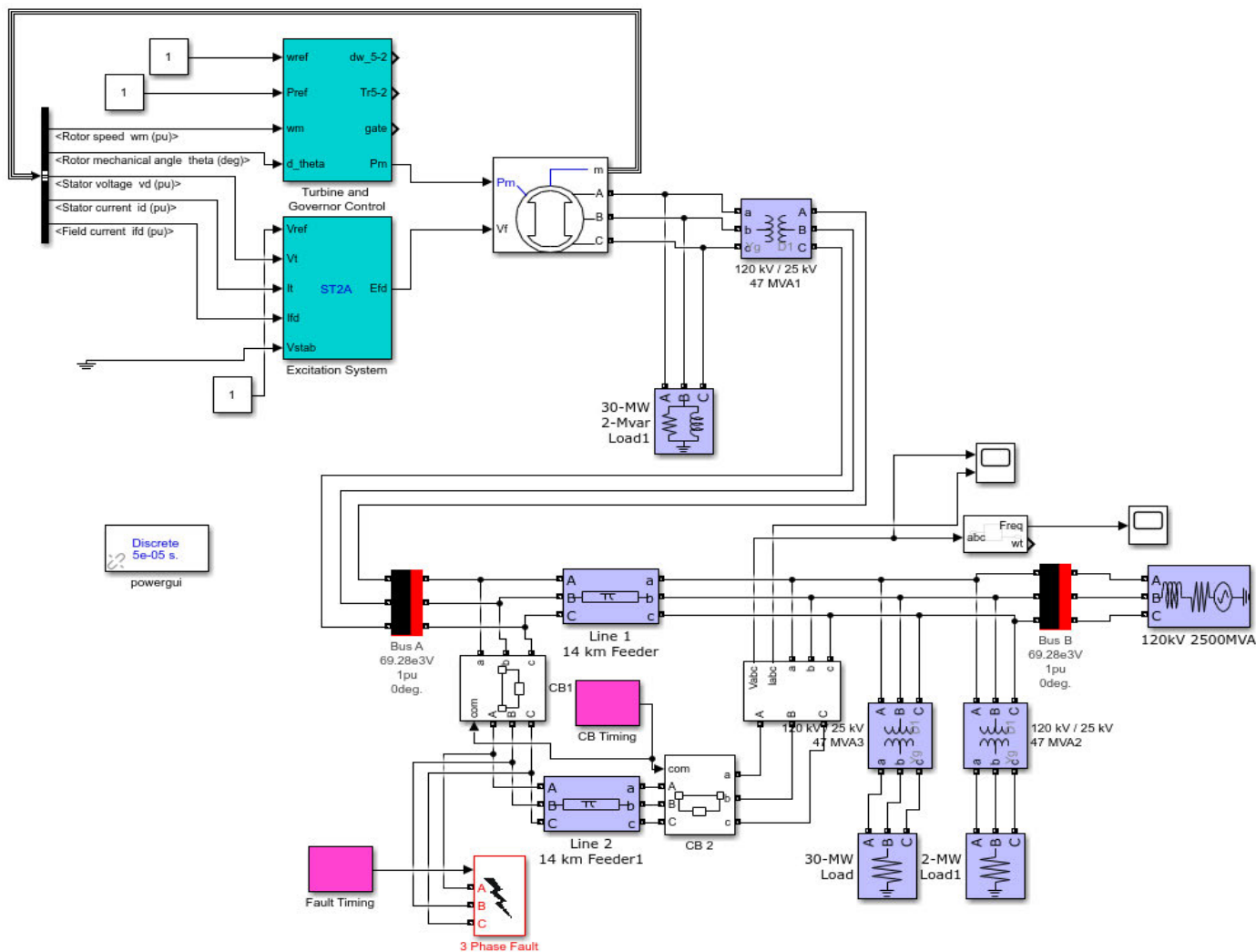


Figure 4.1: Single Synchronous Generator Combined Network

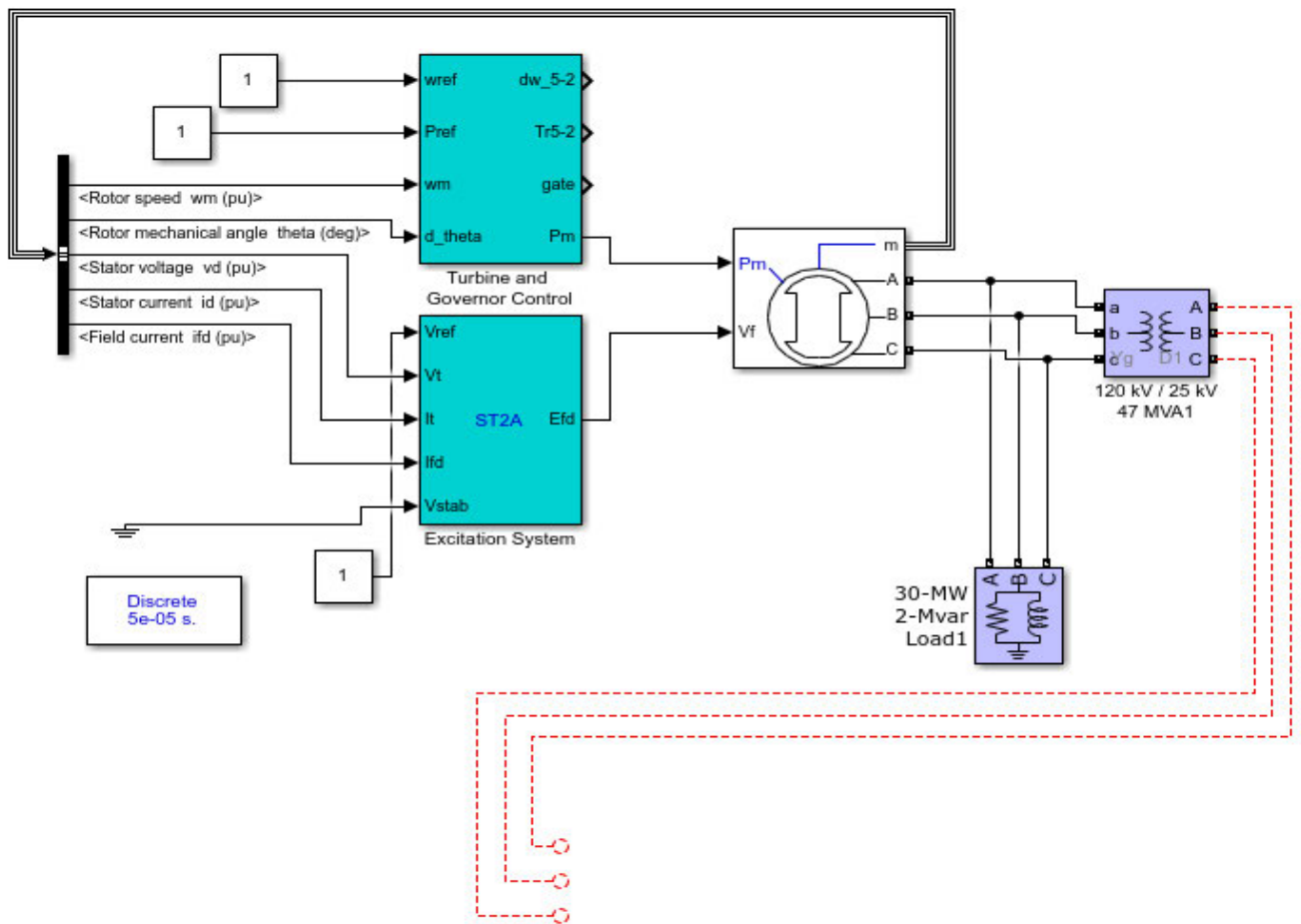


Figure 4.2: Generator Portion of Model

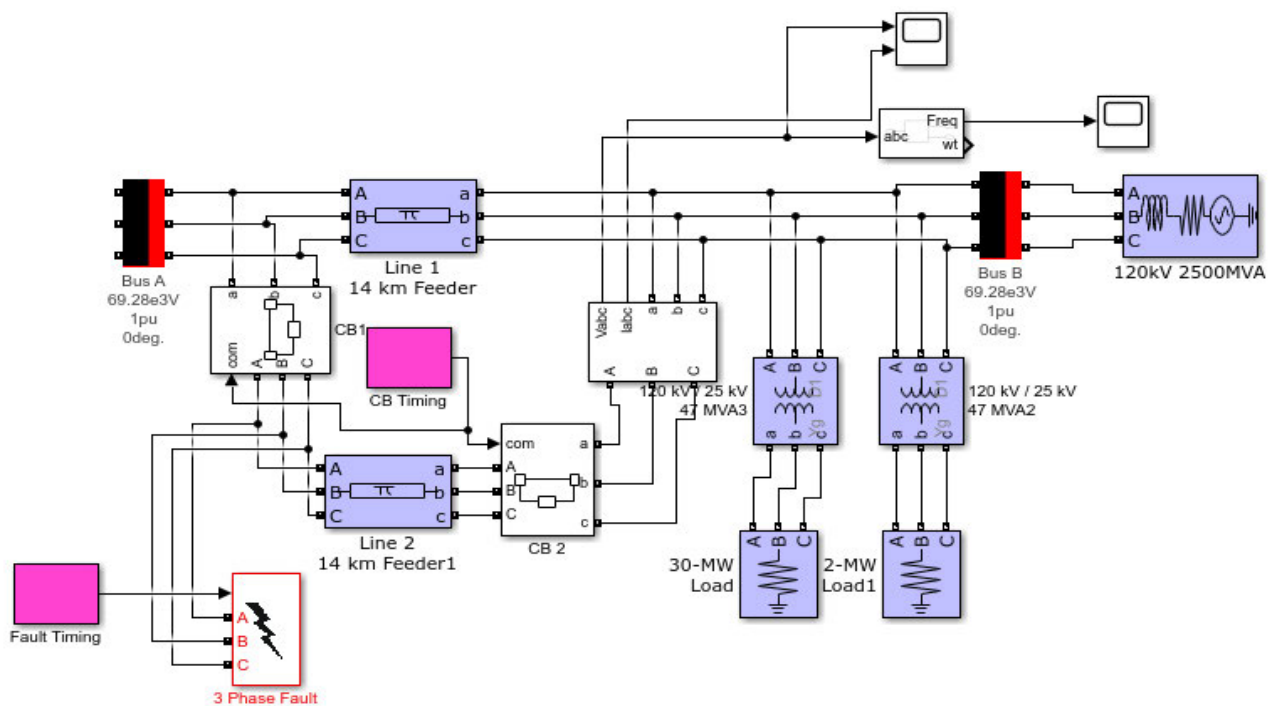


Figure 4.3 Transmission line system and Load

#### 4.2.1 Steady state conditions

The grid section is tested at steady state conditions with no disturbances. Frequency voltage and current readings are taken as shown below.

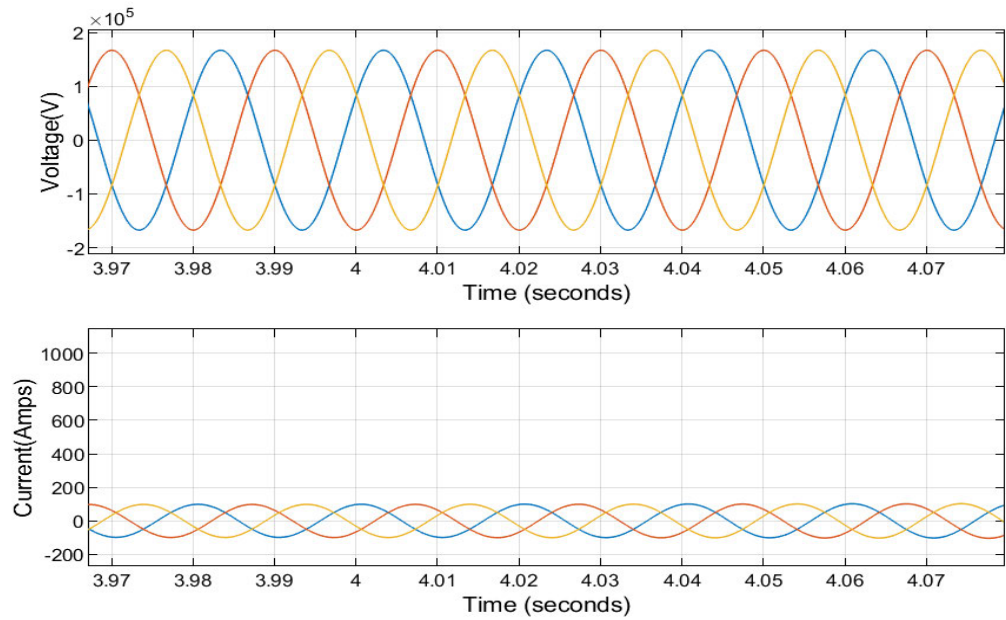


Figure 4.4: Steady state Voltage and Amps

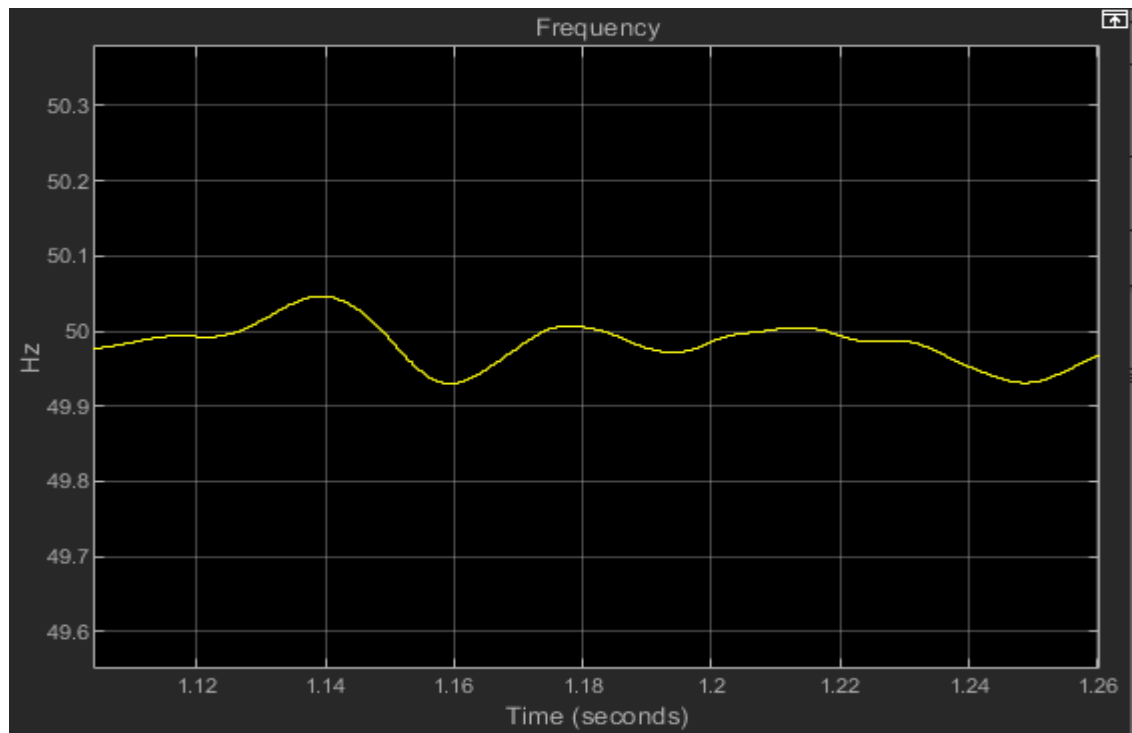


Figure 4.5: Frequency under steady state

#### 4.2.1.2 Results and Analysis

Figure 4.4 and 4.5 above show waveforms for voltage, current and frequency. The voltage and current waveforms are pure sinewaves as expected under state steady conditions. The system frequency ranges between 50.06 Hz and 49.98 Hz. These variations are within the operating variation range of  $\pm 0.15\text{Hz}$  as required by AEMO. Therefore, the model operates within rules and can be used to simulate network conditions. The system parameter measurements are taken from the 120kV transmission line number 2 as shown in the Simulink block diagram in figures 4.1 and 4.3

#### 4.2.2 Three Phase symmetrical Fault Simulation

A three-phase symmetrical fault was applied to transmission line number 2 using the “3 Phase fault” block from Simulink marked in red in figure 4.3. The fault was applied at the 3 seconds time slot. Circuit breakers CB1 and CB2 simultaneously opened to isolate the fault at the 3.1 seconds mark. The 100ms was added to allow for delays in protection relay response and circuit breaker delays. Voltage, Current and frequency measurements were taken on the 120kV transmission system, before, during and after the fault. The measurements obtained are as shown in the waveforms below.

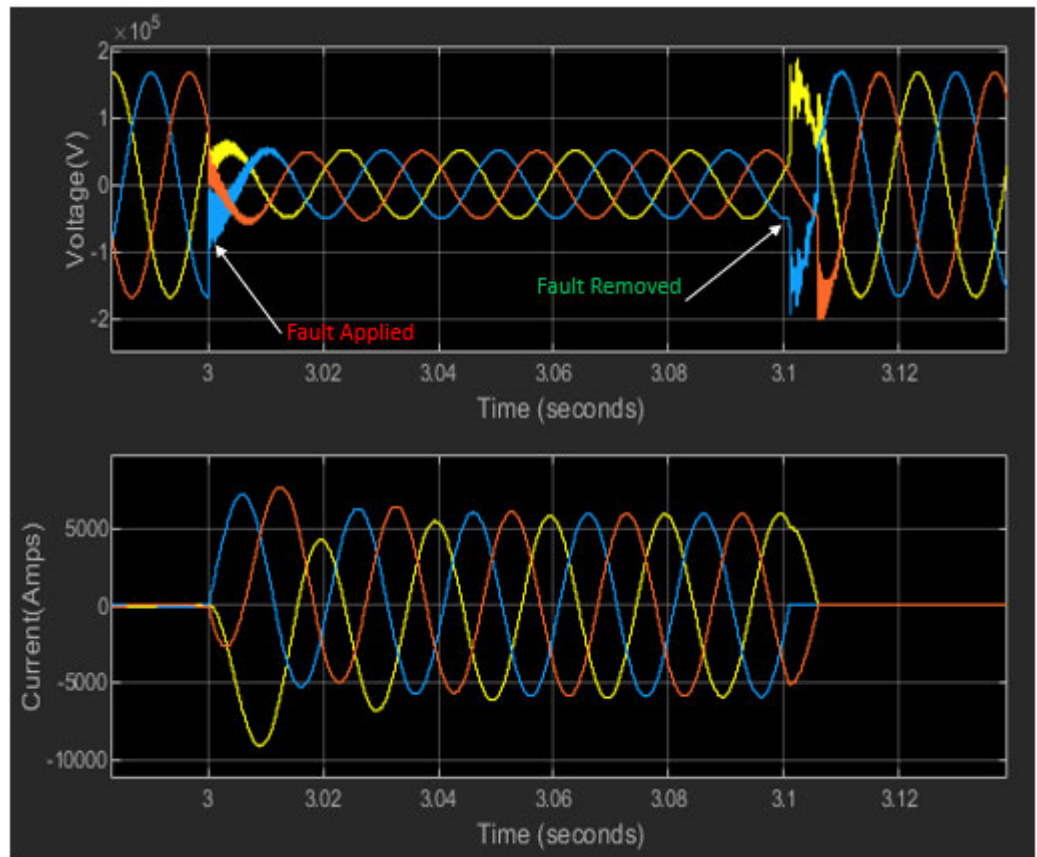
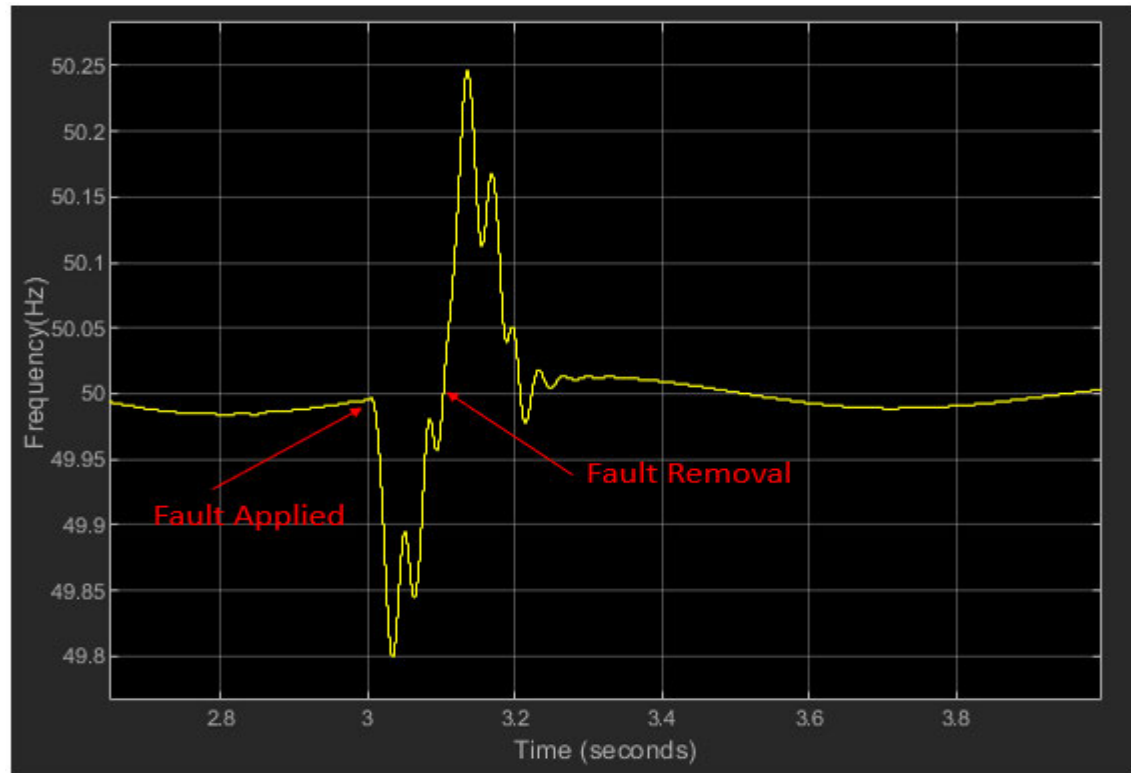


Figure 4.6: Voltage Response to 3 Phase Symmetrical Fault



**Figure 4.7:** Frequency response to a three-phase symmetrical fault

#### 4.2.2.1 Results and Analysis

System voltage dropped to 30% of nominal voltage ( $V_n$ ) at fault inception. The voltage recovered to 100% of  $V_n$  within a time period of about 5ms. The Australian grid codes allow system voltage to drop to 0%  $V_n$  and recover to 80%  $V_n$  in 450ms. The voltage variations and recovery time did not prompt contingency action as they were within the requirements of the National Electricity Rules.

The system current shot to about 9000 A at the introduction of the fault and stabilised at around 5500A. Current quickly went back to load values after fault clearance as expected. The system frequency dropped to 49.8Hz at the inception of fault. This was expected given that a sudden rise in generator stator currents led to an increased opposition to rotor motion due stronger magnetic fields from the stator windings. The opposing fields had a braking effect on the rotor, hence the decrease in frequency. However, the system had reasonable inertia and that helped in slowing down the rate of change of frequency. A reverse effect occurred when the fault current was removed at 3.1 seconds where a reduction in system current led to a momentary rise in frequency to 50.25 Hz before settling at around 50Hz after

According to Australian grid codes, any frequency deviation that satisfies the condition  $47.5 < f < 52$  allows for continuous operation. Frequencies greater than 52 Hz or lower than 47.5 Hz are tolerated for a maximum of 2 seconds beyond which the system trips on over or under frequency respectively. The fault was cleared in less than 120 seconds thus conforming to National Electricity Rules Schedule 5.

#### 4.2.3 Three Phases to Ground Fault Simulation

A three phase to ground fault was simulated by shorting all the three phases together and grounding them. Voltage, frequency and current measurements were performed, and results came out as shown below.

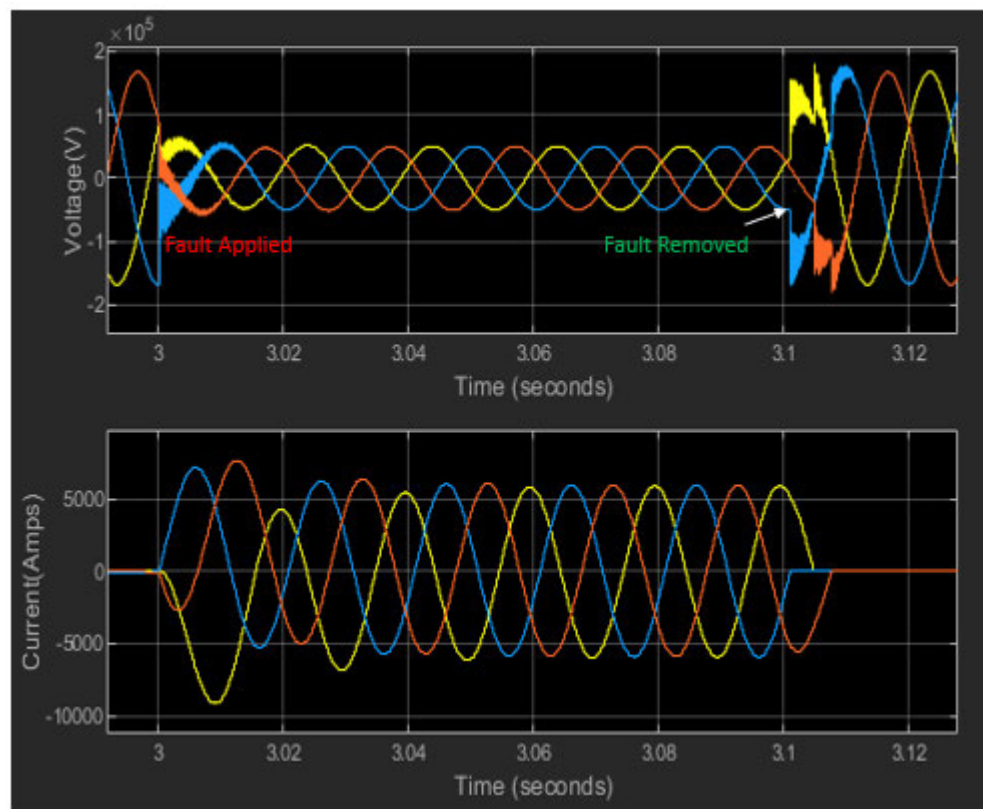


**Figure 4.8:** Volts and Amps after a three-phase to earth fault

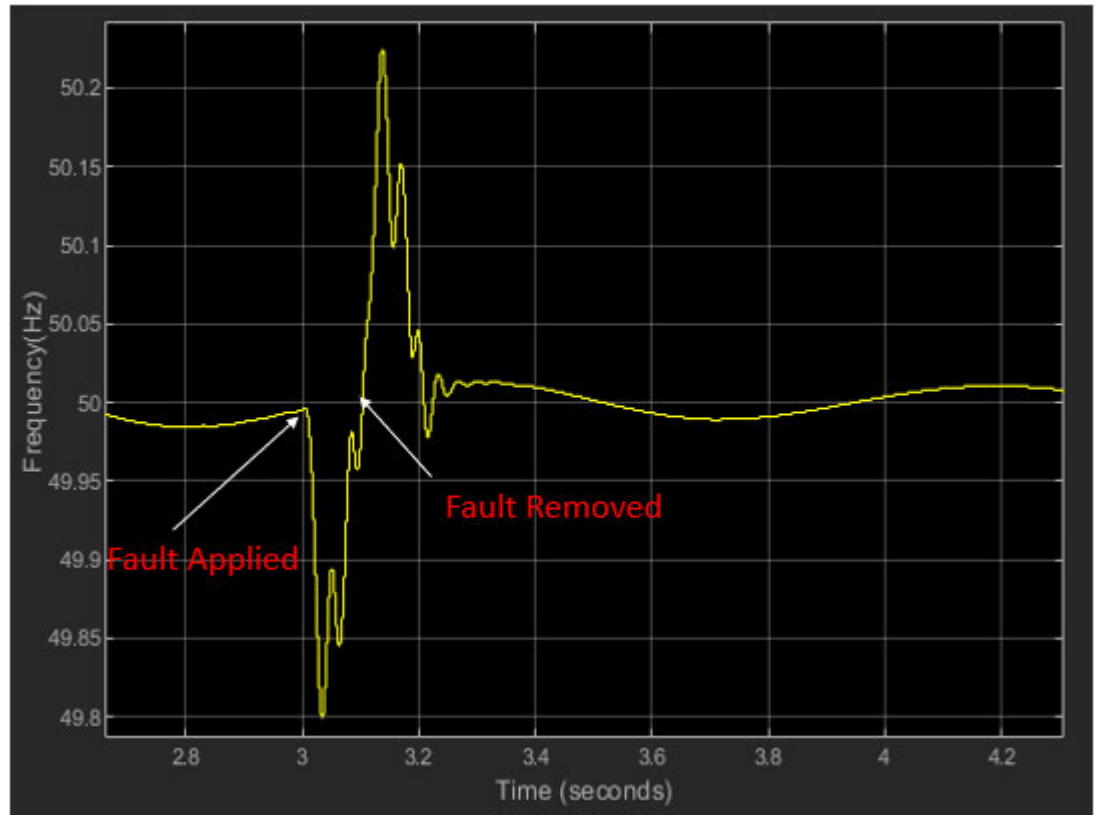


**Figure 4.9:** Frequency Response to a Three Phases to ground fault

#### 4.2.3.1 Results and Analysis

The results obtained from the three-phase to ground fault were like the ones obtained from the three-phase symmetrical fault as expected.

#### 4.2.4 Phase to Phase Fault Simulation

A phase to phase fault on transmission line number 2 was simulated by shorting together A and B phases in figure 4.3. The fault condition was applied at 3 seconds and circuit breakers opened on the 3.1 seconds mark to clear the fault. Network parameter measurements were taken as shown in figures 4.10 and 4.11.

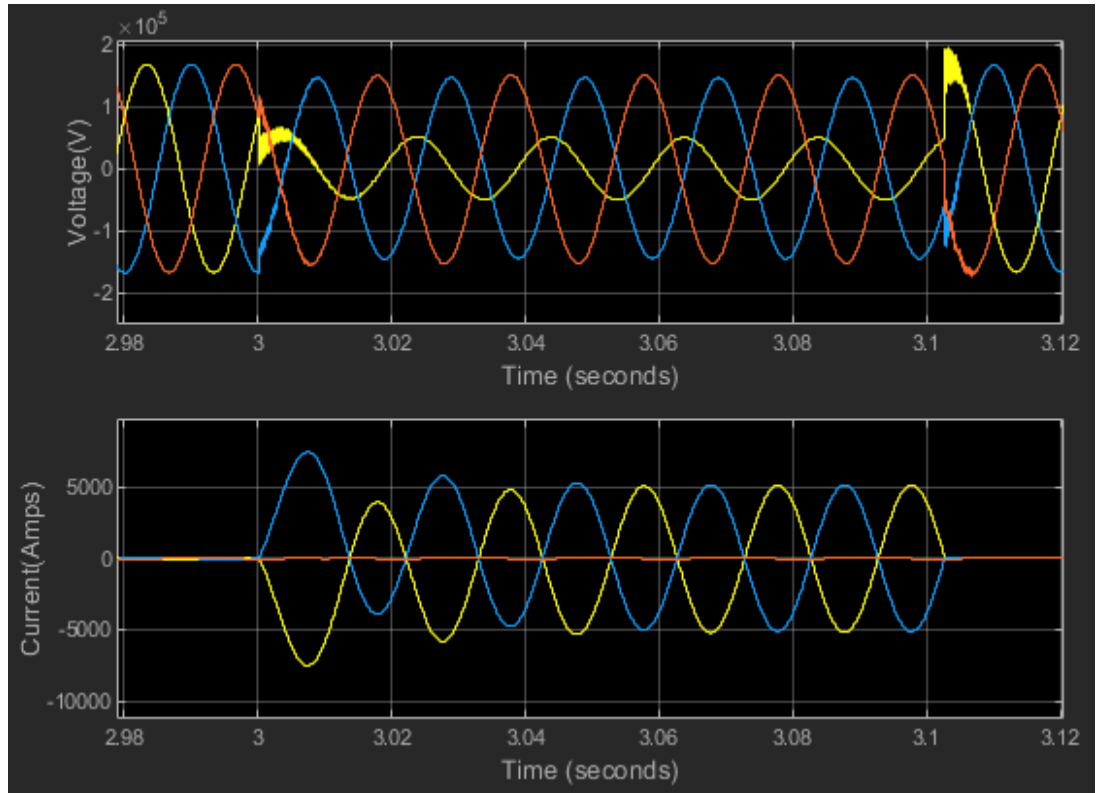


**Figure 4.10:** Voltage and current waveforms, before, during and after a phase to phase fault

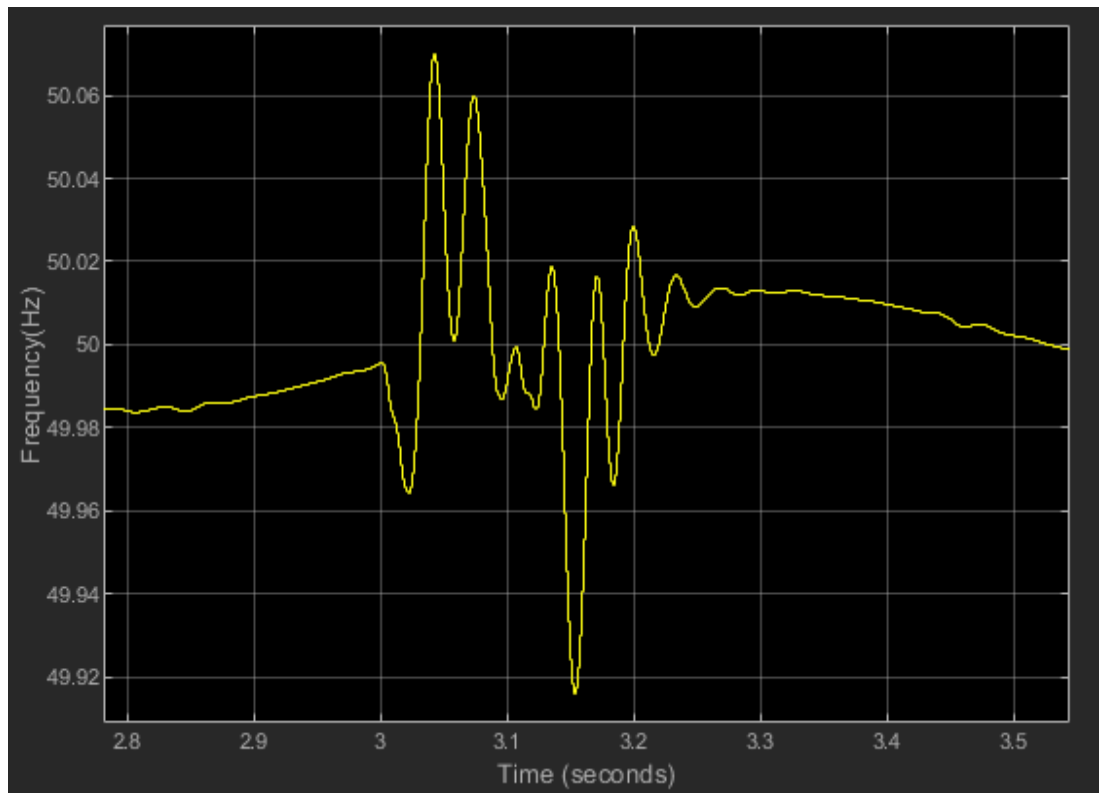


**Figure 4.11:** Frequency Response after Phase to Phase fault

#### 4.2.4.1 Results and Analysis

Phase A volts dropped to 30% of nominal voltage. Phases B and C voltages dropped to approximately 70% of nominal voltage. Phase A and B currents were equal in magnitude by antiphase (180°). Their magnitudes shot to 7000 Amps at introduction of fault, then to about 4000Amps before settling at 5000 Amps for the remainder of the fault period. Voltage recovered after 0.105 seconds.

Frequency variations followed the swings in fault current, dropping with a rise in current and rising with a reduction in fault current as expected. Frequency swung between 50.07 Hz and 49.918 Hz. Frequency recovered to stability in 0.2 seconds.

However, the voltage and frequency variations were within acceptable limits as required by NER, AEMO and the grid codes.

#### 4.2.5 Major Load Rejection

One of the system conditions that is known to upset network stability is the loss of a major load in the network. This could be a factory or a mining site contributing a significant load on the network. The effect is a reverse of losing a generator on the network. The loss of a major load was simulated by disconnecting the 30 MW load (shown in figure 4.12) from the network. A circuit breaker, CB 3 was inserted between the load and transformer 2. The circuit breaker was opened at the 3 seconds mark to remove the load and re-closed at the 6 seconds mark test the effects of connecting a big load into the system.

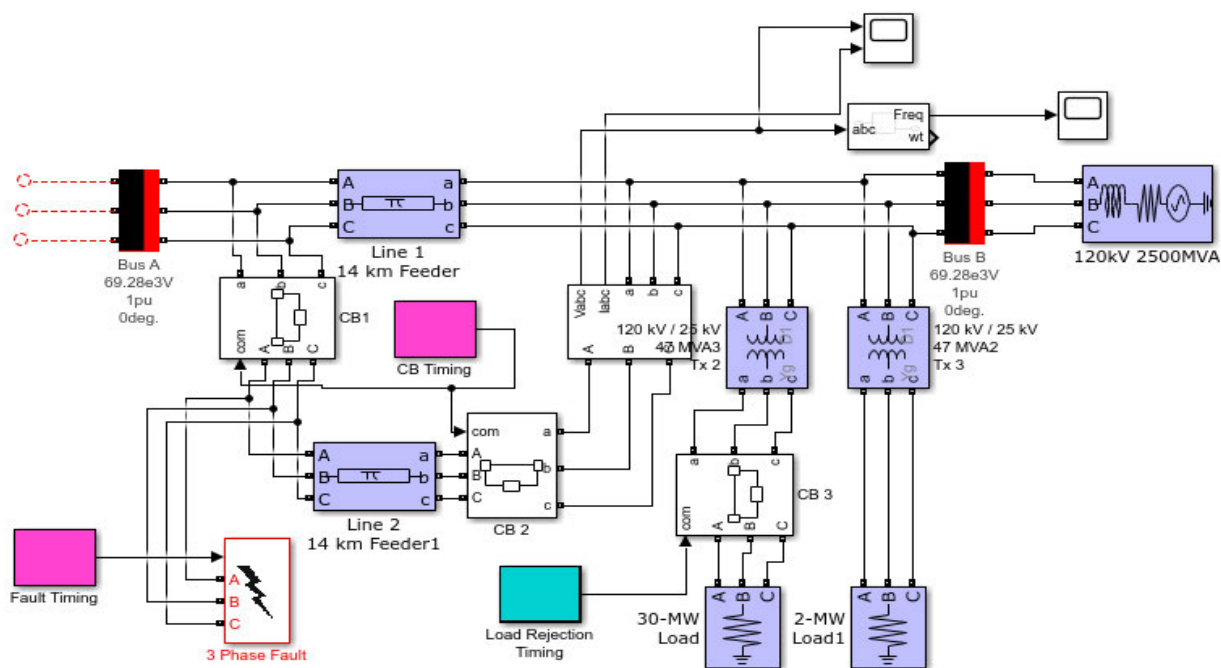
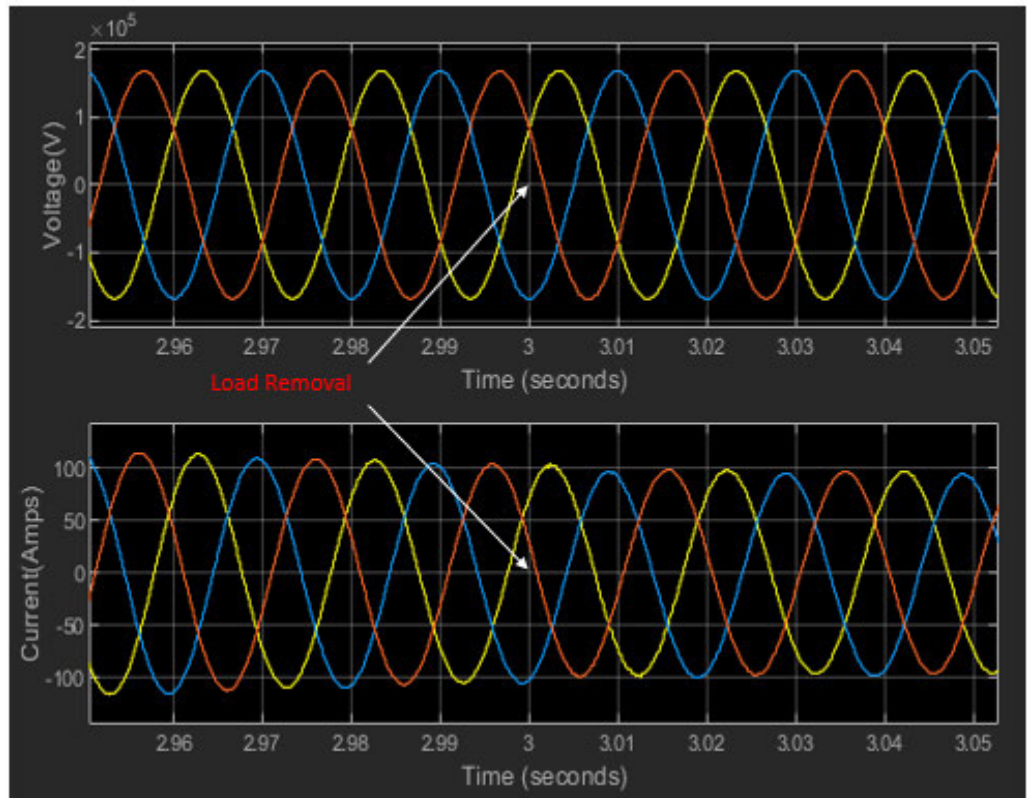
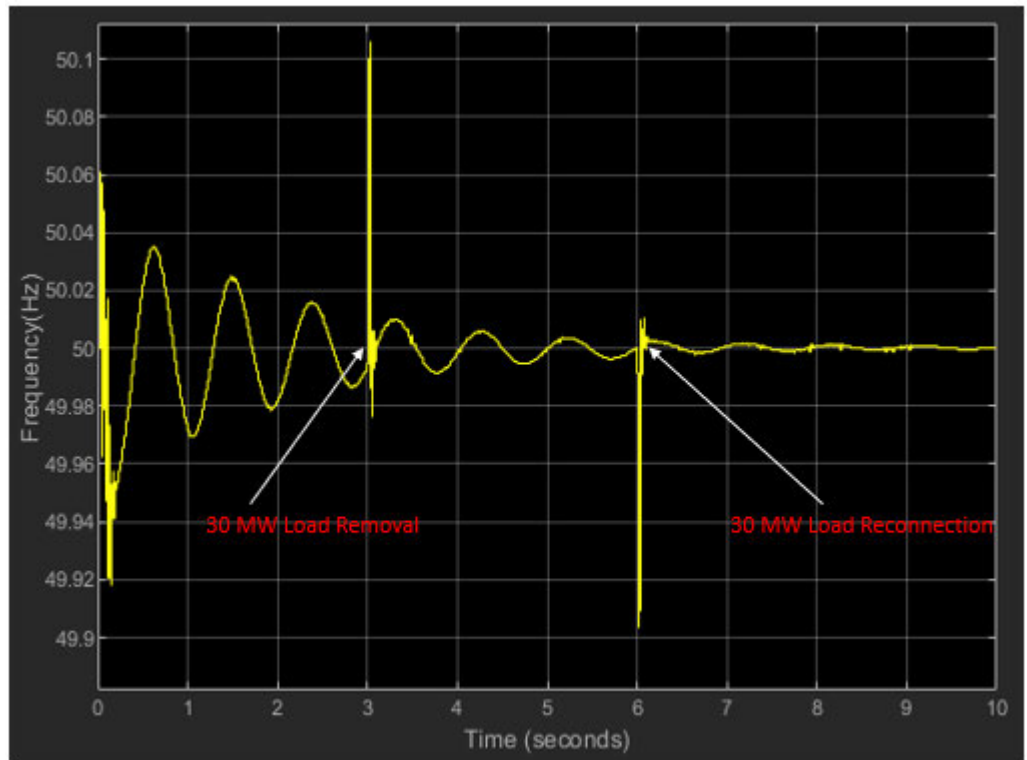


Figure 4.12: Load Rejection using CB 3



**Figure 4.13:** Voltage and Current Waveforms after 30 MW load Removal



**Figure 4.14:** Frequency response during load removal and reconnection

#### 4.2.5.1 Results and Analysis

The results of the simulation test show no visible effect on current and voltage. This could be attributed to low reactive loading on the network and on the load itself. However, frequency spiked at the removal of load and dipped during reconnection of load at 3 seconds and 6 seconds respectively. This was expected since the mechanical torque on the synchronous machine became excessive for the remaining load demand causing momentary acceleration of rotor which was quickly addressed by automatic governor control. A reverse effect was experienced during reconnection of the load.

The frequency variations did not violate NER, AEMO or Grid Codes requirements.

#### 4.3 Network with PV Array ( No Synchronous Machines)

A grid system was modelled in Simulink comprising of a PV system as the main generator, complete with voltage and current feedback systems to assist with Fault Ride Through Capability. The PV system is equipped with varying irradiance at the input of the solar modules to mimic close to a real-life situation. The temperature of the solar panels was modelled as a varying quantity.

A boost converter was included in the model to work in conjunction with the Perturb and Observe algorithm in ensuring that maximum power output is derived from the PV modules. The inverter system is modelled as a voltage source converter. It takes its control input parameters from a point of common coupling. Network disturbances were introduced close to the point of common coupling. Voltage measurements were taken at the point of common coupling in order to capture the effects of disturbances closest to the inverter. Frequency measurements were taken inside the inverter measurement system using a Phase Lock Loop. Part of the inverter measurement control system is shown in figure 4.11 below.

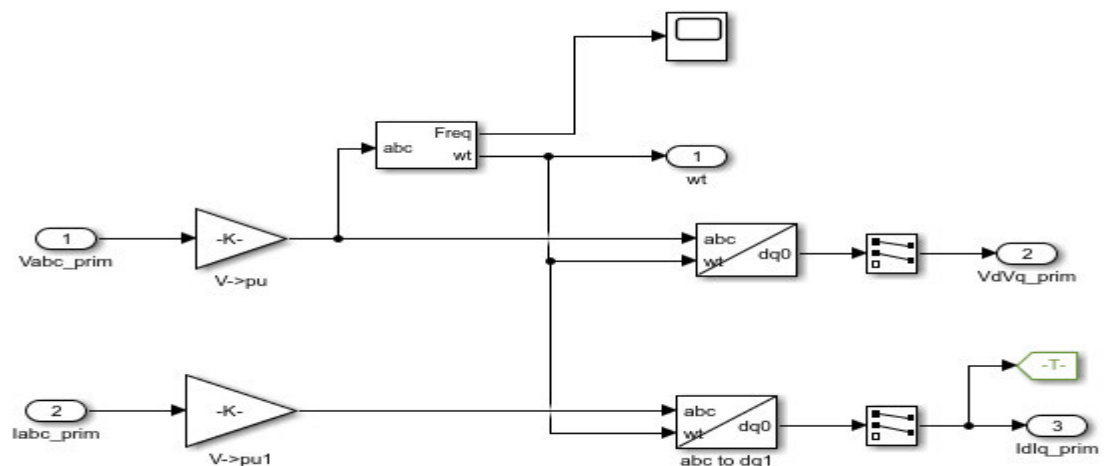


Figure 4.15. Inverter Frequency Measurement

A block diagram of the PV system model is shown in figure 4.12 below.

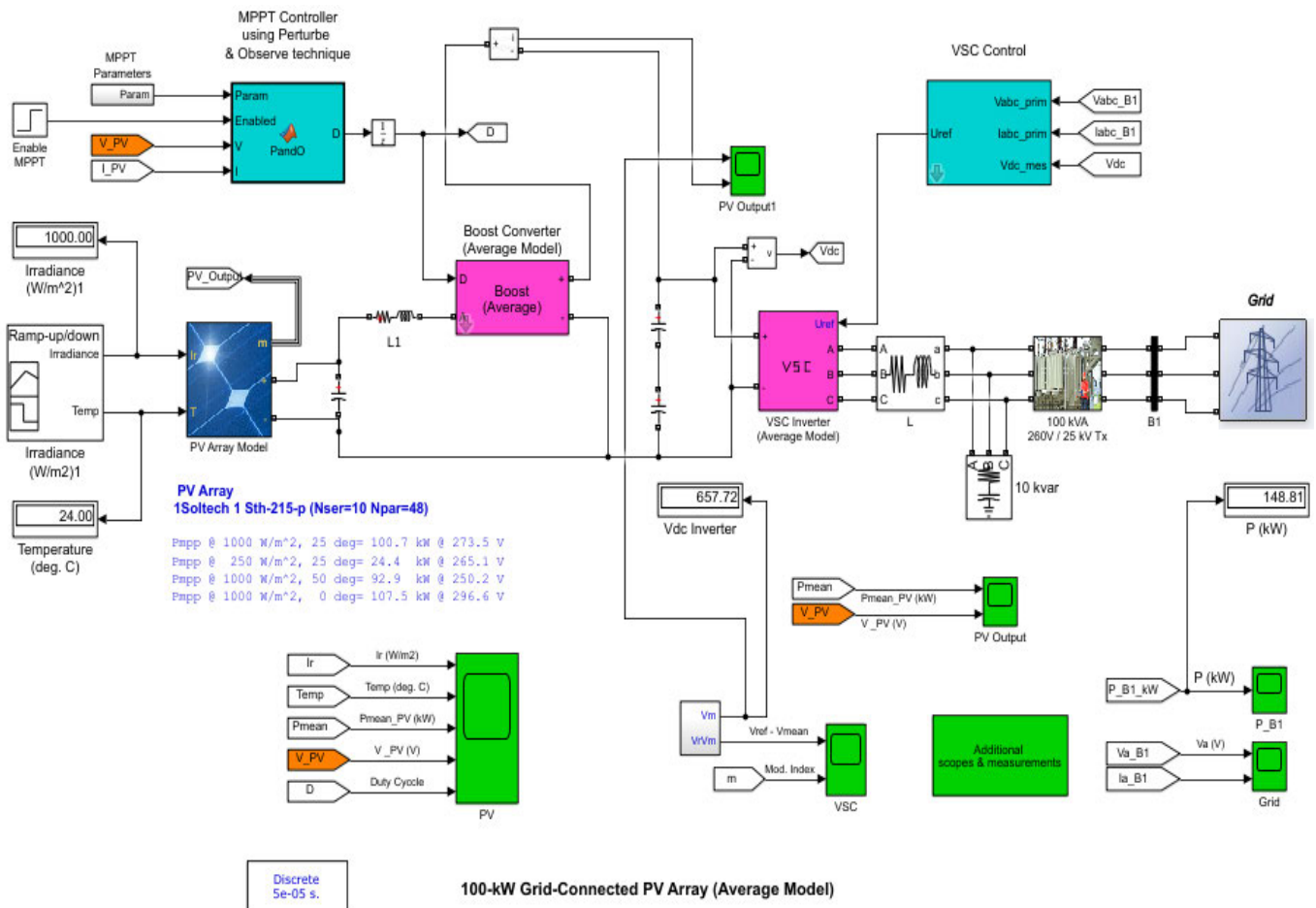
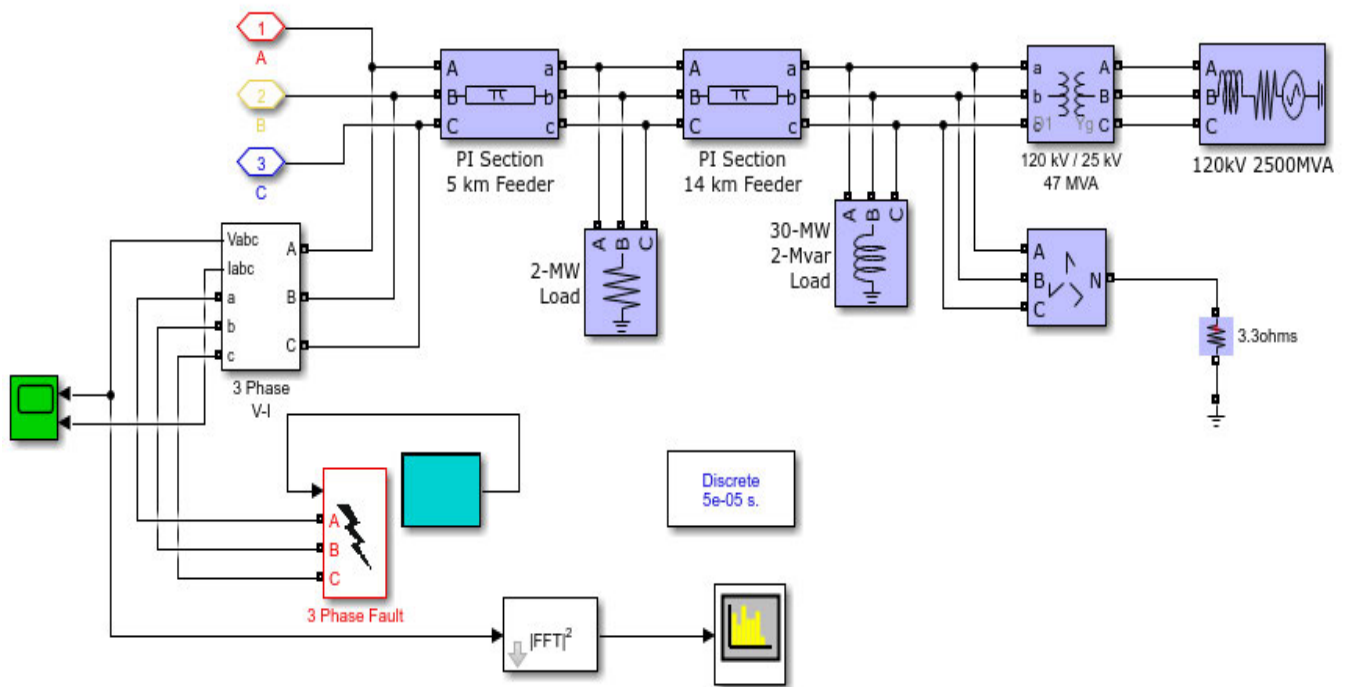


Figure 4.16: PV System Model

The grid portion of the PV system comprises of a 25kV distribution line, a 120kV transmission line, 120/25kV transformer, 2MW load and a 30MW load. The network disturbances are introduced on the distribution line. The disturbances are transient in nature. Software limitations could not accommodate two parallel transmission lines for simulating the disturbance using circuit breakers hence the use of transient conditions where the faults are assumed to be cleared after the first opening of a recloser and gone when the recloser recloses.

The grid portion is shown in figure 4.17 in the next page.



**Figure 4.17:** Grid Portion of PV System

This portion of the model connects to the rest of the PV system shown in figure 4.12 through the hanging terminals marked “1 2 3” or A, B and C. Disturbances are introduced using the fault block labelled as 3 Phase Fault in figure 4.13 above. The disturbances are introduced at various PV penetration levels to test if the amount of penetration influences how the network reacts to abnormalities.

#### 4.3.1 Simulation when PV system Supplies 0.35% of the Load

In this simulation network conditions are introduced when the PV system supplies as low as 0.35% of the load.

##### 4.3.1.1 Simulation of a three-phase symmetrical fault

A three-phase symmetrical fault is introduced at the distribution network and voltage, current, frequency and power waveforms are generated. The fault is introduced at 3 seconds and removed at the 4 seconds mark. The waveforms obtained are as shown in figures 4.14 -4.16 below.

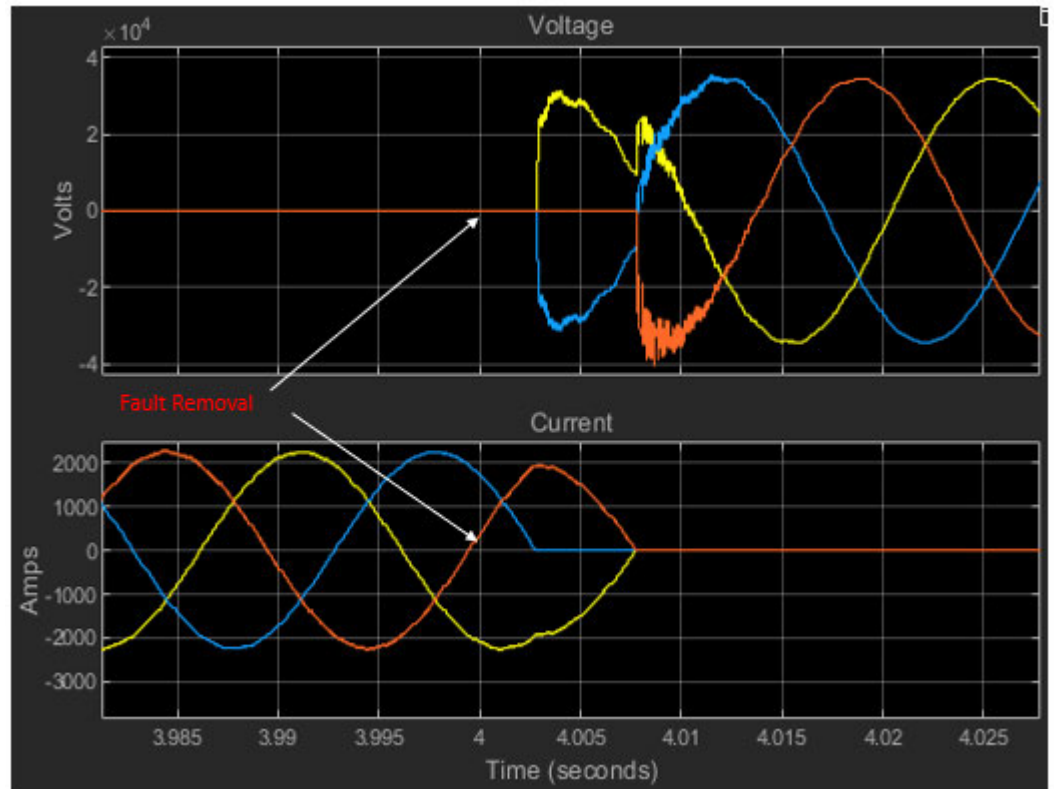


**Figure 4.18:** Voltage and Current waveforms for a three-phase symmetrical fault

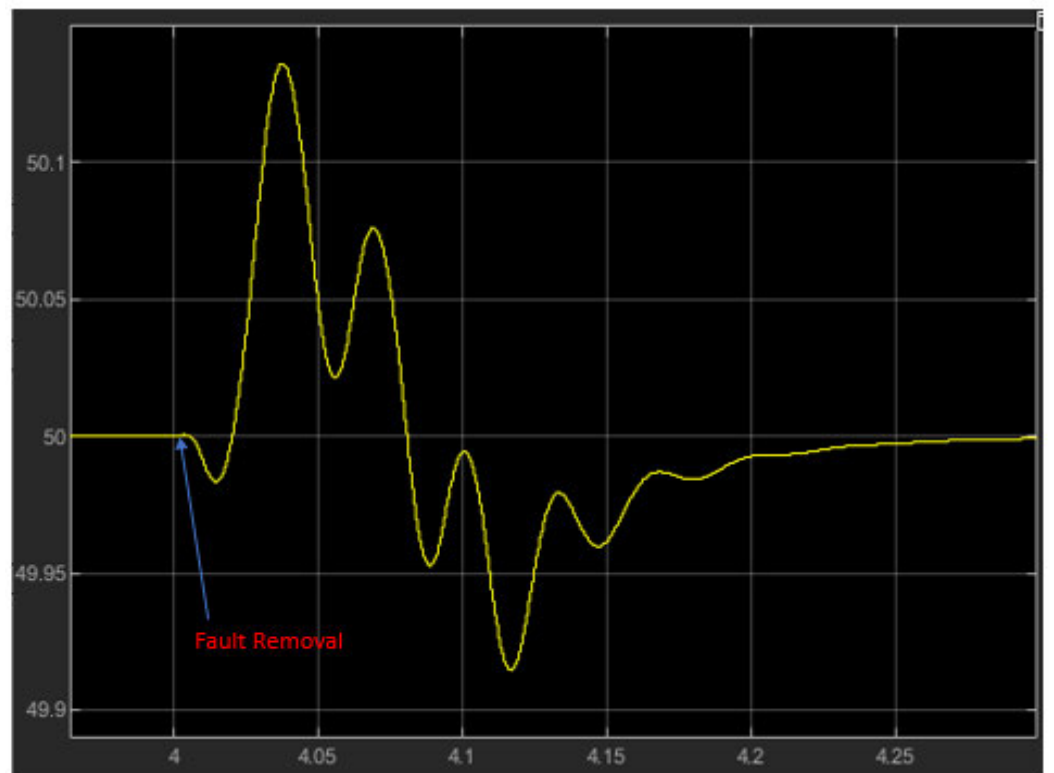


**Figure 4.19:** Frequency response after a three phase Symmetrical Fault

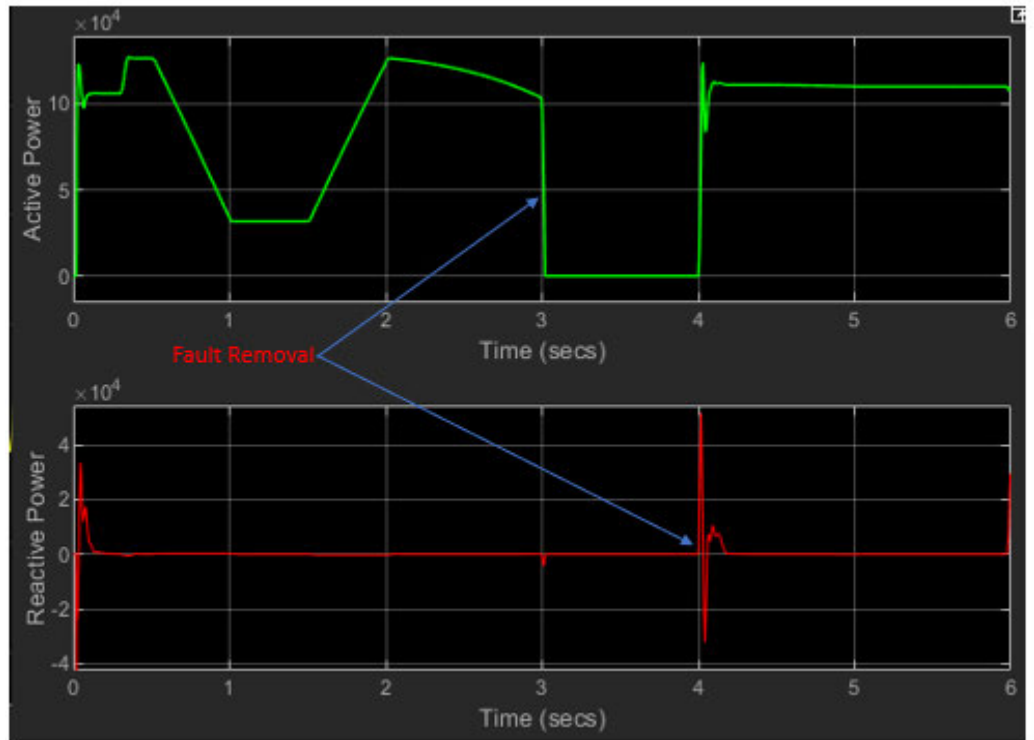


**Figure 4.20:** Active and Reactive Energy Injection During and after fault

#### 4.3.1.1.1 Results and Analysis

The transient fault was introduced on the 3 seconds mark and removed on the 4 seconds mark. However, effect of fault removal was not felt until after 0.0025 seconds due to circuit breaker delay times. All the three phase voltages collapsed to zero during the fault. The voltage recovered to 100% of nominal voltage in 0.02 seconds. Fault current was a balanced 200 Amps per phase and dropped to zero Amps at 4.0025 seconds.

Frequency dropped from about 50 Hz to 49.92 Hz at the time of fault occurrence and then rose to 50.14 Hz after fault removal, before settling at 50 HZ in 0.25 seconds.

Voltage and frequency variations and recovery times did not violate rules that govern network requirements under fault conditions. According to Australia Grid Codes, the frequency can be as low as 47.5 HZ and be as high as 52 Hz for a maximum of 2 seconds. Voltage can drop to 0% of nominal voltage and recover to 80% in 450ms.

Unfortunately, the inverter did not inject visible reactive energy during the fault but injected about 48kVar reactive energy during voltage recovery period. Active energy supply seized during the fault but resumed after the removal of the fault. Ideally, the inverter must remain connected to the system and support voltage recovery under fault conditions.

#### 4.3.1.2 Simulation of Removal of Big Load (30MW)

A 30 MW load is disconnected from the network to test network behaviour after the disturbance. Network parameters were measured and graphically represented as given below:

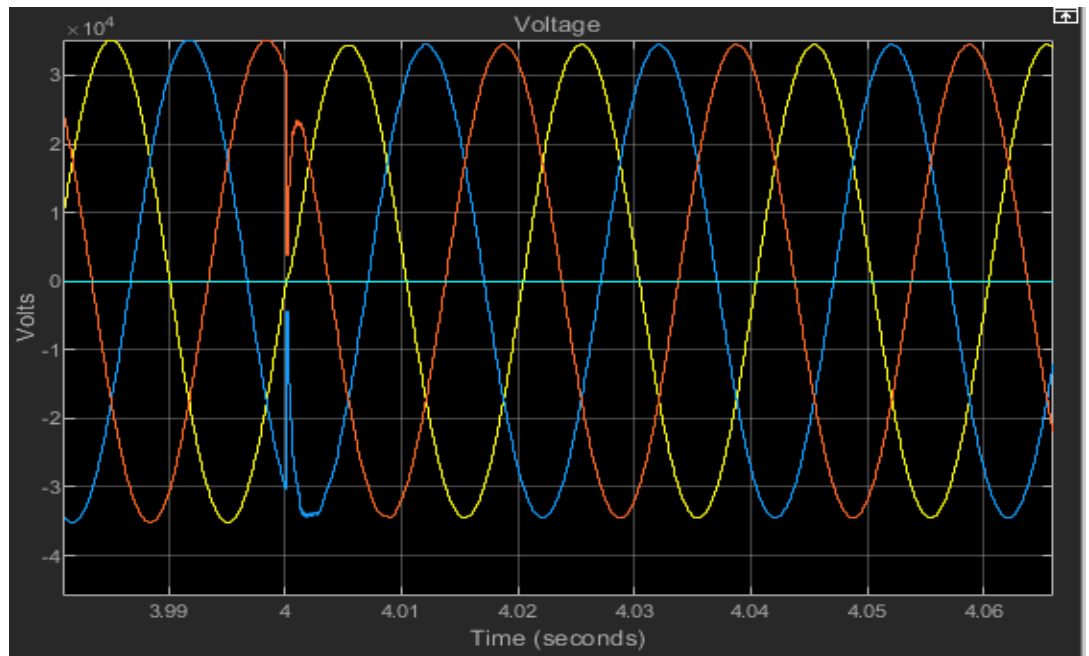


Figure 4.21: Voltage response after removal of 30MW load.

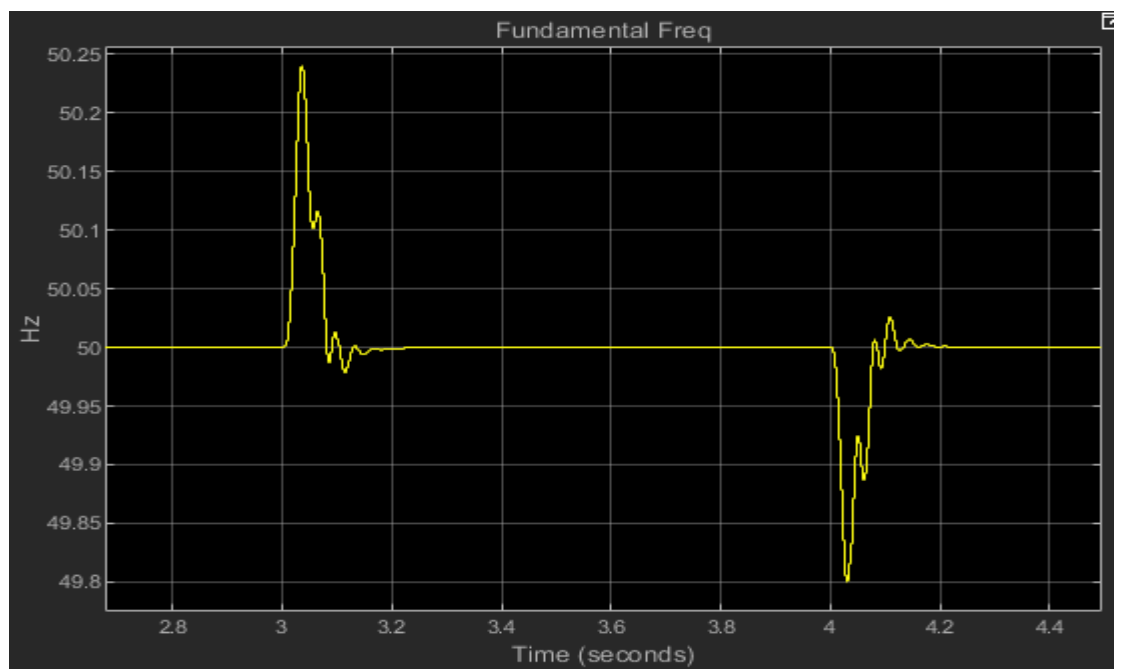


Figure 4.22: Frequency response after removal of 30MW load

#### 4.3.1.2.1 Results and Analysis

B and C phase voltages dropped to about 65% of nominal voltage during load re-connection. It took 0.01 seconds for the system voltage to recover to 100% of nominal voltage after the disturbance. Frequency rose to 50.24 Hz immediately after load rejection and dropped to 49.8 Hz when the load was re-connected. The frequency recovery time in both instances was 0.2 seconds.

The voltage and frequency variations and their time duration did not violate any rules by the bodies that govern the safe and stable operation of the network (AEMO, NER, IEC and IEEE)

#### 4.3.2 Simulation for PV Supplying 1% of Load

The network load was varied so that the PV penetration was enough to supply 1% of total load on network. Disturbances were introduced at the distribution side of the network as explained earlier on.

##### 4.3.2.1 Three-phase symmetrical fault simulation

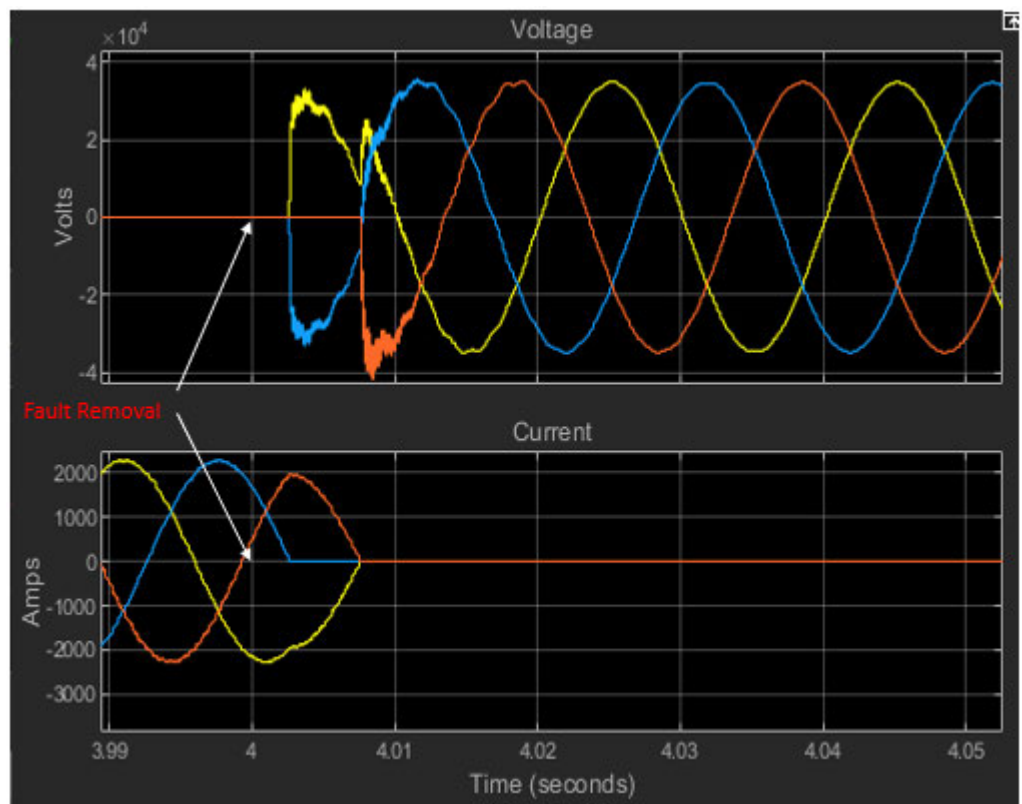
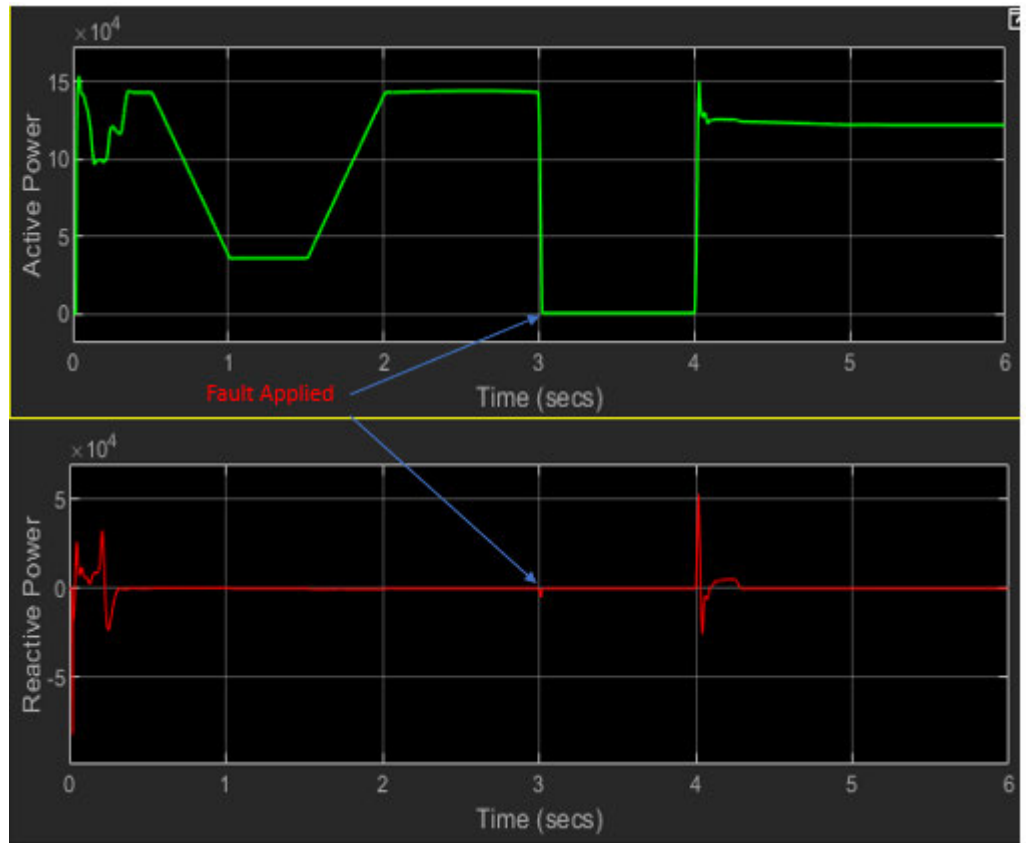


Figure 4.23: Voltage and Current response after a 3-phase symmetrical fault



**Figure 4.24:** Active and Reactive Power injection during and after fault.

#### 4.3.2.1.1 Analysis of Results

The voltage on all three phases dropped to zero during the fault and took 0.035 seconds to return to nominal value with a clean sine wave. Fault current was slightly above 2000 Amps during the fault and took about 0.009 seconds to drop to zero after the fault removal. There was no violation of NER, AEMO or grid codes.

The inverter system did not inject any visible reactive power during the fault but injected about 50 kVar at fault removal time. The inverter remained connected to the network during the fault but partially supported voltage recovery after a depression.

### 4.3.3 PV Supplying 11% of Load

The network loading was altered to enable the PV system to supply 11% of the total connected load. A three-phase symmetrical fault was again simulated to test the network response

#### 4.3.3.1 Three Phase Symmetrical Fault

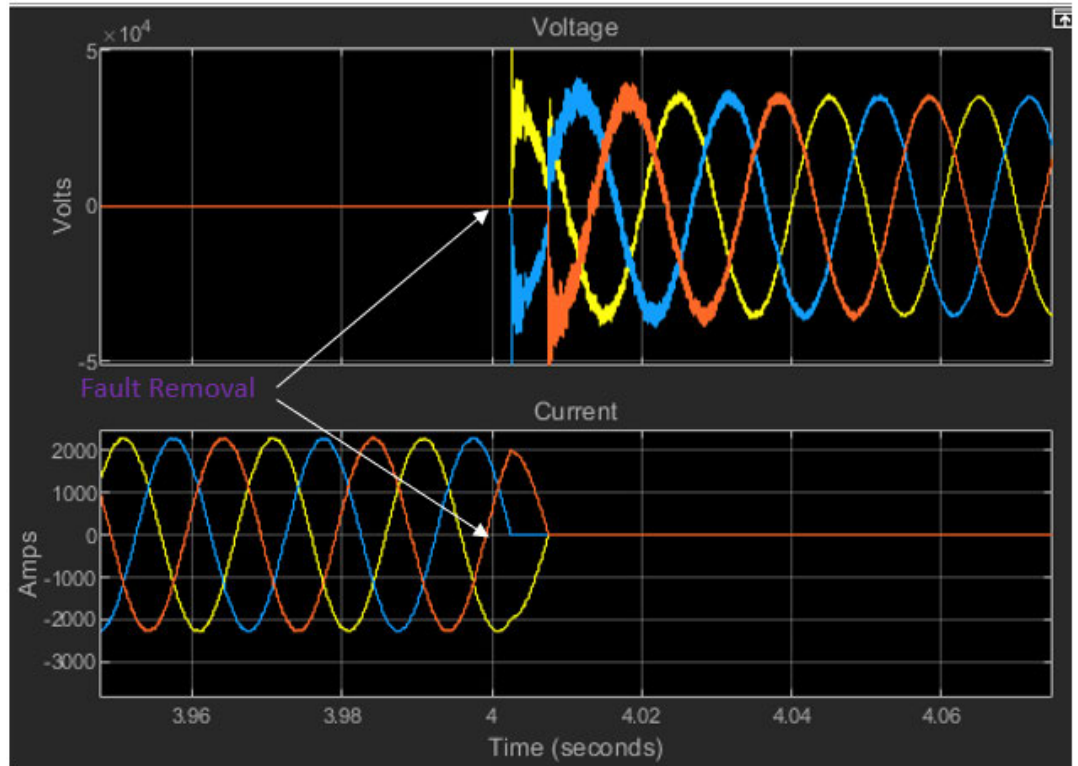


Figure 4.25: Voltage and current response to a three-phase symmetrical fault

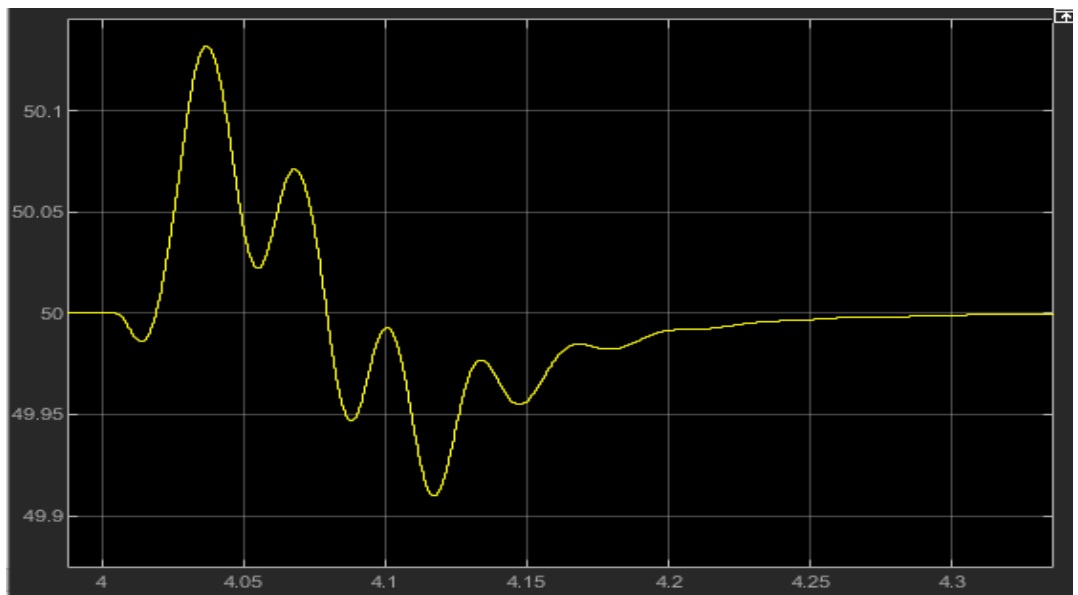
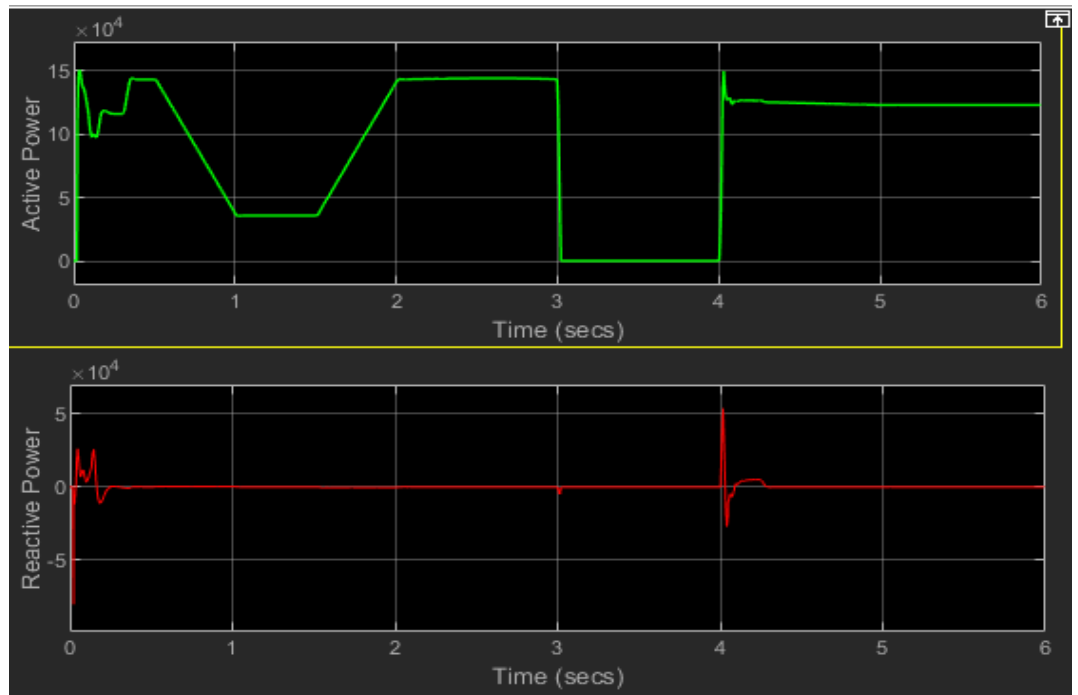


Figure 4.26: Fundamental Frequency Recovery (0.25 sec)



**Figure 4.27:** Reactive and Active power injection during and after fault removal

#### 4.3.3.1.1 Analysis of Results

The fault was introduced at 3 seconds and removed at 4 seconds for this test. The voltage waveform indicates heavy distortion after the fault which could be attributed to the switching nature of the inverter power electronic devices. The voltage on all three phases recovered to nominal values in 0.06 seconds after dropping to zero volts during the fault. Fault current took 0.09 seconds to drop to zero after fault clearance.

The frequency of supply swung between 50.14 Hz and 49.94 Hz and settled back at 50 Hz within 0.25 seconds. Reactive power injection was witnessed during voltage recovery stage after fault clearance like what has been happening in previous tests.

#### 4.3.4 PV System Supplying 100% Load

In this simulation test, the PV system supplies 100% of the load. This creates a weak network given that there are no machines with mechanical parts to provide inertia and stabilise frequency variation. The test seeks to establish how the network responds to disturbances when the main generation is from PV system. Various fault types were introduced to the network as outlined below.

##### 4.3.4.1 Simulation of three-phase symmetrical fault

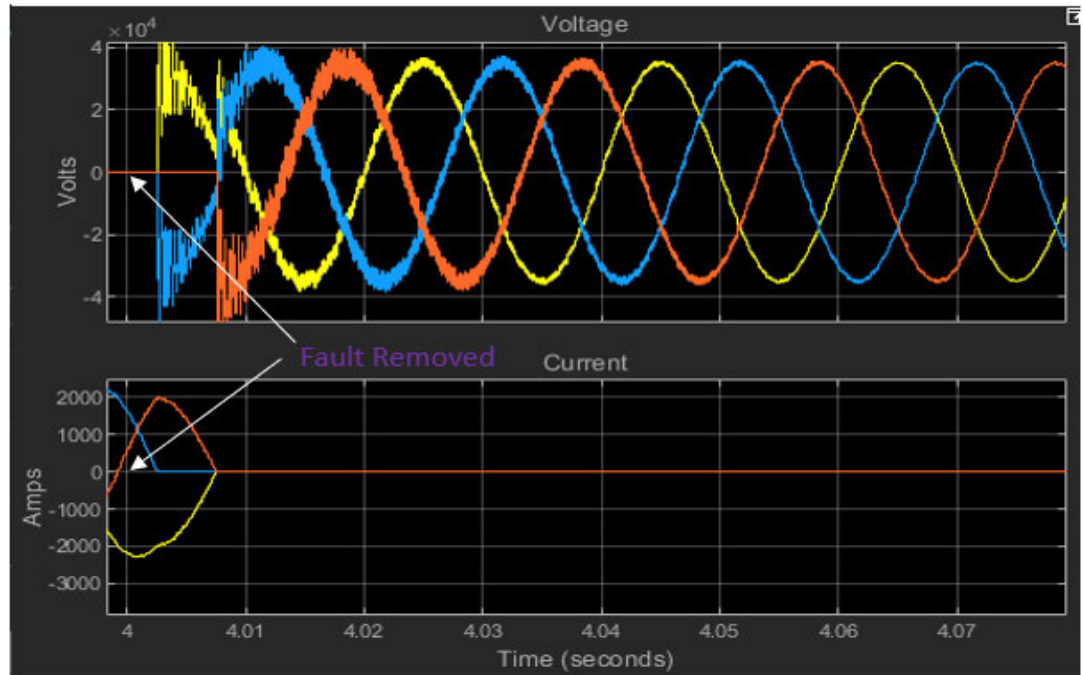


Figure 4.28: Voltage Recovery

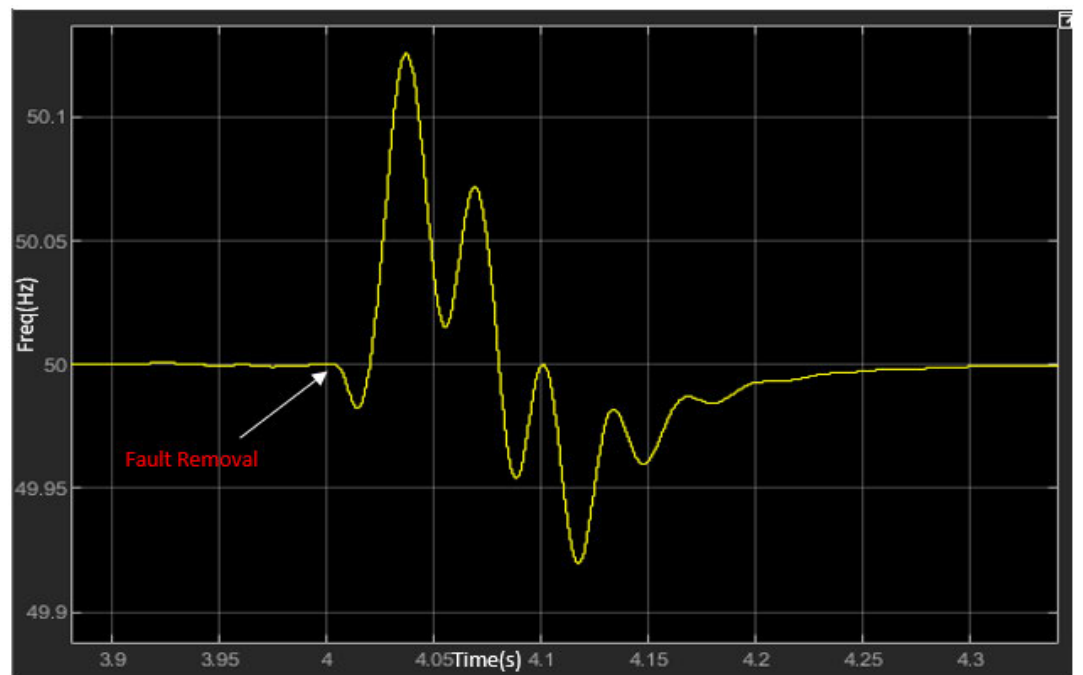


Figure 4.29: Frequency Response

#### 4.3.4.1.1 Analysis of Results

The voltage and current responses were very similar to the responses obtained in similar tests (three-phase Symmetrical fault) under different PV penetration levels. Harmonic distortion seems to have intensified and sustained for a slightly longer period. The voltage recovered from 0% to nominal voltage in 0.065 seconds.

Frequency swung between 49.925 and 50.12 Hz. The variations did not go outside the continuous operation limits prescribed by the Grid Codes and AEMO. Recovery time was 0.3 seconds.

#### 4.3.4.2 Simulation of Three phases to ground fault

A transient fault was introduced to the 25kV distribution network in a similar way as the rest of the tests under section 4.3. The introduction and removal times were 3 seconds and 4 seconds respectively. Voltage and frequency responses were as given in the figures 4.26 and 4.27 below.

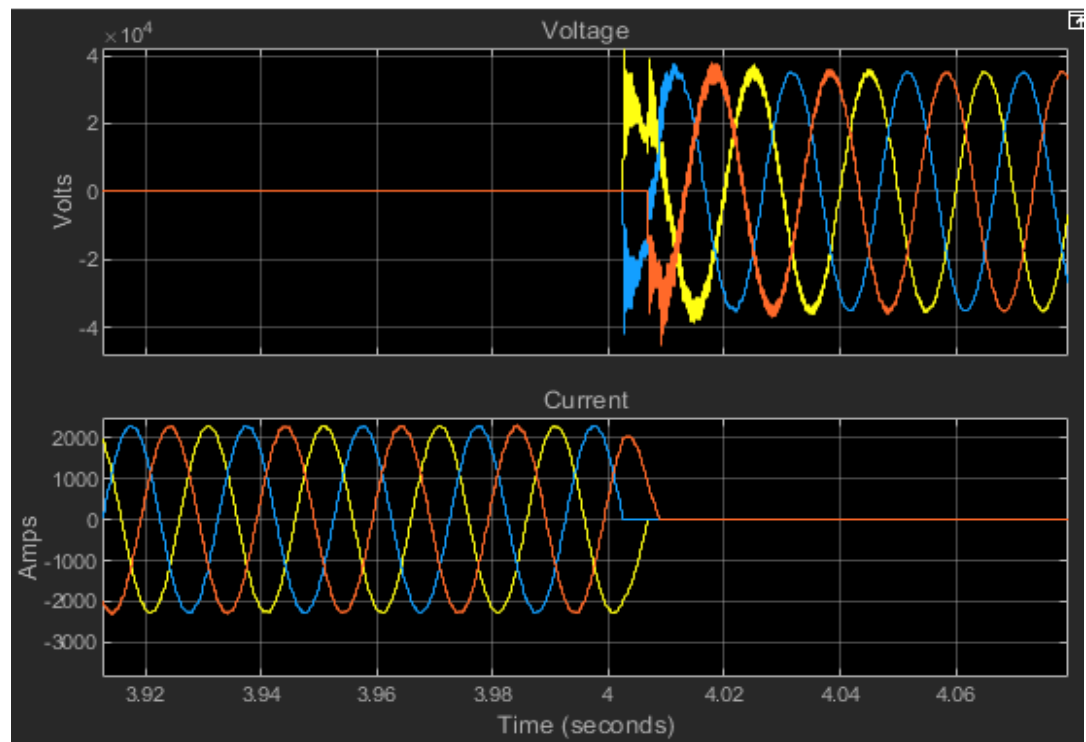


**Figure 4.30:** Voltage recovery for three-phase to ground fault

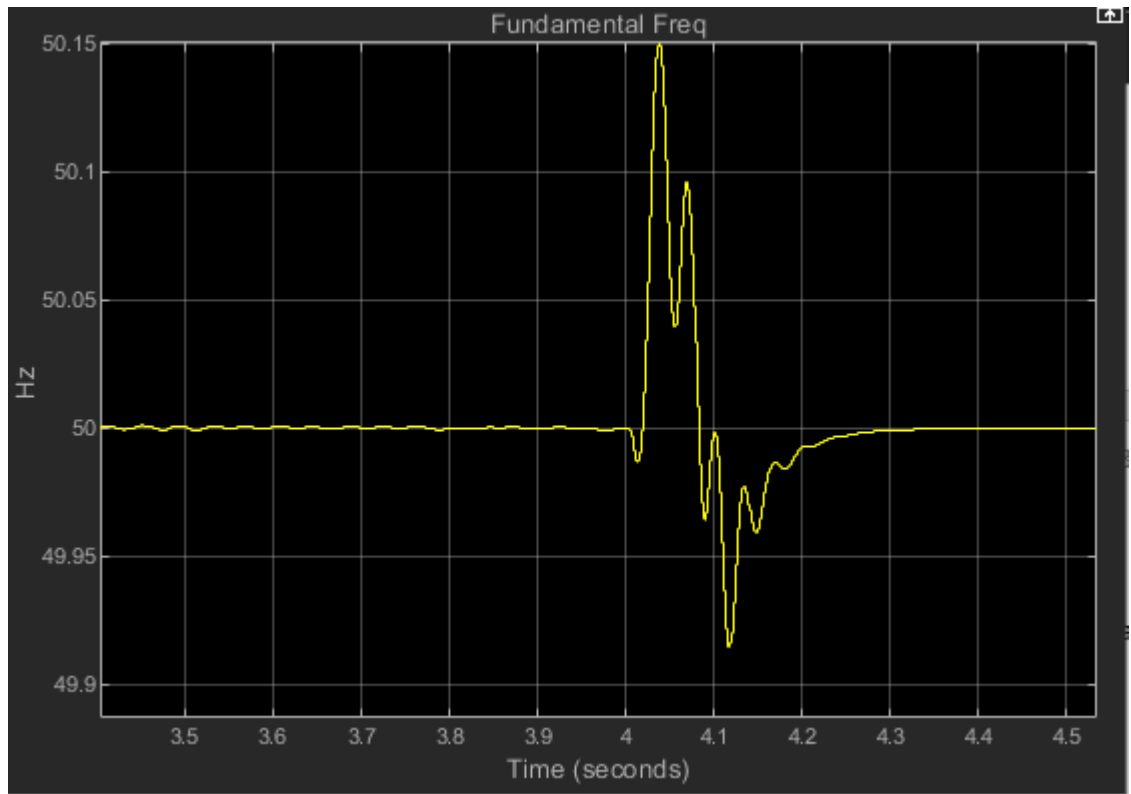


**Figure 4.31:** Frequency recovery from three phase to ground fault

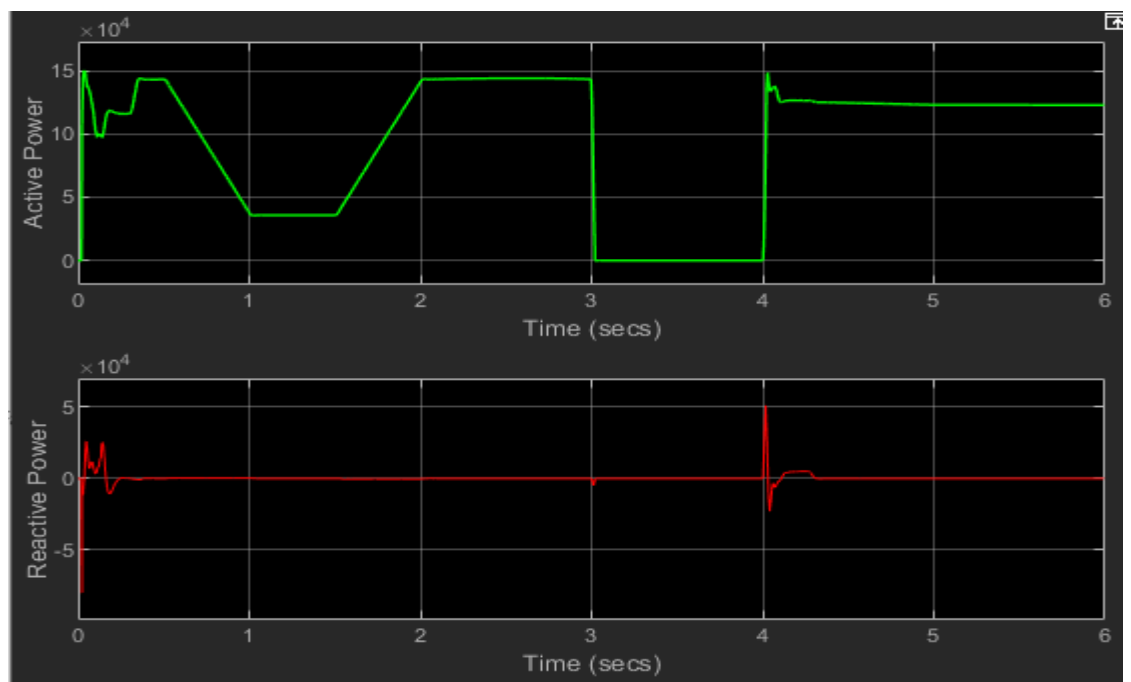


**Figure 4.32:** Active and Reactive power Injection during recovery period

#### 4.3.4.2.1 Analysis of Results

The results obtained here were like the ones obtained in section 4.3.4.1.1. Voltage took 0.06 seconds to recover to nominal value with a clean sine wave. Frequency fluctuated between 50.15 Hz and 49.92 Hz and recovered after 0.31 seconds.

#### 4.3.4.3 Simulation of one Phase to Ground fault

One phase (C phase) was connected to earth via the fault block from Simulink. The same time slots used in the previous tests were also used for the introduction and removal of the fault.

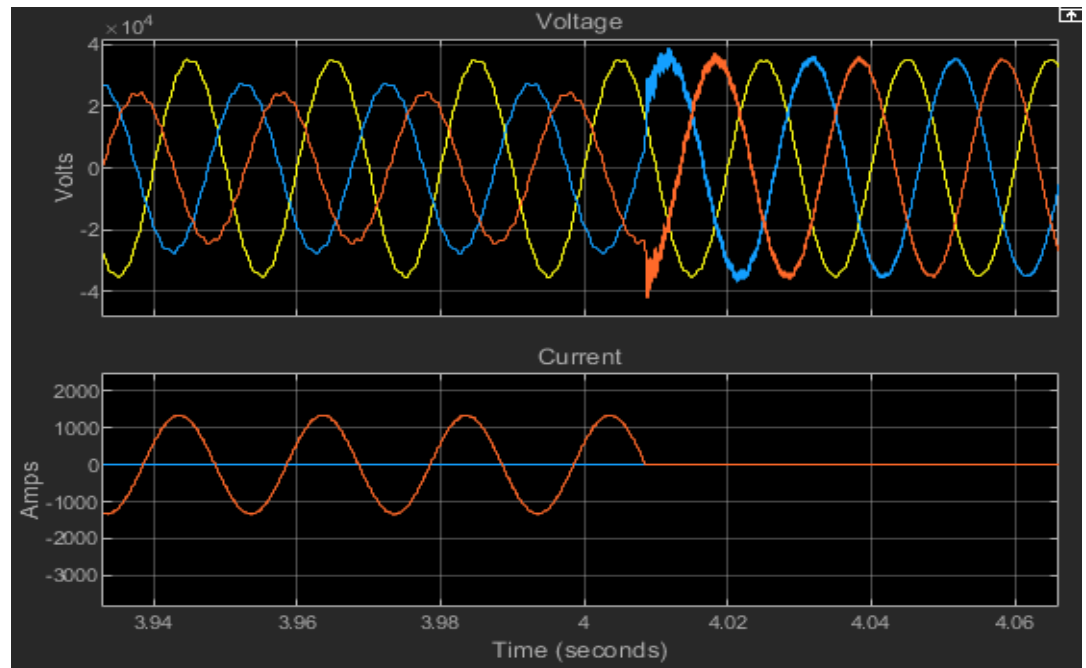


Figure 4.33: Voltage recovery after a single phase to ground fault

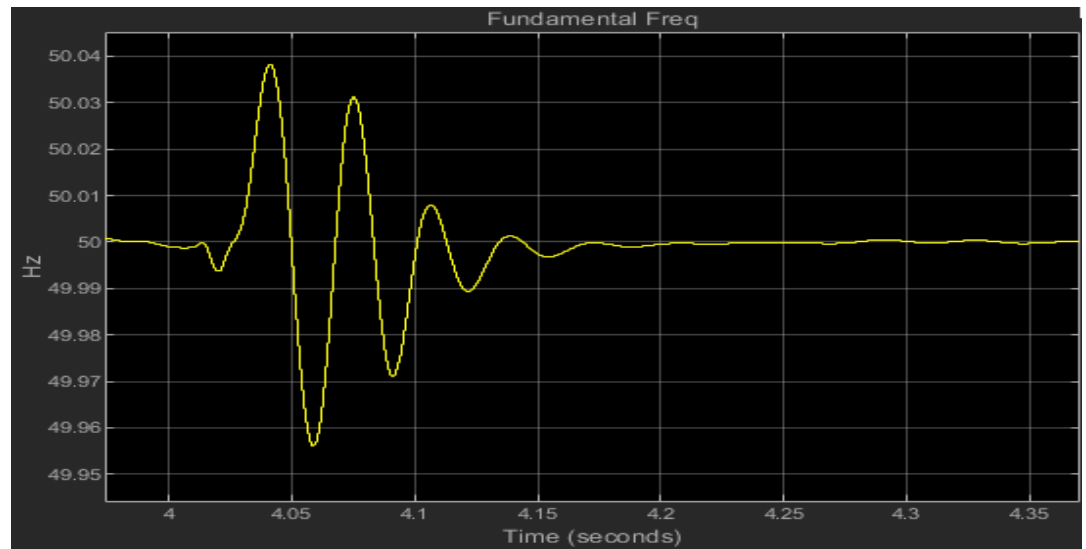
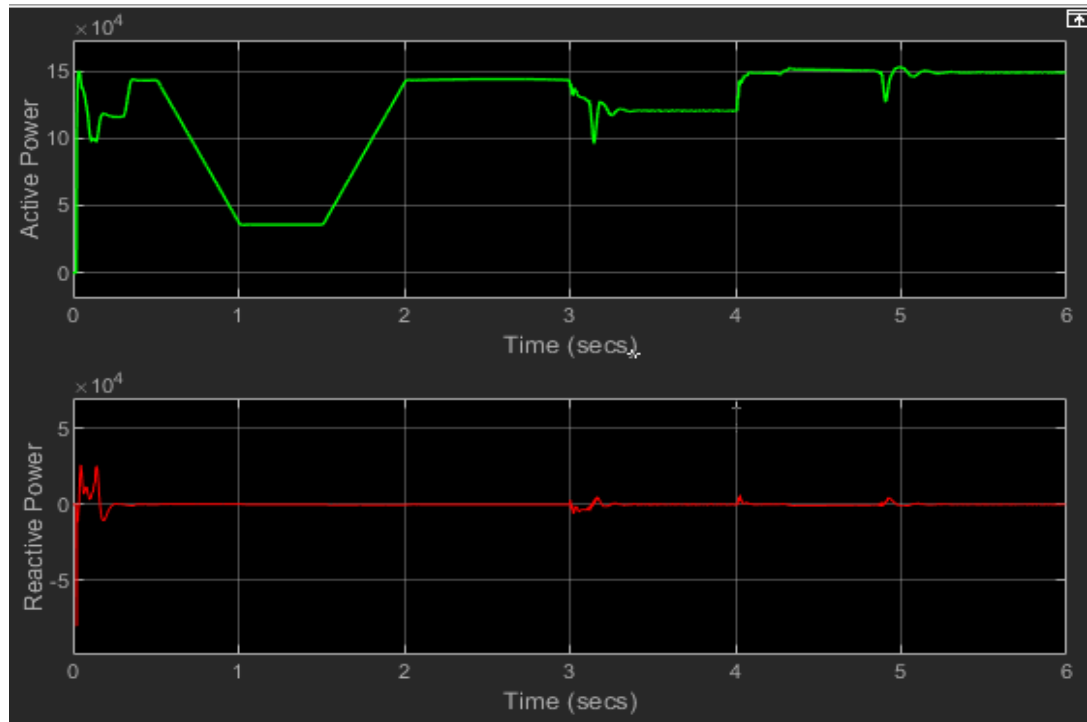


Figure 4.34: Fundamental Frequency Recovery



**Figure 4.35:** Active and Reactive Power injection

#### 4.3.4.3.1 Analysis of Results

Voltages for B and C phases dropped to about 70% of their nominal values but phase A maintained its voltage magnitude. Phase C fault current was constant at 1000A. Voltage recovery took 0.05 seconds.

Frequency variations were within normal operating conditions and recovery time after the fault was 0.25 seconds.

#### 4.3.4.4 Simulation of Phase to phase fault

A fault across phases B and C was introduced using the fault block. The same time slots for introduction and removal of fault were used as in previous tests. Simulation results produced the waveforms as shown in the figures below.

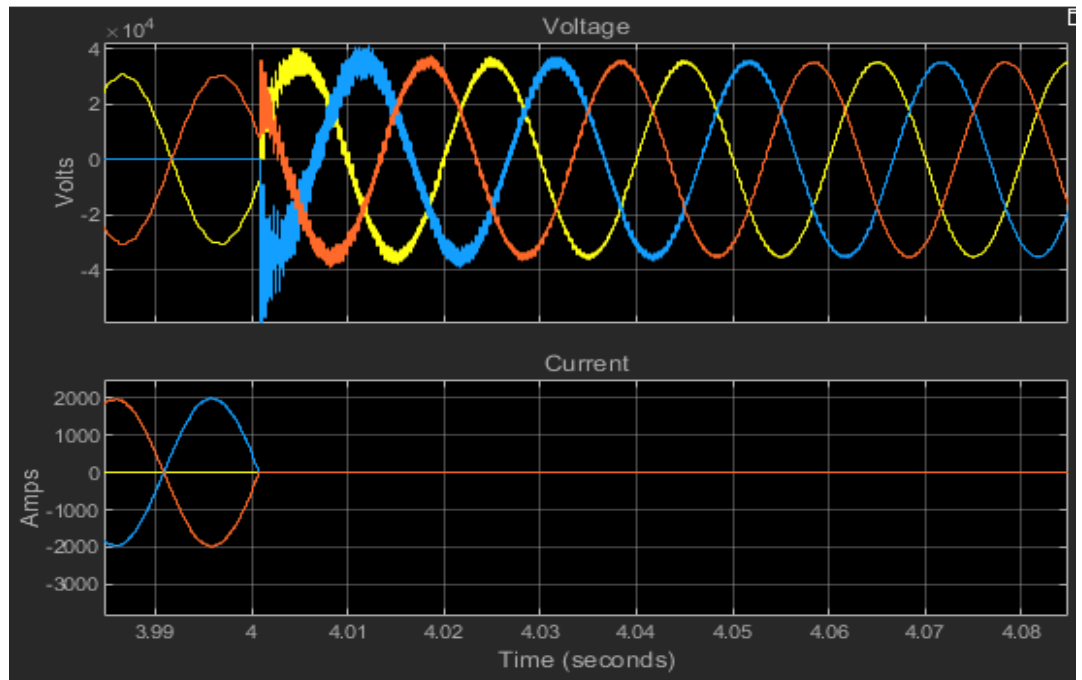


Figure 4.36: Voltage Response after single phase to ground fault.

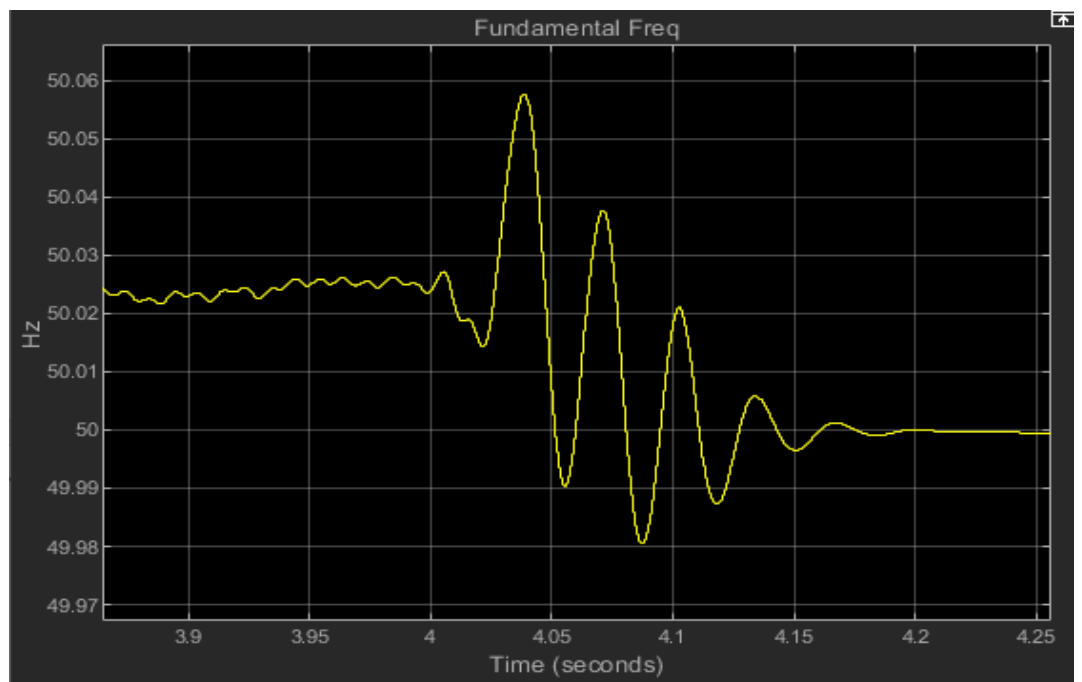
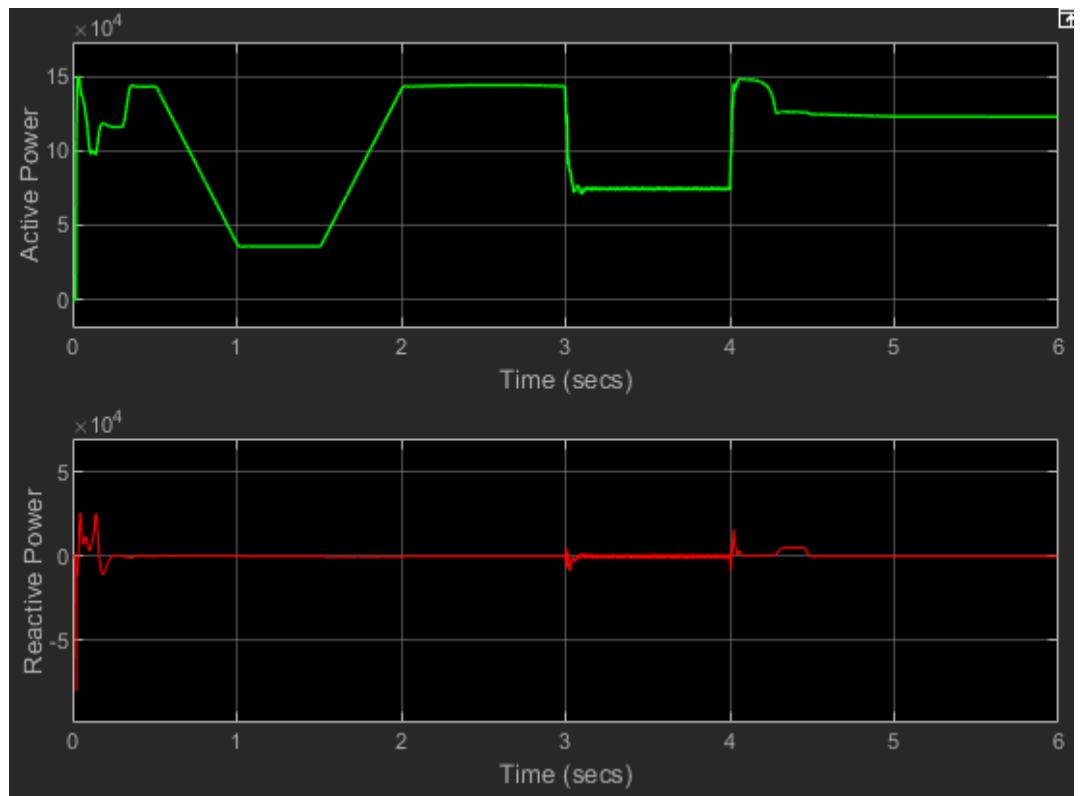


Figure 4.37: Frequency response after single phase to ground fault



**Figure 4.38:** Active and Reactive Power generation during single phase to ground fault.

#### 4.3.4.4.1 Analysis of Results

The simulation results under this test followed the same pattern as the rest of the tests. Voltage and frequency variations did not violate and rules or standards. Voltage recovery took 0.05 seconds and frequency recovery took 0.2 seconds. However, there was insignificant injection of reactive energy from the PV system during the fault but there was reasonable injection of about 20 kVAr at fault removal.

#### 4.4 PV system Combined with Conventional Generators

This section of the simulation test combines PV system with conventional generators. The objective of this combined system was to depict close to a practical network and perform tests with varying percentages of PV penetration. Network responses were noted for different disturbances at these different levels of PV penetration.

A PV system generating up to a maximum of 1.2 MW was connected to a grid system that comprises of two synchronous generators, a transmission line, a distribution line and two loads of 2MW and 30MW. The two synchronous generators were equipped with automatic governor and excitation control systems. The 1.2 MW PV system component of the model was made up of three 400kW systems with their separate DC-DC converters, Inverter system and step up transformers. A simple model was created in Simulink as shown in the block diagram below.

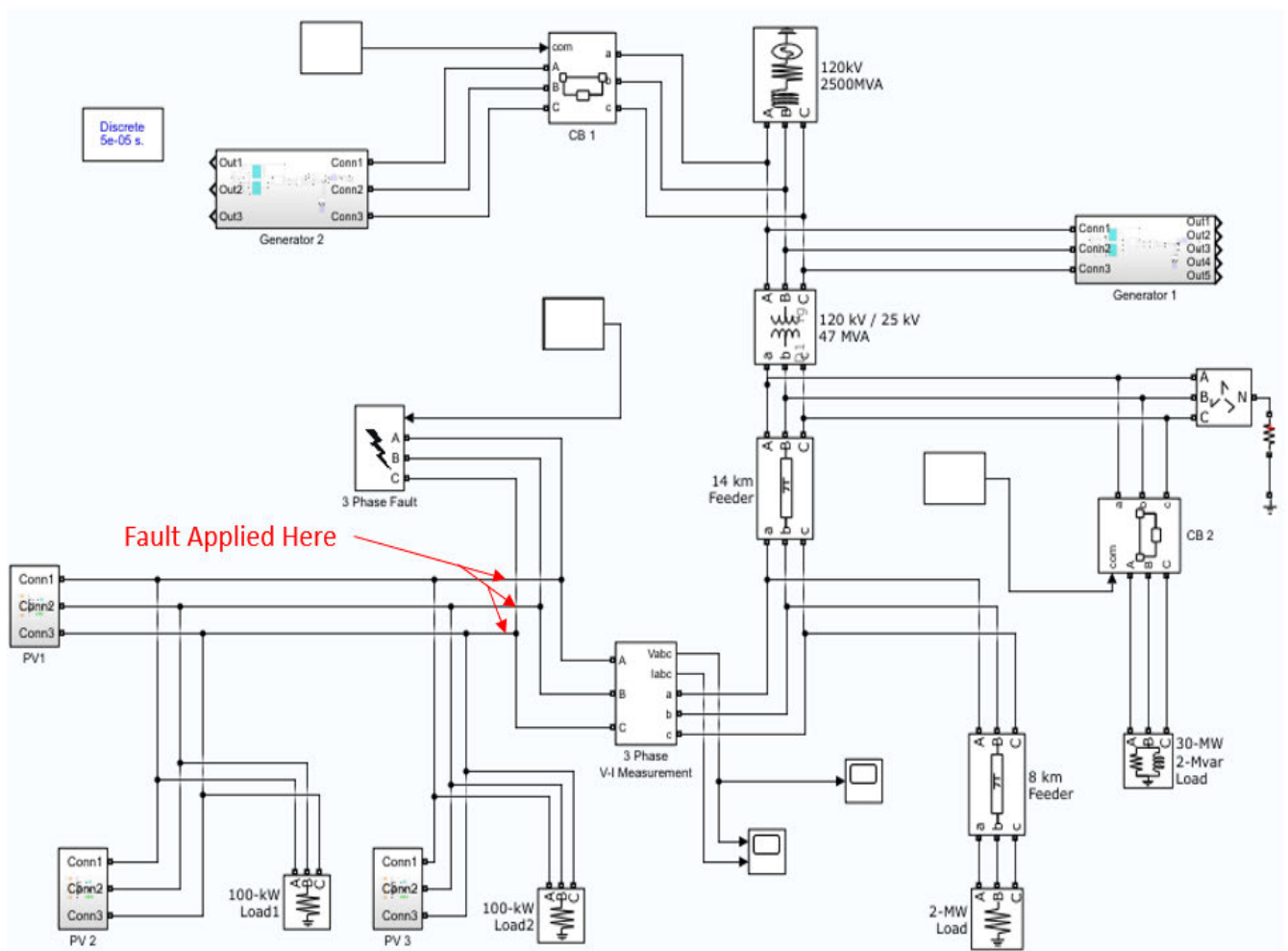


**Figure 4.39:** Combined PV and Synchronous Generator system

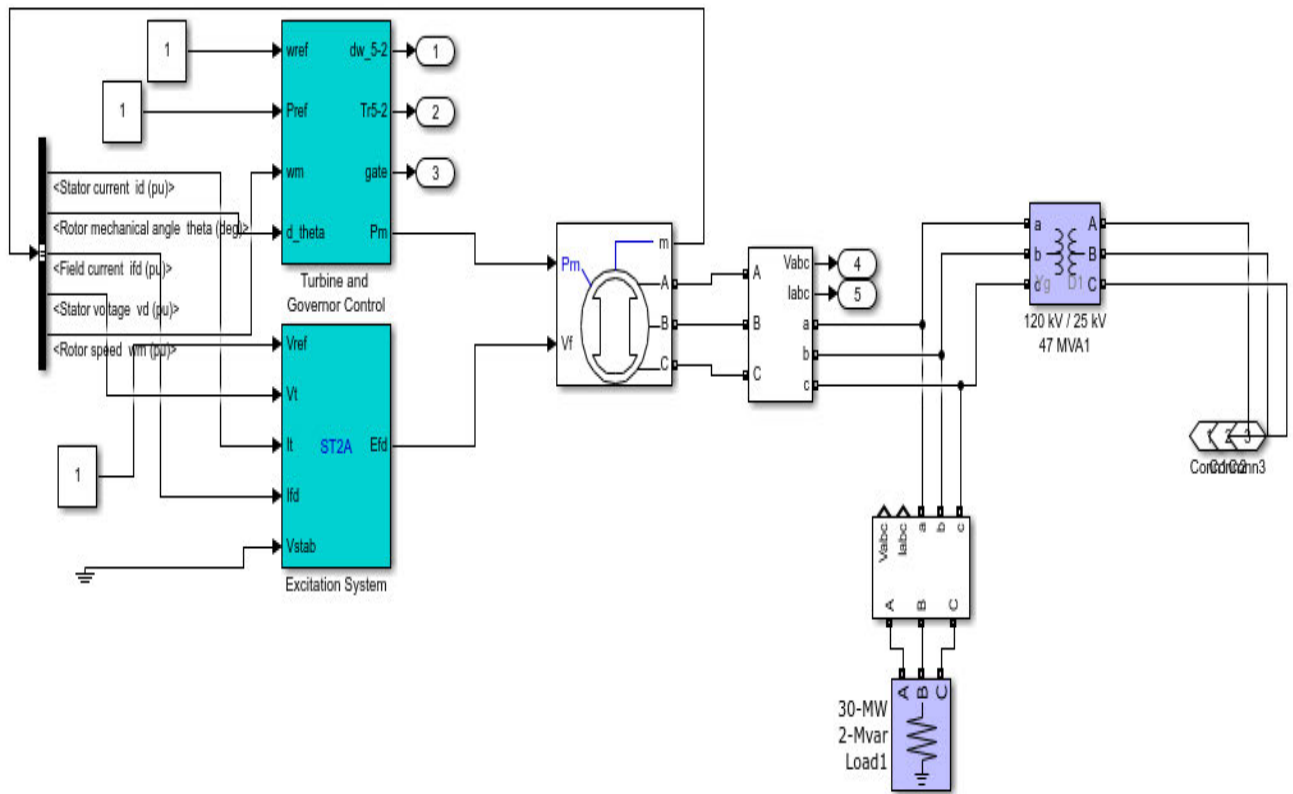


**Figure 4.40:** One of the generator portions of the combined network

#### 4.4.1 PV Supplying 2% Load

The combined grid system was arranged such that the PV system supplied 2% of the grid load. Network disturbances were introduced, and simulation results obtained as shown in the next subsections.

##### 4.4.1.1 Three Phase Symmetrical Fault

A transient three-phase symmetrical fault was introduced to the network by closing a fault breaker marked " 3 Phase faults in figure 4.35 where all three phases were shorted together. Fault inception was at 1 second and removal was on the 2 seconds mark. The fault Results are as shown in the waveforms below.

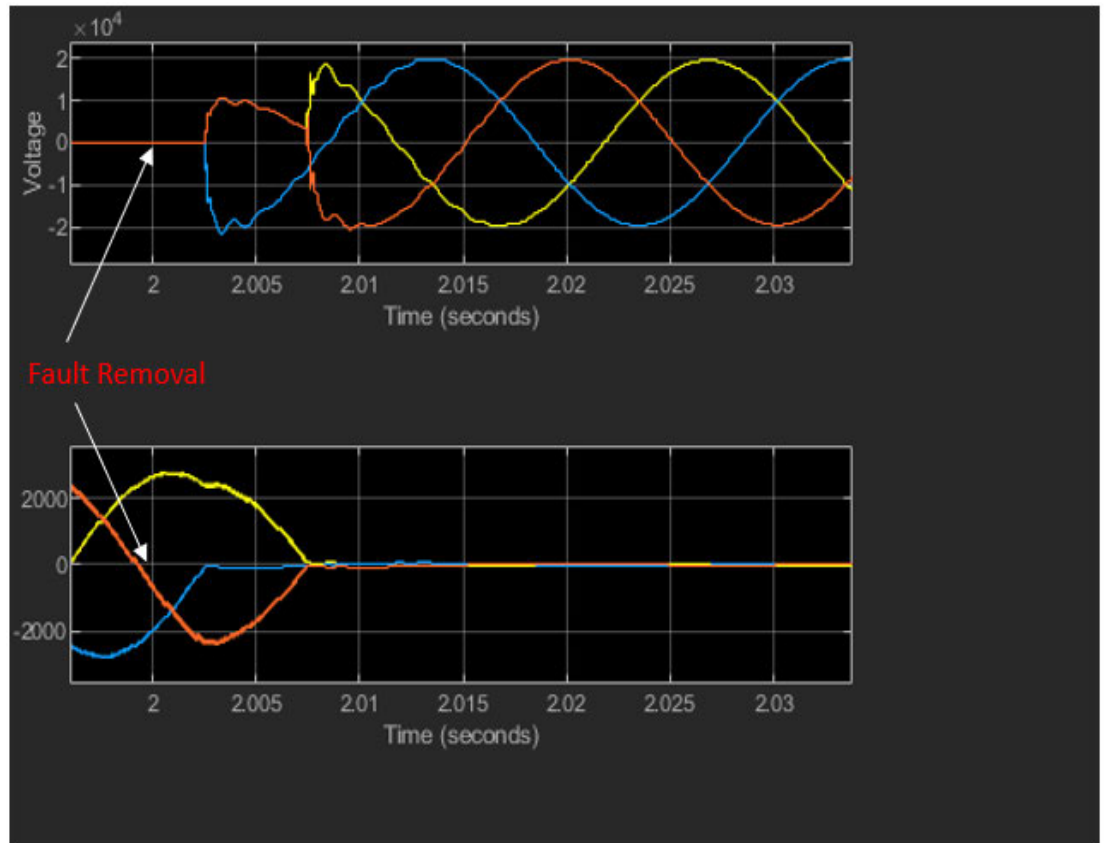


**Figure 4.41:** Voltage response after Three Symmetrical Fault

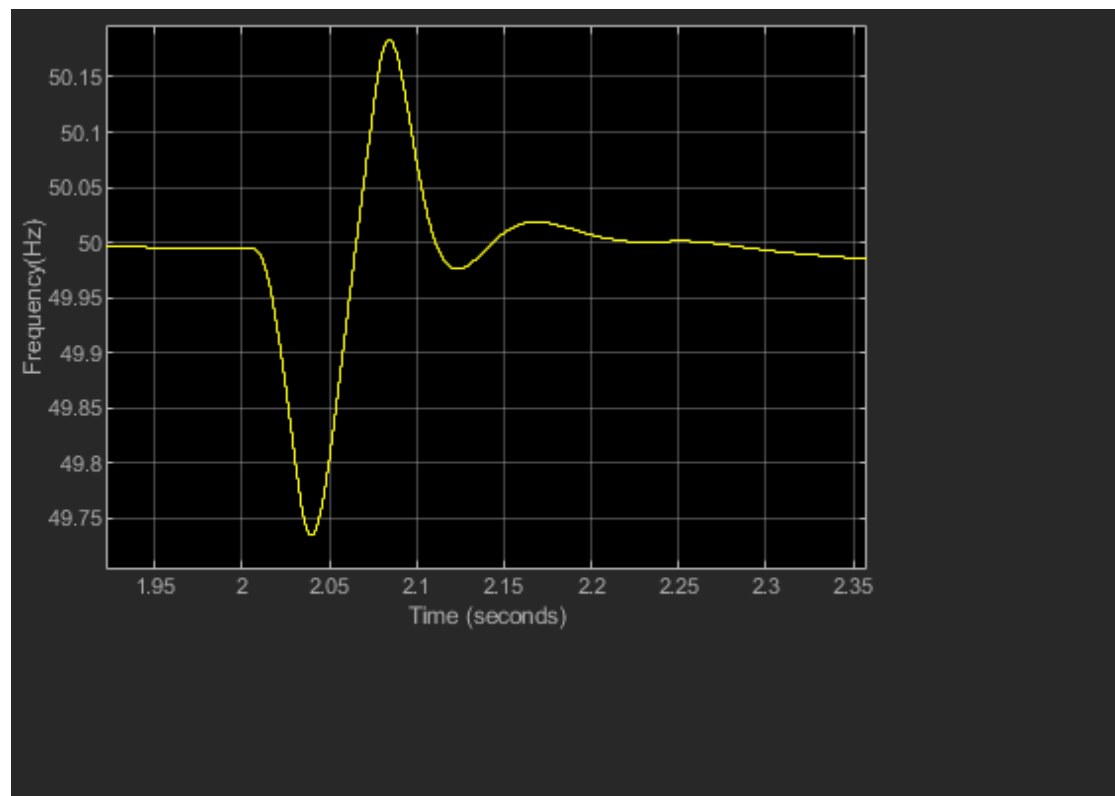


**Figure 4.42:** Frequency Response After Three Phase Symmetrical Fault

#### 4.4.1.1.1 Analysis of Results

The results were not very different from the ones obtained in section 4.2 and 4.3 except that the voltage and current waveforms seem to have less harmonic distortion than tests in section 4.3. Voltage stabilised after 0.021 seconds.

Frequency first dropped to 49.749 Hz before rising to 50.175 Hz and then stabilising after 0.22 seconds. There was no violation of standards.

#### 4.4.1.2 Three Phase to Ground Fault

All the three phases were grounded in this simulation. Fault occurrence and removal times were same as in subsection 4.4.1.1. Results of simulation are as shown in the waveforms below:

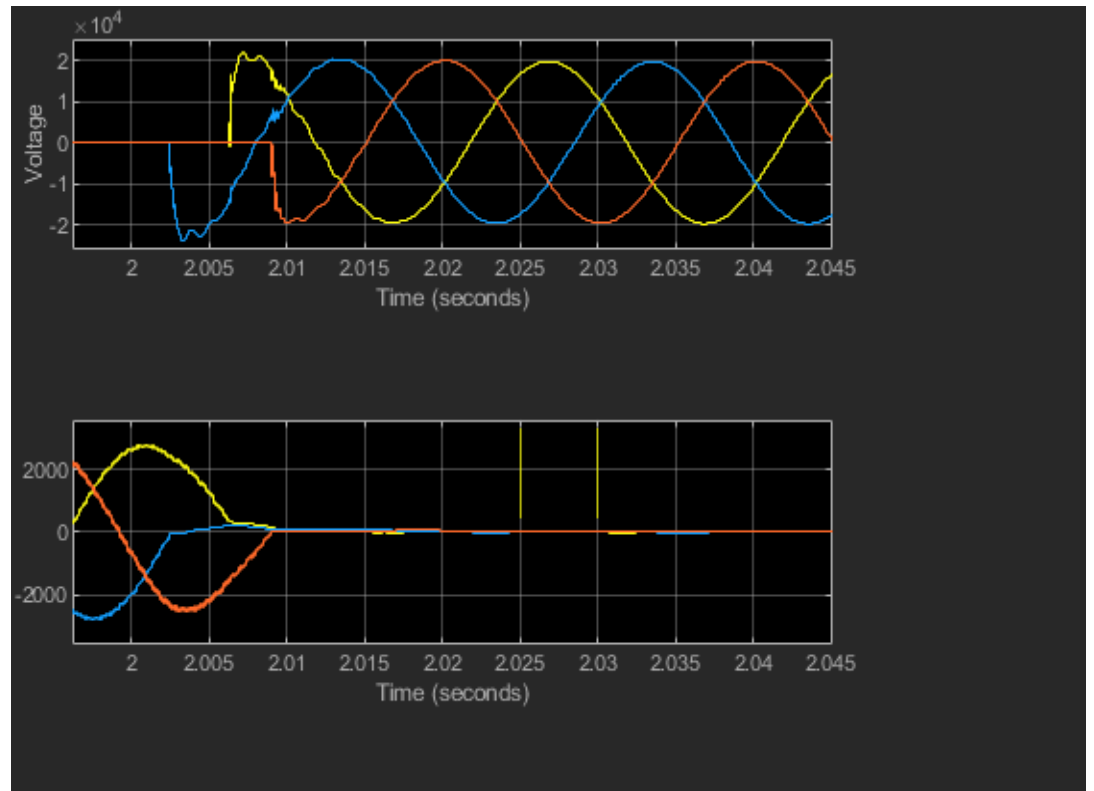


**Figure 4.43:** Voltage response after a three phase to ground fault.

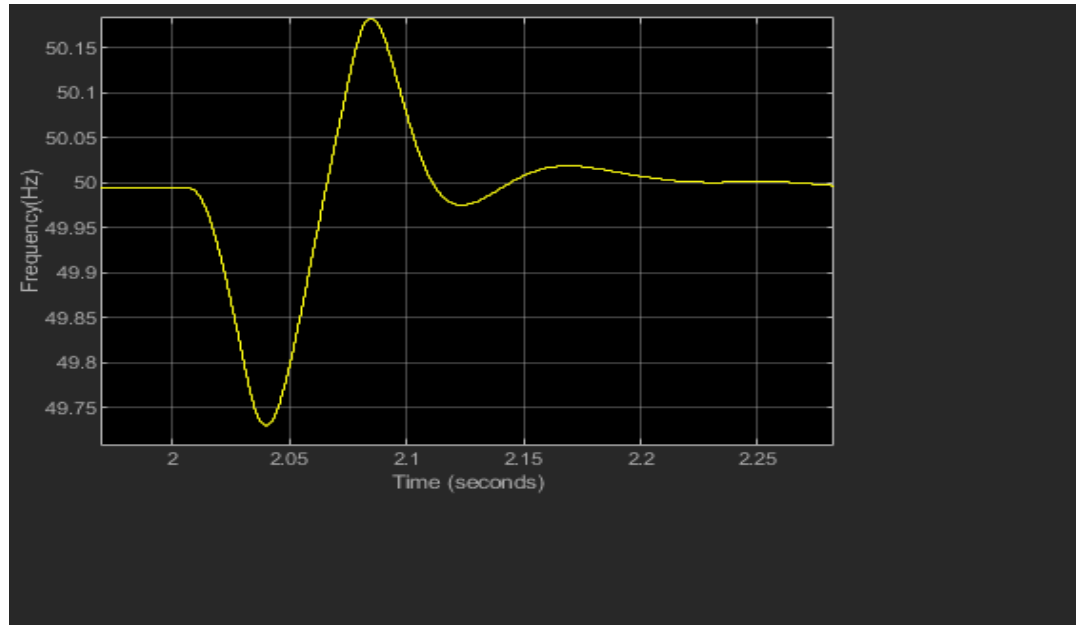


**Figure 4.44:** Frequency response after a three phase to ground fault

#### 4.4.1.2.1 Results and analysis

The results for this test were the same as in subsection 4.4.1.1.1.

#### 4.4.1.3 Phase to ground fault

A single phase to ground fault is simulated using the same inception and removal times as in the previous sections.

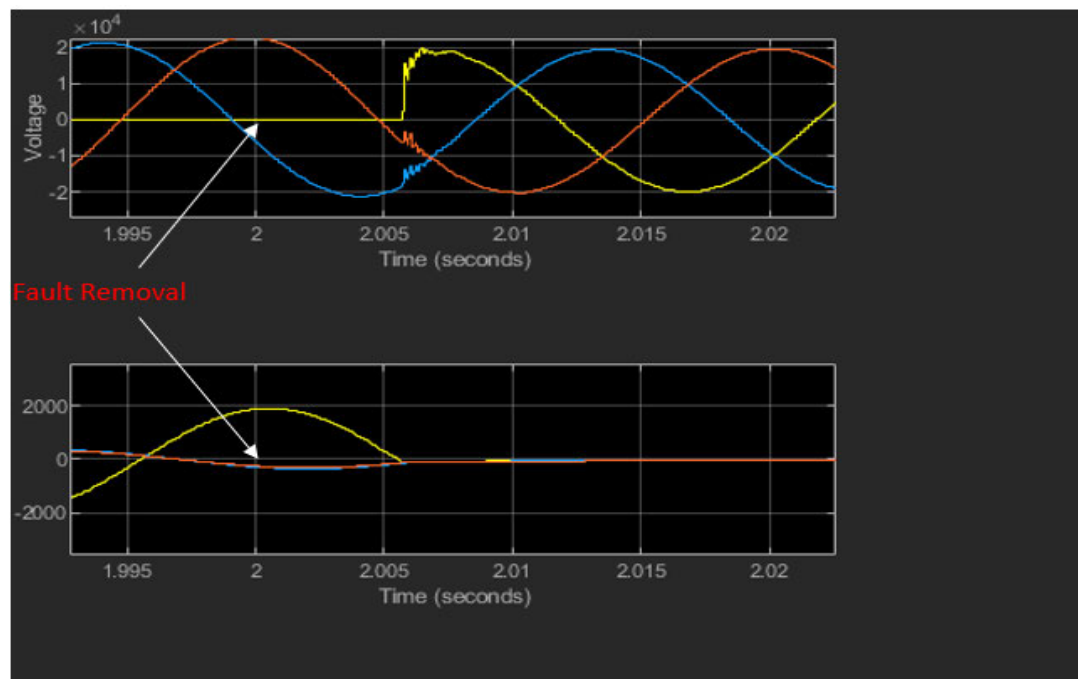


**Figure 4.45:** Voltage response after a single phase to ground fault

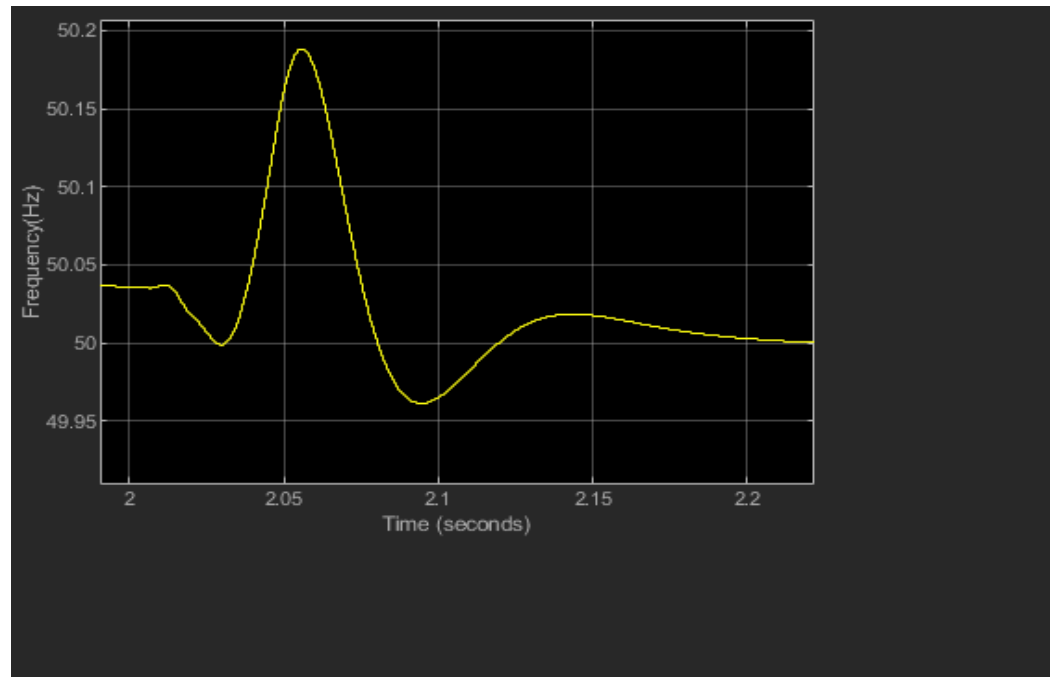


**Figure 4.46:** Frequency Response after a single phase to ground fault

#### 4.4.1.3.1 Analysis of Results

The A phase voltage dropped to zero volts for the duration of the fault. The other two phase voltages had minor distortions but did not lose their magnitudes. Voltage recovery took 0.01 seconds from time of fault removal. Phase A fault current was 2000 A. The other two currents carried small amounts of residual fault current. Frequency went up to 50.18 Hz after the removal of the fault and took 0.2 seconds to go back to 50 Hz.

#### 4.4.1.4 Removal of large load

A load of 30 MW was removed from the network to test response at this level of PV penetration. The introduction and removal times for the fault were not changed. Results came out as shown in the figures below.

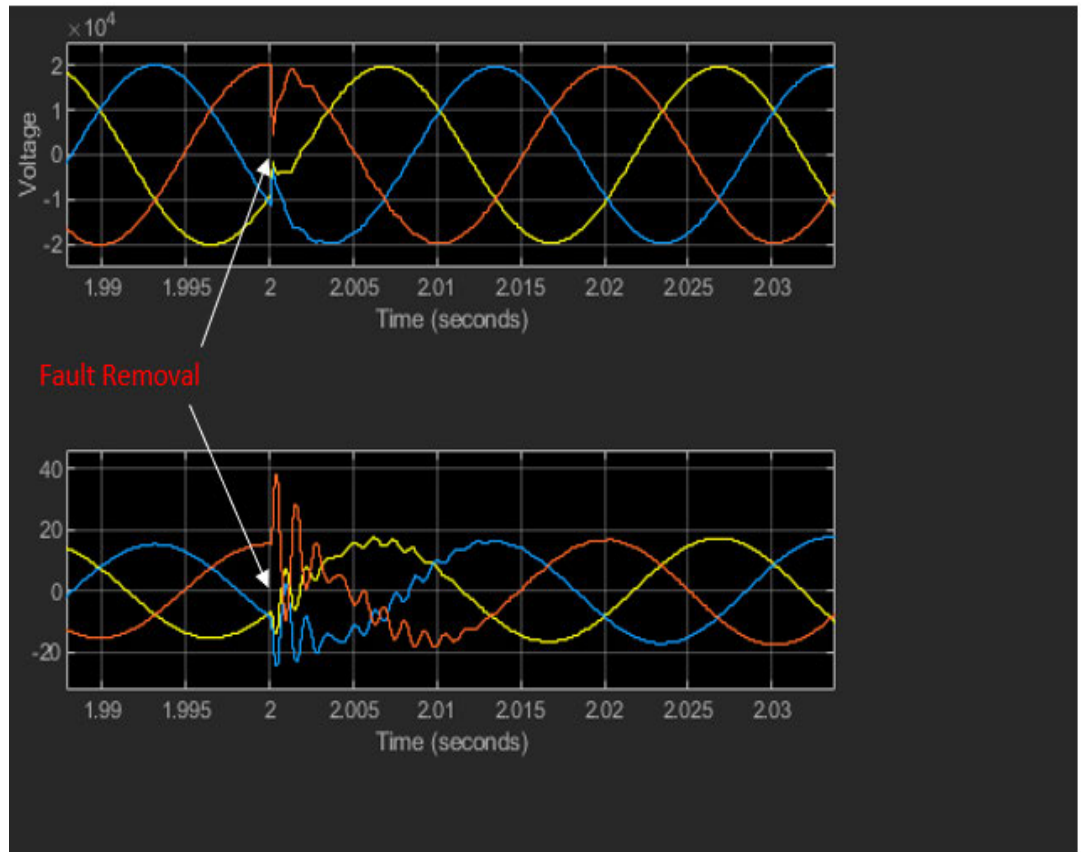


**Figure 4.47:** Voltage Response after removal of 30 MW load

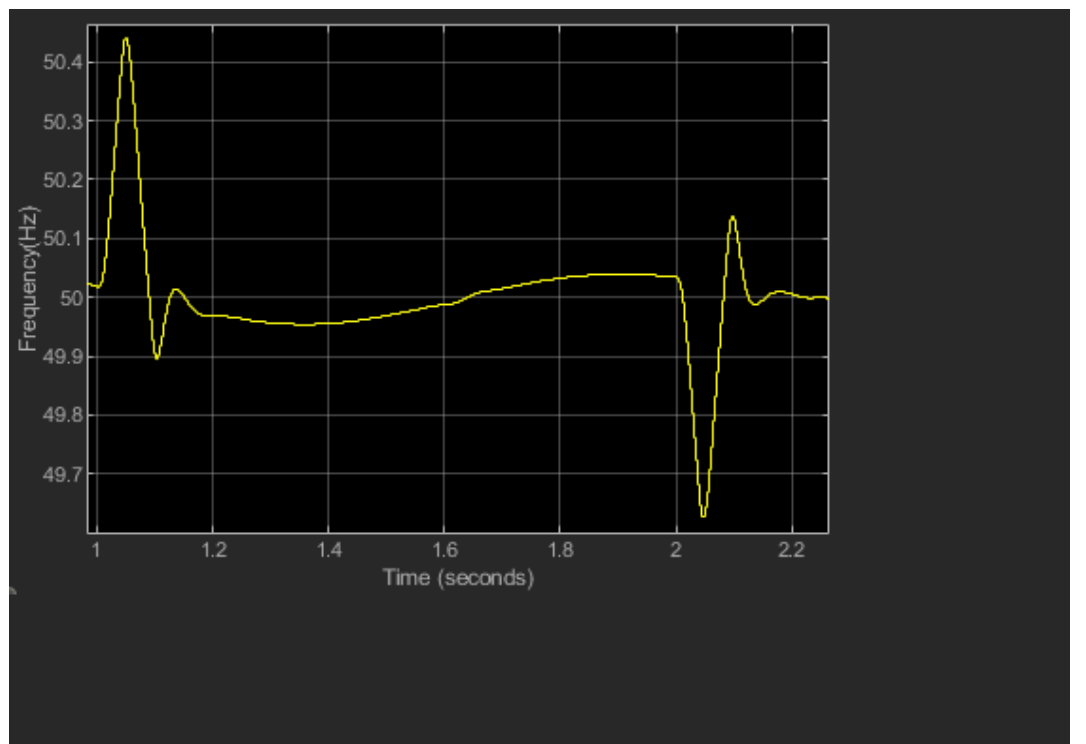


**Figure 4.48:** Frequency Response after Removal of 30MW load

#### 4.4.1.4.1 Analysis of Results

Voltage on all three phases dropped to 25% of nominal value and took 0.015 seconds to recover to 100% nominal value and sinusoidal waveform. The current from the PV system rose from about 20A to close to 40 A when the load was reconnected (shown as fault removal). Frequency rose to 50.42 Hz at the time of load removal and fell to 49.62 when the load was reconnected. The recovery time was 0.2 seconds. There were no violations of standards or rules.

#### 4.4.2 PV Supplying 10% Load

The network loading was re-configured to ensure that the PV system supplied 10% of the load on the network. The same block diagram and fault times used in the previous tests were maintained for uniformity. Fault was applied at 1 second and removed on the 2 seconds mark.

##### 4.4.2.1 Three Phase Symmetrical Fault

A three-phase symmetrical fault was created on 25kV distribution line closest to the PV system on the same spot as the rest of the tests in section 4.4. Voltage and frequency measurements were taken in the form of graphs as shown in the figures below.

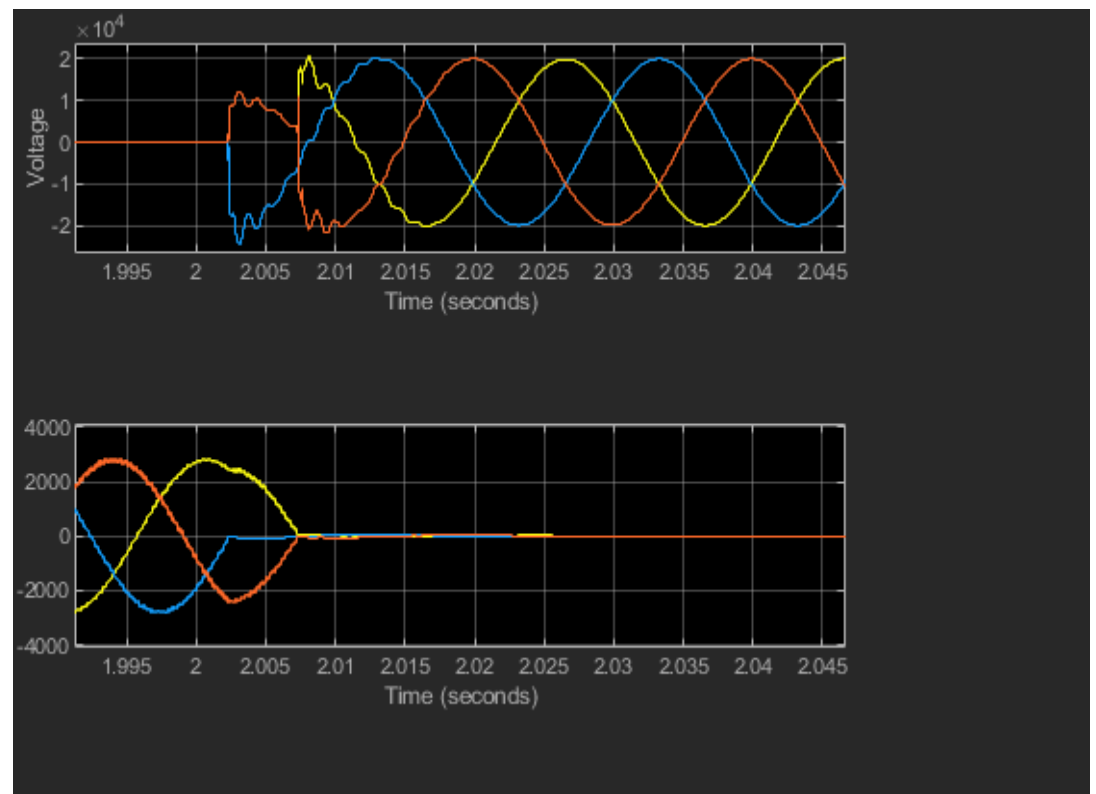
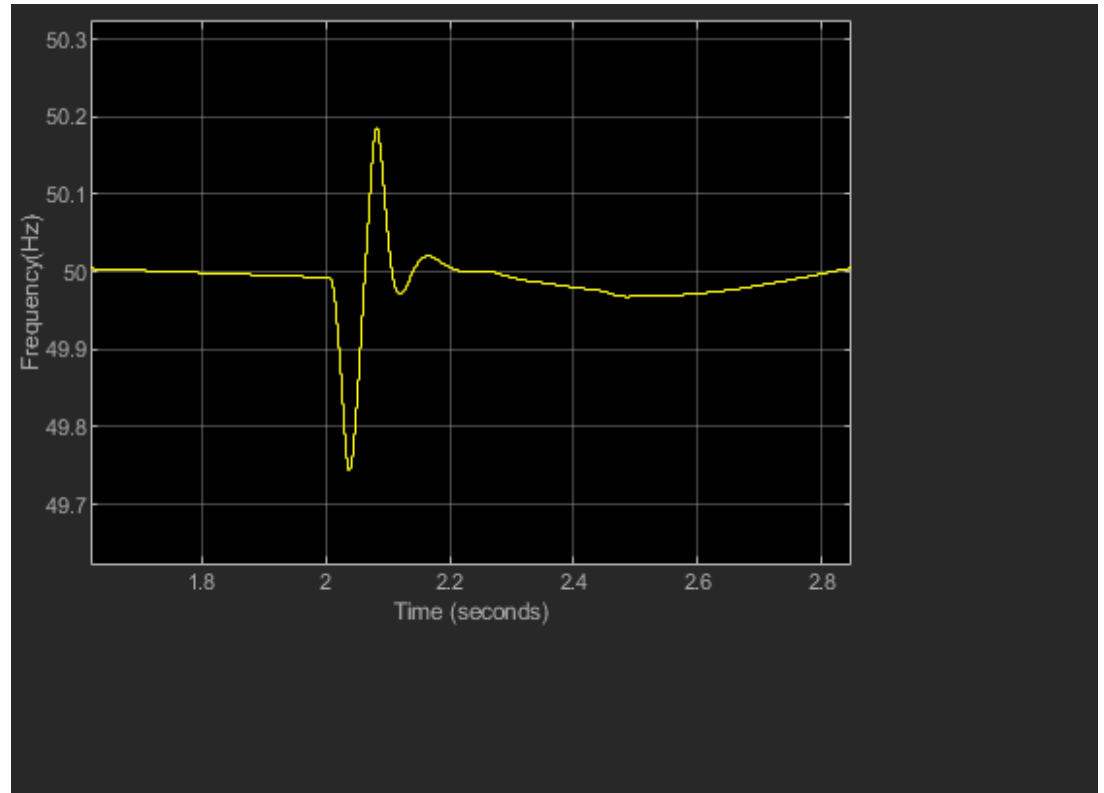


Figure 4.49: Voltage Response after a Three Phase Symmetrical Fault



**Figure 4.50:** Frequency Response after a three-phase symmetrical fault

#### 4.4.2.1.1 Results Analysis

Voltages dropped to zero during fault. There was voltage distortion after fault removal. It took about 0.02 seconds for voltage to recover from the distortion due to the fault. Fault current went close to 3000A. Frequency swung between 49.75 Hz and 50.19 Hz before settling after 0.2 seconds

#### 4.4.2.2 Phase to ground fault

A phase to ground fault was created on C phase under the same conditions as in the previous sections. The figures below show the results in graphical form.

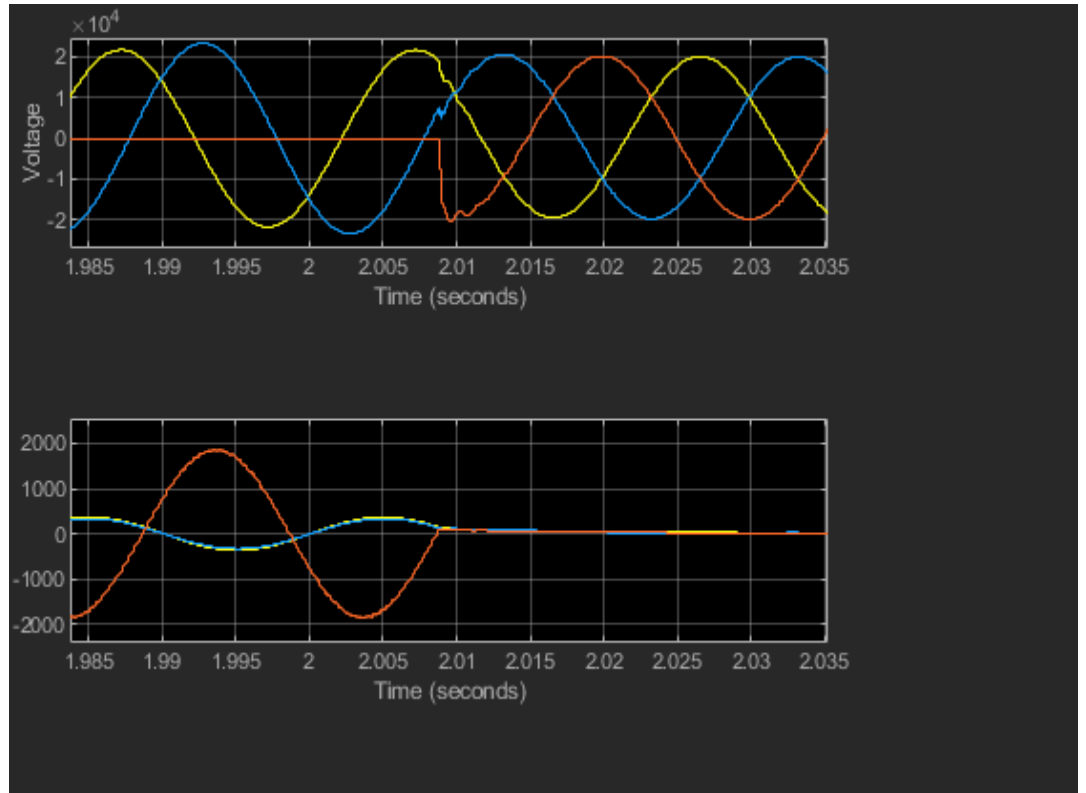


**Figure 4.51:** Voltage response after a single phase to ground fault

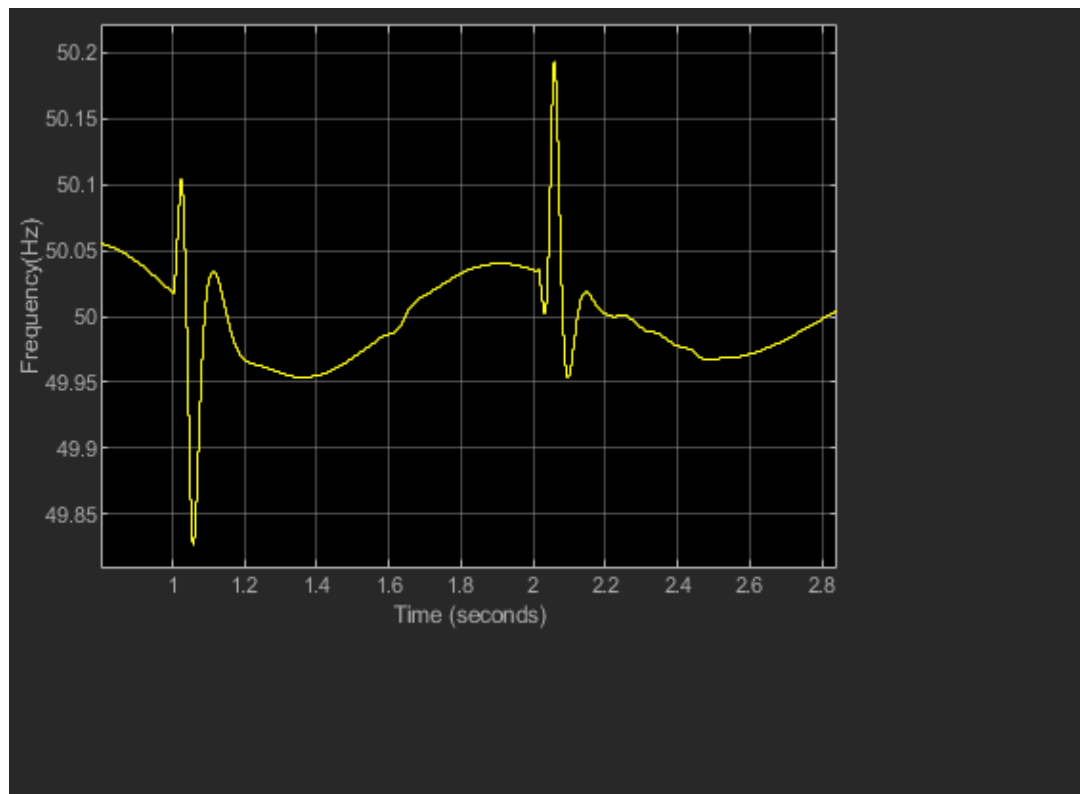


**Figure 4.52:** Frequency response after a single phase to ground fault

#### 4.4.2.2.1 Analysis of Results

C Phase voltage dropped to zero during the fault as expected. The magnitudes of the other two phases were not affected except for minor distortions at inception and removal of fault. C phase current rose to 2000 A during the fault while A and B phase currents were almost in phase but antiphase to the faulted phase.

Frequency dropped to 49.8475 Hz at the introduction of the fault and then rose to 50.19 Hz at removal time of the fault. Recovery time was about 0.6 seconds. No violation of rules noted.

#### 4.4.2.3 Removal of large load

A load of 30MW was removed from the network at the 1 second mark and re-introduced at the 2 seconds mark. Voltage, frequency and current waveforms obtained are shown in the figures below.

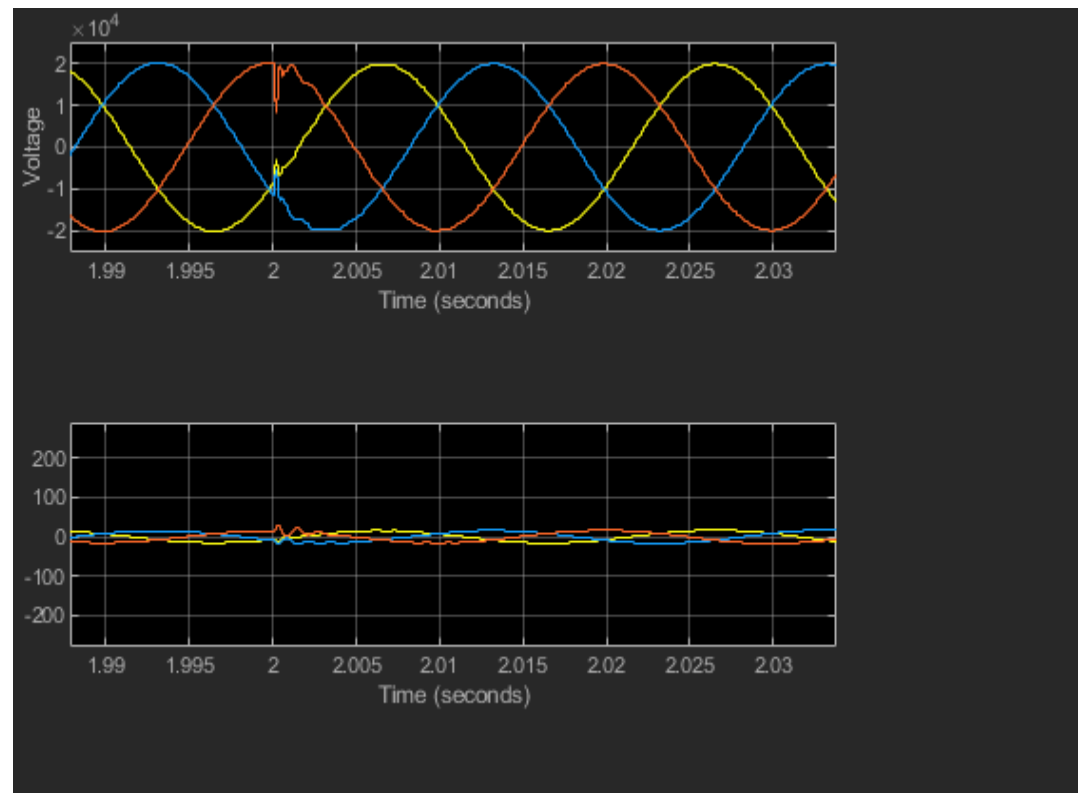


**Figure 4.53:** Voltage response after removal of major load

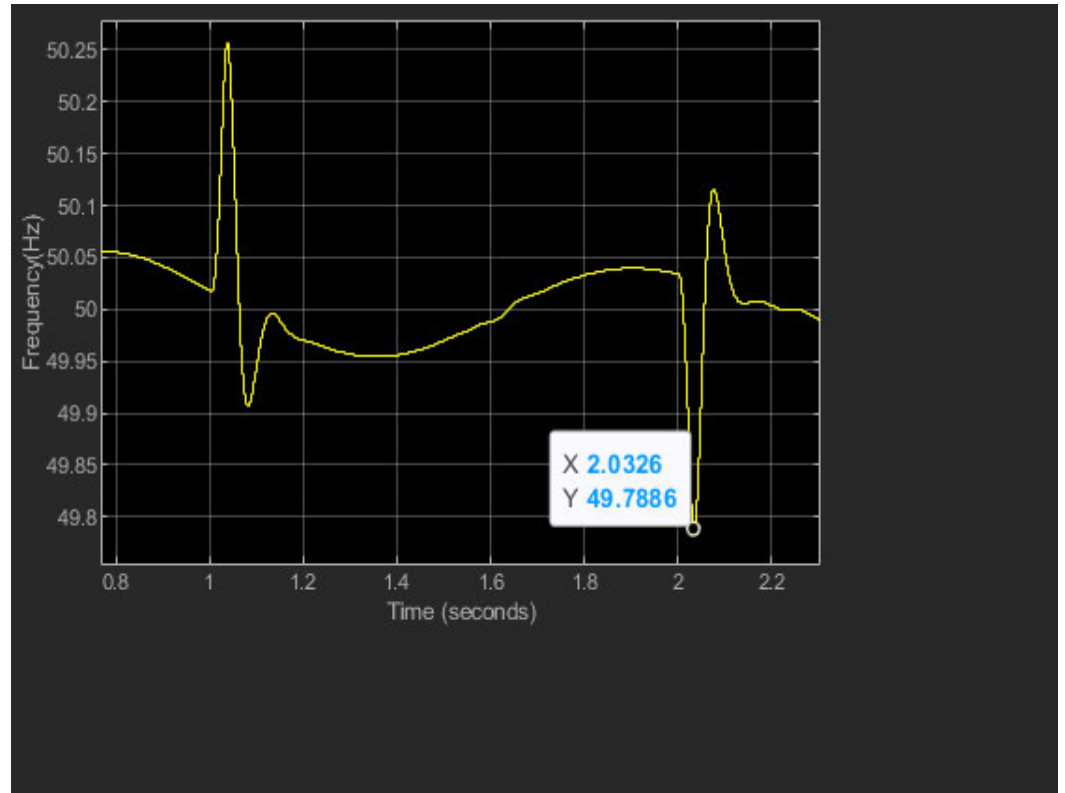


**Figure 4.54:** Frequency Response after removal of large load

#### 4.4.2.3.1 Analysis of Results

Voltage dropped to 50% during re-connection of load. Recovery was less than 0.01 seconds. Frequency went up slightly above 50.25 Hz during removal of load and dropped to 49.7886 Hz when the load was connected back to the system. Recovery time was 0.2 seconds. Voltage drop was excessive for normal operation although the recovery time was within limits for a contingency event.

#### 4.4.3 PV Supplying 50% Load

A simulation test was performed on the combined network with PV system supplying 50% of the total load. This was meant to test how the network responds to disturbances when PV generation has penetrated up to 50%. Three tests were repeated at this level of penetration. The tests being: Three phase symmetrical fault, Single phase to ground and removal of major load. A fourth test was performed where one of the generators was disconnected from the network to create a contingency event. The results of these tests are shown in the subsections that follow.

#### 4.4.3.1 Three Phase Symmetrical Fault

A three-phase symmetrical fault was simulated in the same way as in preceding subsections. Results of the test are shown in the figures below.

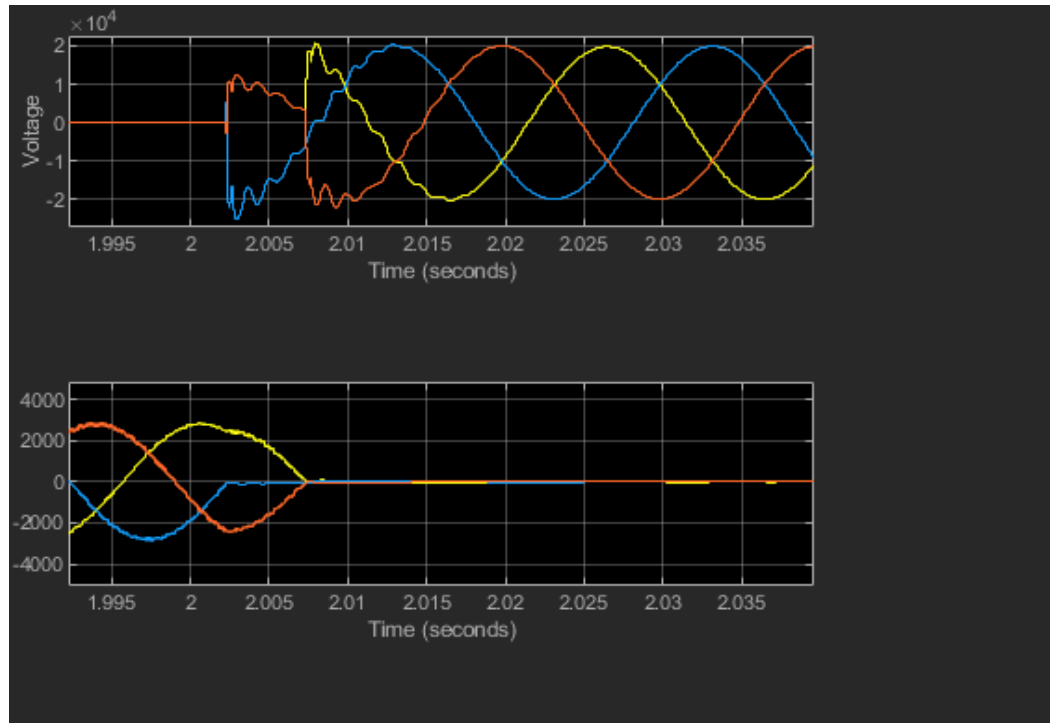


**Figure 4.55:** Voltage response after three phase symmetrical fault

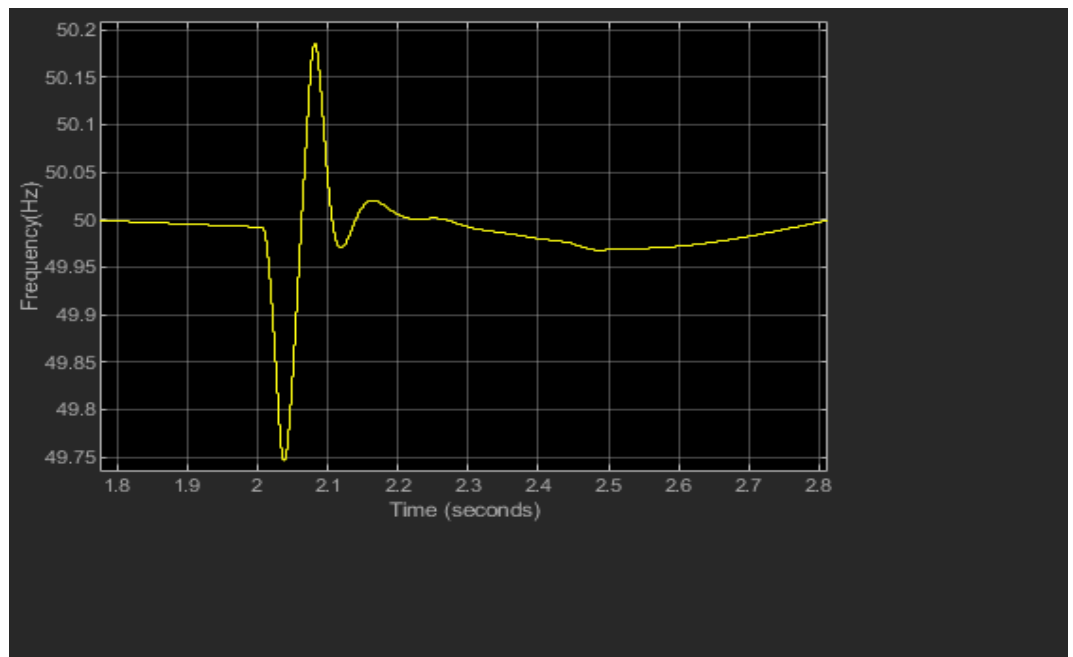


**Figure 4.56:** Frequency Response after three phase symmetrical fault

#### 4.4.3.1.1 Analysis of Results

Voltage on all three phases dropped to zero during the fault as expected at such high fault currents. The voltage fully recovered to nominal value in 0.02 seconds on all three phases. Significant distortions were noticeable on the voltage waveforms from the time of fault removal at 2 seconds up to 2.019 seconds. Fault current reached the 3000A mark and dropped to zero in 0.0055 seconds after fault removal time.

Frequency fluctuated between 49.75 and 50.157 Hz before settling at close to 50 Hz in 0.2 seconds. Neither voltage nor frequency magnitudes and recovery times violated national Electricity Rules or any relevant standards.

#### 4.4.3.2 Phase to Phase to ground fault

In this test, phases A and C were grounded. The results of the test are shown in figures 4.52 and 4.53.

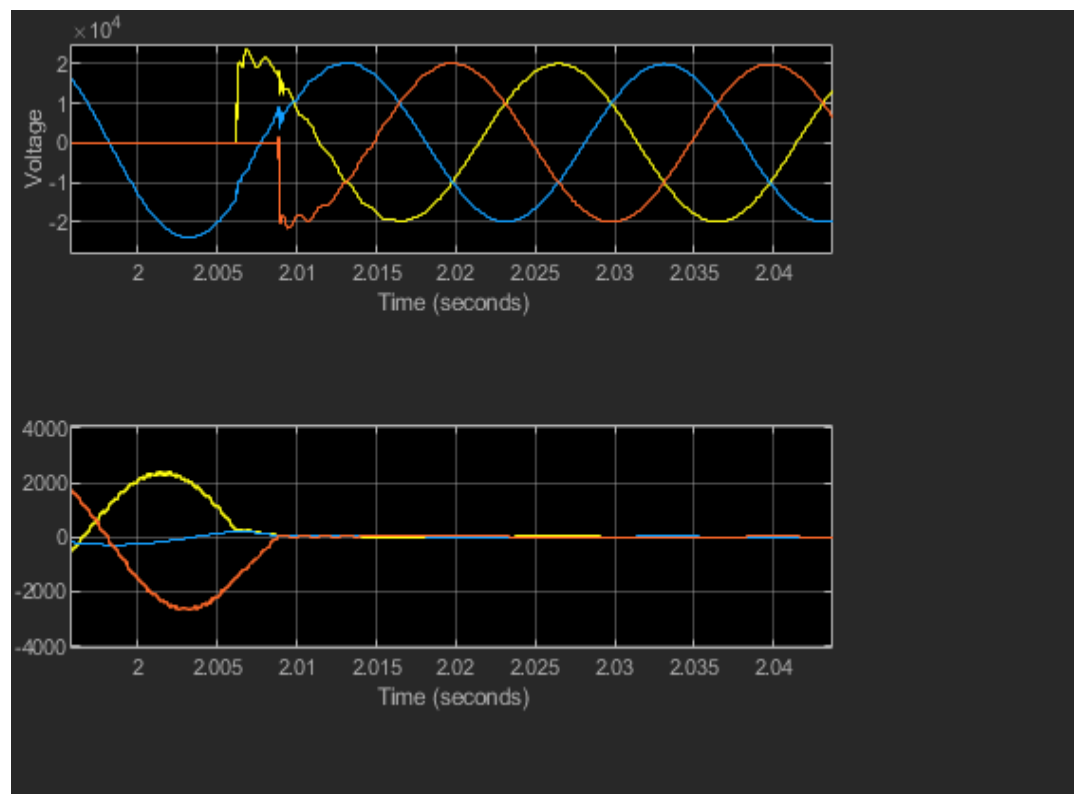


**Figure 4.57:** Voltage and current response after a phase to phase to ground fault.

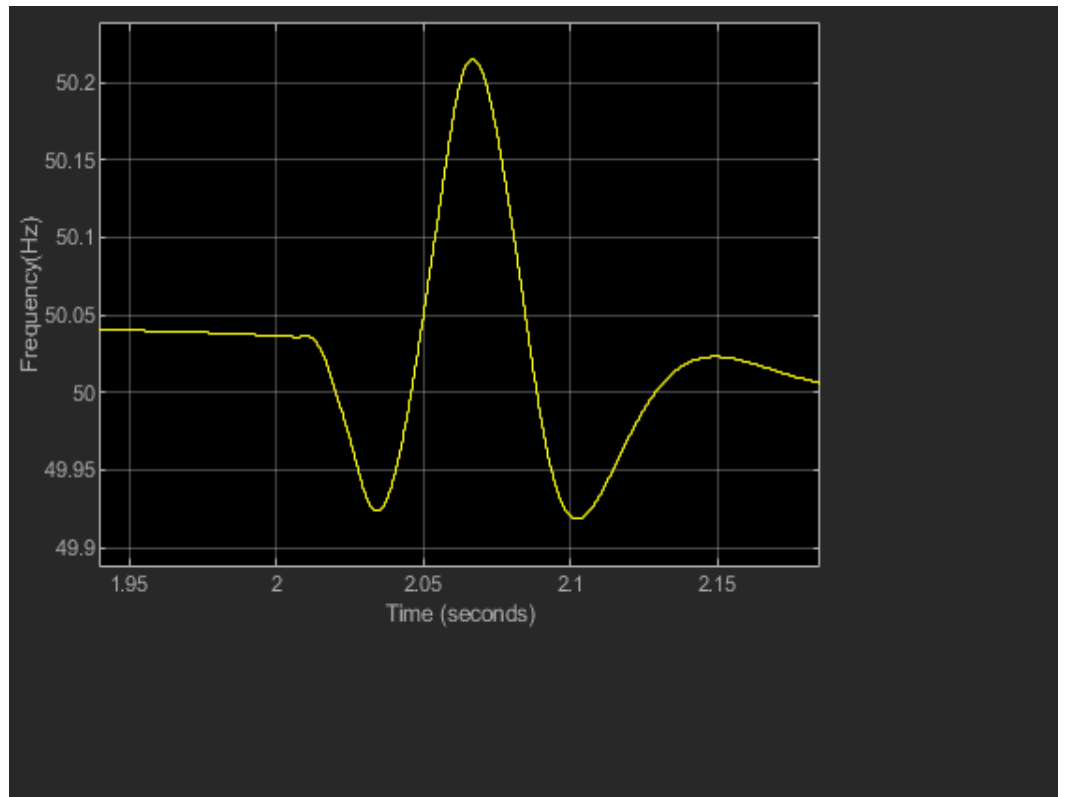


**Figure 4.58:** Frequency response after a phase to phase to ground fault

#### 4.4.3.2.1 Analysis of Results

The middle phase voltage maintained a close to clean sinewave during the fault with noticeable distortions at introduction and removal of fault. Phases A and C voltages dropped to zero during the fault as expected. These two phases had their currents going up to slightly above 2000A and dropping to zero at approximately 0.0056 seconds after removal of the fault. Voltage recovered after 0.02 seconds.

Frequency rose to 50.22Hz after the removal of fault but had two bottom lobes of around 49.9475Hz.

There were no noticeable violations to standards or rules during this test. Frequency stability was attained after 0.15 seconds.

#### 4.4.3.3 Removal of “large” load

In this test, a load was removed from the network. However, with a limited PV generation of 1.2MW, the “large” load that was previously 30MW had been reduced to 2 MW to ensure that the PV system supplied 50% of the total load.

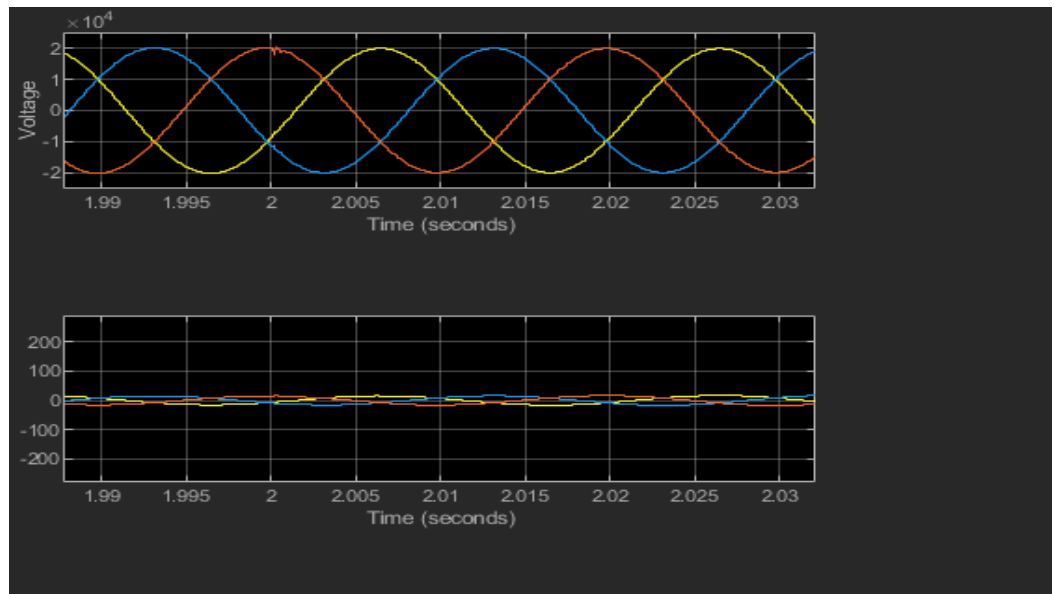


Figure 4.59: Voltage response after load rejection

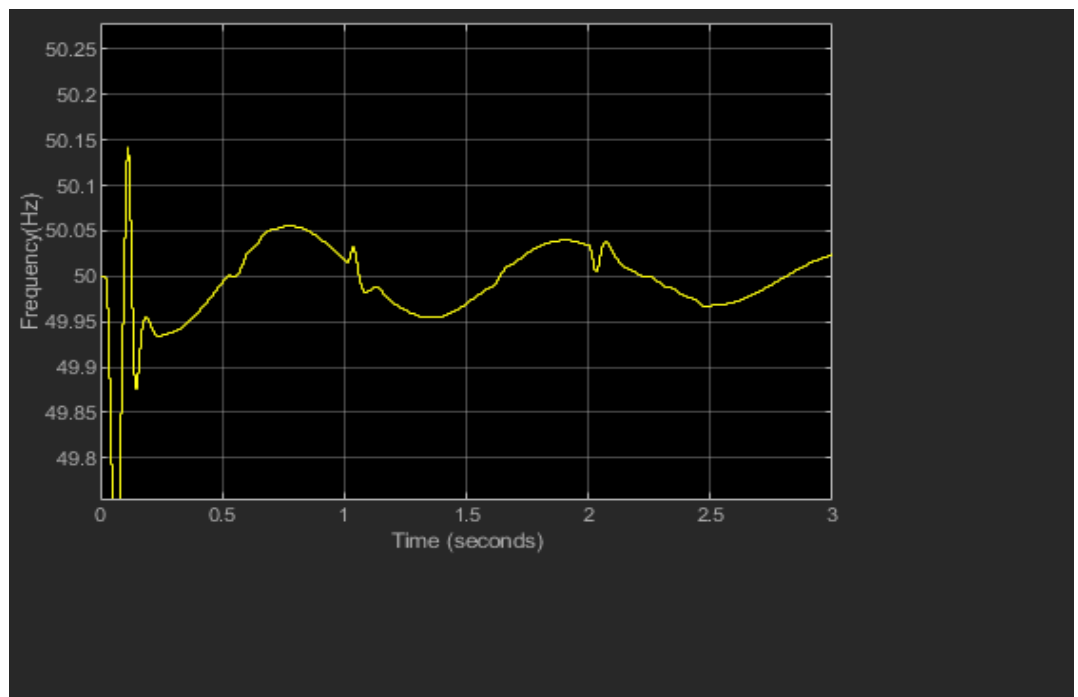


Figure 4.60: Frequency Response after load rejection

#### 4.4.3.3.1 Analysis of Results

The test results indicated an insignificant effect on both voltage and frequency owing to reduced size of the load and reduced amount of total energy in the network. This was attributed to the software limitations in modelling larger PV system that could deliver hundreds of MW into the network. There was no violation of standards.

#### 4.4.3.4 Disconnection and Reconnection of a Synchronous Generator

In this test one of the generators was disconnected from the network. The intention was to test how the network responds to a loss in generation from a synchronous machine when the main generation is predominantly from PV generators with no mechanical inertia to aid in stabilising the network. The scenario resembled close to a weak network. Disconnection and reconnection of the generator was accomplished using circuit breaker CB 1 as shown in figure 4.61 below.

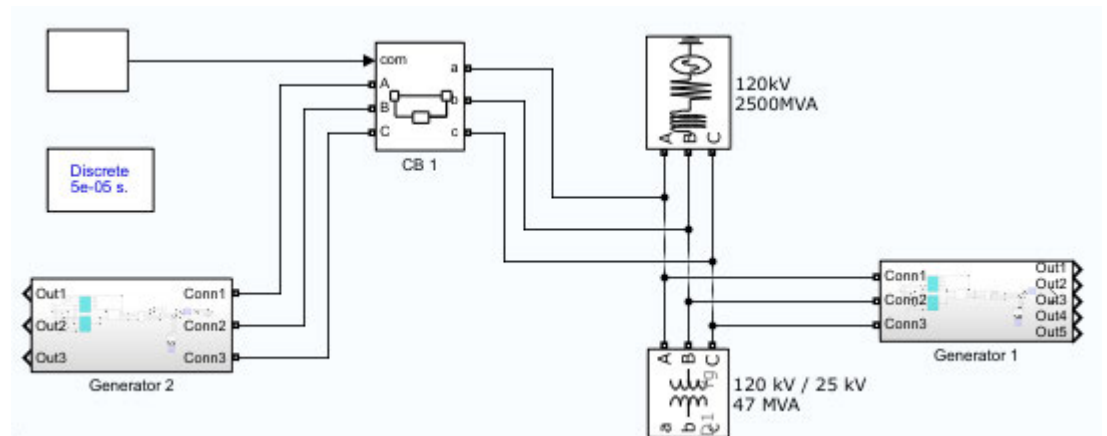
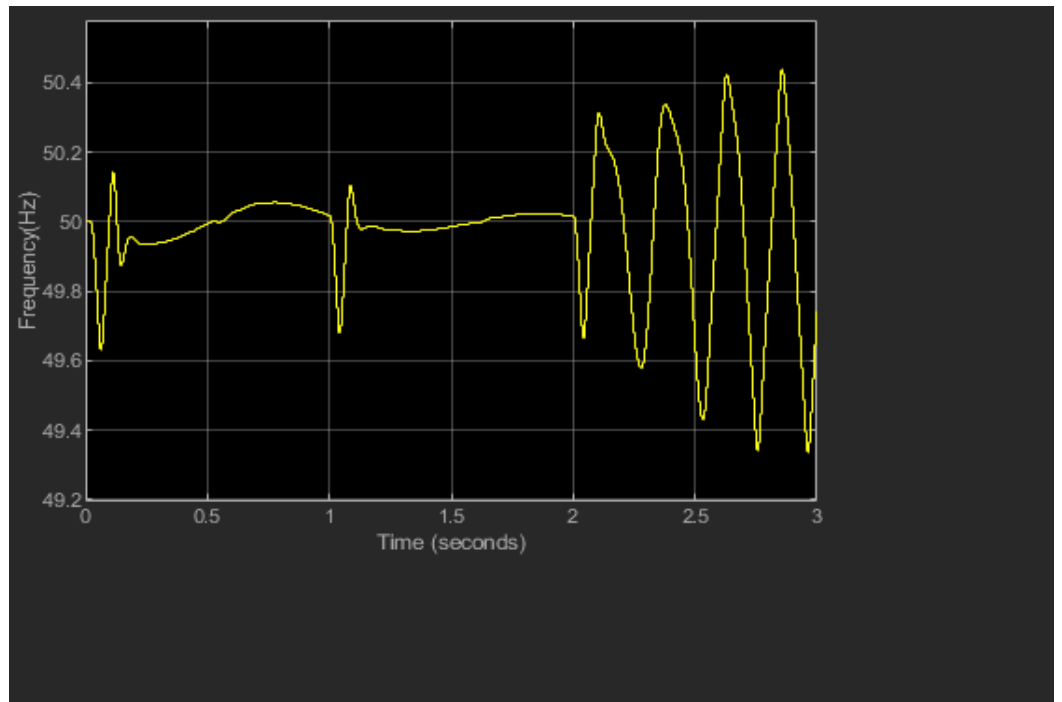


Figure 4.61: Generator Disconnection Using CB 1

The test results came out as shown in figure 4.62



**Figure 4.62:** Frequency Response after synchronous generator disconnection.

#### 4.4.3.4.1 Results Analysis

Frequency dropped to 49.7 Hz when the generator was disconnected from the network and stabilised after 0.15 seconds. However, the network experienced frequency oscillations after reconnection of the synchronous generator. The oscillations had very steep gradients that kept rising till the end of the simulation period. This could violate the rate of change of frequency requirements leading to over or under frequency trips.

# Chapter 5

## 5 Conclusions and Recommendations

### 5.1 Introduction

This chapter of the project contains conclusions drawn from individual test results and their respective analyses as outlined in chapter 4. The validity and accuracy of the results is critiqued in this section. Recommendations are also explored for improvements and future works. A summary is drawn at the end of the chapter.

### 5.2 Summary of Results and conclusions

#### 5.2.1 Model with Synchronous Machine( Without PV)

The table below shows a summary of results for various disturbances

Table 5.1: Voltage and Frequency Response for Synch Gen Model

Synchronous Generator Model				
Type of Disturbance	Voltage Recovery		Frequency Recovery	
	Volts(Fault)	Time(s)	Freq(Hz)	Time(s)
3 Phase Symmetrical Fault	30% Vn	0.005	49.8-50.25	0.3
Pase to Phase fault	30% Vn	0.15	49.918-50.07	0.2
Load Rejection	No effect	N/A	No effect	N/A

The network responded to disturbances in a stable and robust manner. The voltage remained at 30% of its nominal value. The intention of creating this model was to mimic a weak network that compares well with a scenario where most generation comes from a PV system with minimum or no moment of inertia. An ideal model would have been one comprising of a single synchronous generator feeding a bus, two transmission lines and a load on the receiving end bus. However, Simulink could not run a simulation without an AC source for synchronisation. An attempt to include a slack bus failed because of student licence limitations.

In view of the above-mentioned complications and limitations, the frequency responses may not depict ideal responses for a weak network as the AC source may have provided infinite bus characteristic where frequency was maintained almost constant even under disturbances.

### 5.2.2 Model with PV Array ( Without Synchronous Machine)

The table below summarises the voltage and frequency recovery times after a three-phase symmetrical fault.

**Table 5.2:** Voltage and frequency Response to a three-phase symmetrical fault

PV Array Model					
Type of Disturbance	Penetration(%)	Voltage Recovery		Frequency Recovery	
		Volts(Fault)	Time(s)	Freq(Hz)	Time(s)
3 Phase Symmetrical Fault	0.35	0% Vn	0.02	49.92-50.14	0.25
	1	0%	0.035	N/A	N/A
	11	0%	0.06	49.94-50.14	0.25
	100	0%	0.065	49.925-50.12	0.3

The above results indicate very minimum disturbance to frequency profile, perhaps due to the inevitable inclusion of an AC source in the model. The trend in the voltage recovery times is summarised in the graph in figure 5.1

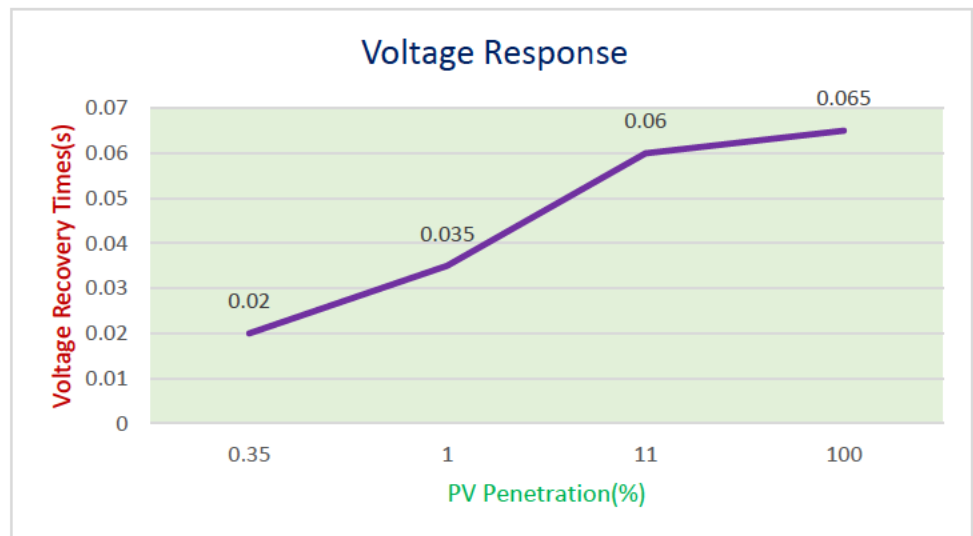


**Figure 5.1:** Voltage recovery times for various PV penetration levels

In the above graph, voltage recovery times increase linearly with an increase in PV penetration. If this trend is a true reflection of a practical situation then there is high probability that voltage levels below 80% of nominal voltage may be sustained in the network for longer periods beyond the maximum permissible time of 450ms as stipulated in the Australian Grid Codes.

However, the model was tested with only 120kW PV system supplying part of a combined load of 32MW. The low energy levels from the PV system may not necessarily validate these results as correct for a network taking PV output in the range of hundreds of MW. Furthermore, the inverter system did not inject significant amounts of reactive energy during the fault although it did during fault clearance and remained connected to the network as required by AEMO, IEC, IEEE and AS/NZS 4777.2:2015.

### 5.2.3 Combined PV and Two Synchronous Generators

**Table 5.3:** Voltage and frequency Responses

Combined PV Array Model and Synchronous generator					
Type of Disturbance	Penetration(%)	Voltage Recovery		Frequency Recovery	
		Volts(Fault)	Time(s)	Freq(Hz)	Time(s)
3 Phase Symmetrical Fault	2	0% Vn	0.021	49.75-50.18	0.22
	10	0% Vn	0.02	49.75-50.19	0.2
	50	0% Vn	0.02	49.75-50.16	0.2
Removal of Load	2	25% Vn	0.015	49.62-50.42	0.2
	10	50% Vn	0.01	49.79-50.25	0.2
	50	N/A	N/A	N/A	N/A

The results in the above table show that there were minor discrepancies in recovery times for the same disturbances at various PV penetration levels. While the total PV output was 1.2MW, the percentages for PV penetration were arrived at by reducing the load. The initial plan was to keep the load at its maximum and vary the PV penetration, but this could not be achieved because of the limited PV output otherwise the penetration would have started at very low percentages and ended at 2%.

The tests, therefore, were performed with limited energy on the network which could have compromised the results. There was no visible effect on the network when a load of 2MW was removed from the network compared to removal of a 30MW load. This leads to the conclusion that perhaps better results can be obtained with greater energy levels on the network especially from the PV system.

The test could not explicitly confirm the level of PV penetration where network stability gets compromised. However, the reconnection of one of the generators led to frequency oscillations which might mean that a network with at least 50% PV penetration might suffer from instability whenever a synchronous generator is introduced to provide spinning reserve for example.

#### **5.2.4 Summary**

Most results did not indicate any violation of standards or rules. A network comprising of only PV generation may suffer from longer durations of voltage dips after disturbances and may experience frequency oscillations when a synchronous generator is introduced at high levels of PV penetration. PV system failure to inject reactive energy during faults could imply insufficient fault current leading to protection equipment insensitivity. When protection equipment fails to detect a fault or takes too long to isolate the fault lives and equipment could be at risk and the consequences could be catastrophic.

It is not possible to completely replace synchronous generators now due to a mismatch between maximum PV generation times and peak demand on the network. Nowadays a normal network demand curve takes the shape of what is called a “duck Curve” where maximum generation from rooftop solar panels reduces the midday grid demand curve portion to the shape of a duck’s belly. The grid demand curve rises steeply around 5pm when solar ceases to generate. This makes it impractical to completely replace synchronous generators as they provide peak load and spinning reserves. It might be possible soon when battery storage systems and other storage methods become more accessible and affordable. The use of virtual inertia devices may assist in replicating the necessary inertia that is currently provided by synchronous machines.

#### **5.2.5 Recommendations**

A commercial software package that can accommodate simulation of large PV systems, in the range of hundreds of MW, could be used to produce more reliable results. Future models must include other network equipment especially protection devices and associated gear.

#### **5.2.6 Further Work**

Further work should include storage (batteries), wind turbines and virtual inertia devices in the models. The models must accommodate, as much as possible, all modern equipment associated with safe integration of renewable energy into electricity networks.

# Chapter 6

## 6 References

- AEMO 2017, *South Australian Renewable Energy Report*, South Australian Advisory Functions. viewed 18 October 2018, <[https://www.aemo.com.au/-/media/Files/Electricity/NEM/Planning\\_and\\_Forecasting/SA\\_Advisory/2017/South-Australian-Renewable-Energy-Report-2017.pdf](https://www.aemo.com.au/-/media/Files/Electricity/NEM/Planning_and_Forecasting/SA_Advisory/2017/South-Australian-Renewable-Energy-Report-2017.pdf)>.
- AbdelHady, R 2017, 'Modeling and simulation of a micro grid-connected solar PV system', *Water Science*, vol. 31, no. 1, pp. 1-10.
- Albadi, MH, El-Rayani, YM, El-Saadany, EF & Al-Riyami, HA 2018, 'Impact of solar power projects on LMP and transmission losses in Oman', *Sustainable Energy Technologies and Assessments*, vol. 27, pp. 141-9.
- Aliyu, AK, Modu, B & Tan, CW 2018, 'A review of renewable energy development in Africa: A focus in South Africa, Egypt and Nigeria', *Renewable and Sustainable Energy Reviews*, vol. 81, pp. 2502-18.
- Al-Shetwi, A. Q., Sujod, M. Z., & Blaabjerg, F. (2018). Low voltage ride-through capability control for single-stage inverter-based grid-connected photovoltaic power plant. *Solar Energy*, 159, 665-681. doi:<https://doi.org/10.1016/j.solener.2017.11.027>
- Atsu, D, Agyemang, EO & Tsike, SAK 2016, 'Solar electricity development and policy support in Ghana', *Renewable and Sustainable Energy Reviews*, vol. 53, pp. 792-800.
- Bensmaine, F., Barakat, A., Tnani, S., Champenois, G., & Mouni, E. (2012). Dual control of synchronous generator for terminal voltage regulation-comparison with a single control. *Electric Power Systems Research*, 91, 78-86. doi:<https://doi.org/10.1016/j.epr.2012.05.010>
- Bouchakour, S., Arab, A. H., Abdeladim, K., Amrouche, S. O., Semaoui, S., Taghezouit, B., . . . Razagui, A. (2017). Investigation of the voltage quality at PCC of grid connected PV system. *Energy Procedia*, 141, 66-70. doi:<https://doi.org/10.1016/j.egypro.2017.11.013>
- Chattopadhyay, D 2014, 'Modelling renewable energy impact on the electricity market in India', *Renewable and Sustainable Energy Reviews*, vol. 31, pp. 9-22.
- Chaudhary, P., & Rizwan, M. (2018). Voltage regulation mitigation techniques in distribution system with high PV penetration: A review. *Renewable and Sustainable Energy Reviews*, 82, 3279-3287. doi:<https://doi.org/10.1016/j.rser.2017.10.017>
- Díez-Maroto, L, Rouco, L & Fernández-Bernal, F 2016, 'Fault ride through capability of round rotor synchronous generators: Review, analysis and discussion of European grid code requirements', *Electric Power Systems Research*, vol. 140, pp. 27-36.
- Dreidy, M., Mokhlis, H., & Mekhilef, S. (2017). Inertia response and frequency control techniques for renewable energy sources: A review. *Renewable and Sustainable Energy Reviews*, 69, 144-155. doi:<https://doi.org/10.1016/j.rser.2016.11.170>
- Etzegarai, A, Eguia, P., Torres, E., Buigues, G., & Iturregi, A. (2017). Current procedures and practices on grid code compliance verification of renewable power generation. *Renewable and Sustainable Energy Reviews*, 71, 191-202. doi:<https://doi.org/10.1016/j.rser.2016.12.051>
- Faranda, R & Leva, S 2008, 'Energy comparison of MPPT techniques for PV Systems', *J. Electromagn. Anal. Appl.*, vol. 3.
- Fiedler, T 2019, 'Simulation of a power system with large renewable penetration', *Renewable Energy*, vol. 130, pp. 319-28.

Hajjaki Fani, M & Hamedani Golshan, ME 2018, 'Determining optimal virtual inertia and frequency Hamrouni, N, Younsi, S & Jraidi, M 2019, 'A Flexible Active and Reactive Power Control Strategy of a LV Grid Connected PV System', *Energy Procedia*, vol. 162, pp. 325-38.

control parameters to preserve the frequency stability in islanded microgrids with high penetration of renewables', *Electric Power Systems Research*, vol. 154, pp. 13-22.

Hansen, K, Mathiesen, BV & Skov, IR 2019, 'Full energy system transition towards 100% renewable energy in Germany in 2050', *Renewable and Sustainable Energy Reviews*, vol. 102, pp. 1-13.

Haidar, AMA & Julai, N 2019, 'An improved scheme for enhancing the ride-through capability of grid-connected photovoltaic systems towards meeting the recent grid codes requirements', *Energy for Sustainable Development*, vol. 50, pp. 38-49.

Hernández, JC, Ortega, MJ, De la Cruz, J & Vera, D 2011, 'Guidelines for the technical assessment of harmonic, flicker and unbalance emission limits for PV-distributed generation', *Electric Power Systems Research*, vol. 81, no. 7, pp. 1247-57.

Hota, P 2016, 'Fault Analysis of Grid Connected Photovoltaic System', *American Journal of Electrical Power and Energy Systems*, vol. 5, p. 35.

IRENA 2018, *Total Renewable Power Generation Capacity 2011-2017*, viewed 19 October 2018, <<https://www.rambuenergy.com/2018/04/irena-global-renewable-generation-continues-strong-growth-indonesia-leads-in-geothermal>>.

Inzunza, A, Moreno, R, Bernales, A & Rudnick, H 2016, 'CVaR constrained planning of renewable generation with consideration of system inertial response, reserve services and demand participation', *Energy Economics*, vol. 59, pp. 104-17.

Jacobson, MZ, Cameron, MA, Hennessy, EM, Petkov, I, Meyer, CB, Gambhir, TK, Maki, AT, Pflieger, K, Clonts, H, McEvoy, AL, Miccioli, ML, von Krauland, A-K, Fang, RW & Delucchi, MA 2018, '100% clean and renewable Wind, Water, and Sunlight (WWS) all-sector energy roadmaps for 53 towns and cities in North America', *Sustainable Cities and Society*, vol. 42, pp. 22-37.

Jaalam, N., Rahim, N. A., Bakar, A. H. A., & Eid, B. M. (2017). Strategy to enhance the low-voltage ride-through in photovoltaic system during multi-mode transition. *Solar Energy*, 153, 744-754. doi:<https://doi.org/10.1016/j.solener.2017.05.073>

Jamal, T., Urme, T., Calais, M., Shafiullah, G. M., & Carter, C. (2017). Technical challenges of PV deployment into remote Australian electricity networks: A review. *Renewable and Sustainable Energy Reviews*, 77, 1309-1325. doi:<https://doi.org/10.1016/j.rser.2017.02.080>

Jian-Bin, H, Shao-Wu, W, Yong, L, Zong-Ci, Z & Xin-Yu, W 2012, 'Debates on the Causes of Global Warming', *Advances in Climate Change Research*, vol. 3, no. 1, pp. 38-44.

Turcotte, D & Katiraei, F 2009, 'Fault contribution of grid-connected inverters', *IEEE Electrical Power Conference*.

Karimi, M, Mokhlis, H, Naidu, K, Uddin, S & Bakar, AHA 2016, 'Photovoltaic penetration issues and impacts in distribution network – A review', *Renewable and Sustainable Energy Reviews*, vol. 53, pp. 594-605.

Kenneth, AP & Folly, K 2014, 'Voltage Rise Issue with High Penetration of Grid Connected PV', *IFAC Proceedings Volumes*, vol. 47, no. 3, pp. 4959-66.

Koutroulis, E., Chatzakis, J., Kalaitzakis, K., Manias, S., & Voulgaris, N. C. (2003). A system for inverter protection and real-time monitoring. *Microelectronics Journal*, 34(9), 823-832. doi:[https://doi.org/10.1016/S0026-2692\(03\)00134-4](https://doi.org/10.1016/S0026-2692(03)00134-4)

Kuriyama, A & Abe, N 2018, 'Ex-post assessment of the Kyoto Protocol – quantification of CO<sub>2</sub> mitigation impact in both Annex B and non-Annex B countries', *Applied Energy*, vol. 220, pp. 286-95.

Kilickaplan, A., Bogdanov, D., Peker, O., Caldera, U., Aghahosseini, A., & Breyer, C. (2017). An energy transition pathway for Turkey to achieve 100% renewable energy powered electricity, desalination and non-energetic industrial gas demand sectors by 2050. *Solar Energy*, 158, 218-235.

doi:<https://doi.org/10.1016/j.solener.2017.09.030>

[Yamashita, K, Renner, H, Martinez Villanueva, S, Vennemann, K, Martins, J, Aristidou, P, Van Cutsem, T, Song, Z, Lammert, G, Pabon, L, Zhu, L, Green, I, Irwin, G, Geibel, D, Jankovic, S, Zhan, C, Ciausiu, F, Karoui, K, Chan, K & Steurer, M 2018, \*Modelling of inverter-based generation for power system dynamic studies\*, vol. No. 298.](#)

[Lasheen, M, Rahman, AKA, Abdel-Salam, M & Ookawara, S 2016, 'Performance Enhancement of Constant Voltage Based MPPT for Photovoltaic Applications Using Genetic Algorithm', \*Energy Procedia\*, vol. 100, pp. 217-22.](#)

Lin, X., Zhang, R., Tong, N., Li, X., Li, M., & Yang, D. (2015). Regional protection scheme designed for low-voltage micro-grids. *International Journal of Electrical Power & Energy Systems*, 64, 526-535.

doi:<https://doi.org/10.1016/j.ijepes.2014.07.050>

Lucas, A 2017, 'Confected conflict in the wake of the South Australian blackout: Diversionary strategies and policy failure in Australia's energy sector', *Energy Research & Social Science*, vol. 29, pp. 149-59.

McKenna, R 2018, 'The double-edged sword of decentralized energy autonomy', *Energy Policy*, vol. 113, pp. 747-50.

Naderi, SB, Negnevitsky, M, Jalilian, A & Hagh, MT 2016, 'Efficient fault ride-through scheme for three phase voltage source inverter-interfaced distributed generation using DC link adjustable resistive type fault current limiter', *Renewable Energy*, vol. 92, pp. 484-98.

NERC 2018, *Short\_Circuit Modelling and System Strength*, viewed 19 October 2018, <[https://www.nerc.com/pa/RAPA/ra/Reliability%20Assessments%20DL/Short\\_Circuit\\_whitepaper\\_Final\\_1\\_26\\_18.pdf](https://www.nerc.com/pa/RAPA/ra/Reliability%20Assessments%20DL/Short_Circuit_whitepaper_Final_1_26_18.pdf)>

Newbery, D 2018, 'Shifting demand and supply over time and space to manage intermittent generation: The economics of electrical storage', *Energy Policy*, vol. 113, pp. 711-20.

Notton, G., Nivet, M.-L., Voyant, C., Paoli, C., Darras, C., Motte, F., & Fouilloy, A. (2018). Intermittent and stochastic character of renewable energy sources: Consequences, cost of intermittence and benefit of forecasting. *Renewable and Sustainable Energy Reviews*, 87, 96-105.

doi:<https://doi.org/10.1016/j.rser.2018.02.007>

Obi, M & Bass, R 2016, 'Trends and challenges of grid-connected photovoltaic systems – A review', *Renewable and Sustainable Energy Reviews*, vol. 58, pp. 1082-94.

Perpinias, II, Papanikolaou, NP & Tatakis, EC 2015, 'Fault ride through concept in low voltage distributed photovoltaic generators for various dispersion and penetration scenarios', *Sustainable Energy Technologies and Assessments*, vol. 12, pp. 15-25.

Perpinias, I. I., Papanikolaou, N. P., & Tatakis, E. C. (2015). Fault ride through concept in low voltage distributed photovoltaic generators for various dispersion and penetration scenarios. *Sustainable Energy Technologies and Assessments*, 12, 15-25. doi:<https://doi.org/10.1016/j.seta.2015.08.004>

Peydayesh, M., & Baldick, R. (2012). The effects of very fast response to frequency fluctuation. *International Association for Energy Economics*.

- Prakash Kumar Hota, Babita Panda, Bhagabat Panda. Fault Analysis of Grid Connected Photovoltaic System. *American Journal of Electrical Power and Energy Systems*. Vol. 5, No. 4, 2016, pp. 35-44. doi: 10.11648/j.epes.20160504.12
- Sanchez-Hidalgo, M.-A., & Cano, M.-D. (2018). A survey on visual data representation for smart grids control and monitoring. *Sustainable Energy, Grids and Networks*. doi:<https://doi.org/10.1016/j.segan.2018.09.007>
- Saravanan, S., & Ramesh Babu, N. (2016). RBFN based MPPT algorithm for PV system with high step up converter. *Energy Conversion and Management*, 122, 239-251. doi:<https://doi.org/10.1016/j.enconman.2016.05.076>
- Seck, GS, Krakowski, V, Assoumou, E, Maïzi, N & Mazauric, V 2017, 'Reliability-constrained scenarios with increasing shares of renewables for the French power sector in 2050', *Energy Procedia*, vol. 142, pp. 3041-8.
- Shivashankar, S, Mekhilef, S, Mokhlis, H & Karimi, M 2016, 'Mitigating methods of power fluctuation of photovoltaic (PV) sources—A review', *Renewable and Sustainable Energy Reviews*, vol. 59, pp. 1170-84.
- Simon Abourida, JB, Vahid Jalili-Marandi 2016, 'Real time Power System Simulation'.
- Simshauser, P 2018, 'On intermittent renewable generation & the stability of Australia's National Electricity Market', *Energy Economics*, vol. 72, pp. 1-19.
- Sivaneasan, B, Lim, ML & Goh, KP 2017, 'Overcoming Solar PV Intermittency using Demand Response Management in Buildings', *Energy Procedia*, vol. 143, pp. 210-5.
- Sivaneasan, B., Lim, M. L., & Goh, K. P. (2017). Overcoming Solar PV Intermittency using Demand Response Management in Buildings. *Energy Procedia*, 143, 210-215. doi:<https://doi.org/10.1016/j.egypro.2017.12.673>
- Sovacool, BK 2009, 'The intermittency of wind, solar, and renewable electricity generators: Technical barrier or rhetorical excuse?', *Utilities Policy*, vol. 17, no. 3, pp. 288-96.
- Sovacool, B. K. (2009). The intermittency of wind, solar, and renewable electricity generators: Technical barrier or rhetorical excuse? *Utilities Policy*, 17(3), 288-296. doi:<https://doi.org/10.1016/j.jup.2008.07.001>
- Tielens, P., & Van Hertem, D. (2012). *Grid inertia and frequency control in power systems with high penetration of renewables*. Paper presented at the Young Researchers Symposium in Electrical Power Engineering.
- Tielens, P & Van Hertem, D 2016, 'The relevance of inertia in power systems', *Renewable and Sustainable Energy Reviews*, vol. 55, pp. 999-1009.
- Xavier, P. N. V. K., & Muthukumar, S. (2010). *Frequency regulation by free governor mode of operation in power stations*. Paper presented at the IEEE International Conference on Computational Intelligence and Computing Research.
- Zappa, W, Junginger, M & van den Broek, M 2019, 'Is a 100% renewable European power system feasible by 2050?', *Applied Energy*, vol. 233-234, pp. 1027-50.
- Kilickaplan, A, Bogdanov, D, Peker, O, Caldera, U, Aghahosseini, A & Breyer, C 2017, 'An energy transition pathway for Turkey to achieve 100% renewable energy powered electricity, desalination and non-energetic industrial gas demand sectors by 2050', *Solar Energy*, vol. 158, pp. 218-35.
- Zhu, X, Wang, J, Mulcahy, D, Lubkeman, DL, Lu, N, Samaan, N & Huang, R 2017, 'Voltage-load sensitivity matrix based demand response for voltage control in high solar penetration distribution feeders', in *2017 IEEE Power & Energy Society General Meeting*, IEEE, pp. 1-5.

# Appendix A

## ENG4111/4112 Research Project

### Project Specification

**For:** Mkululi Mpofu

**Title:** Impact of Large-Scale Solar Energy Penetration on the Electricity Network  
With a View of Replacing Synchronous Generators

**Major:** Electrical and Electronic Engineering

**Supervisors:** Dr Andrew Hewitt  
(Yet to Secure a supervisor from Ergon Energy)

**Enrolment:** ENG4111 – EXT S1, 2019  
ENG4112 – EXT S2, 2019

**Project Aim:** To develop a simple network model to aid in investigating the impact of large-scale solar energy penetration on electricity networks.

**Program:** Version 1, 18<sup>th</sup> March 2019

- Research literature on the effects of large-scale solar generation systems on power network dynamic behavior.
- Develop suitable models using PowerFactory, ETAP and/or SimPowerSystems software for the analysis of power system dynamic responses for varying levels of solar generation penetration.
- Using the developed network models, analyze the dynamic response of a simplified power network with differing levels of solar generation penetration. These studies will be based on various practical situations such as fault recovery and load variations.
- Time permitting, other impacts of large solar penetration like harmonics and effects of solar connection to a weak network among others, will be investigated.



Figure B.1 above shows the project schedule that was formulated with the major tasks in mind. Most activities started after the approval of the project in April. However, most activities happened simultaneously. Work on software and compilation of the project was an on-going task until the completion of the project in week. The gun chart activities were not necessarily been put in order of importance but in in the order of chronological sequence of events. While there are breaks in University calendar, the researcher did not enjoy the break as an external student.

## B1.2 Resources

The project required some resources for successful implementation. Part of the resources included the ones listed below:

### B1.2.1 Hardware

Table B1.1: Hardware Requirements

Hardware Name	Source	Function	Estimated Cost AUD
Memory Stick	Shops	Data Transfer	120
Back up Memory	Shops	Backup	110
Laptop Computer Desktop Computer	Available Available	Document Processing Report Writing	Available 2000
Headphones	Unknown	Decoding Instructions	Unknown

### B1.2.2 Software

Table B1.2: Software Requirements

Software	Source	Function	Estimated Cost AUD
Windows 10	Desktop Computer	Report Writing	300
Microsoft Office	Available	Report Writing	120
Matlab/Simulink	Mathworks	Simulation	300
Simscape Electrical	Mathworks	Modelling	179
Faston Capture	Available	Image capture	30

### **B1.2.3 Financial Resources**

Finance was required to assist in the purchase of various software and hardware as shown in the tables above. Additional capital was required for printing and printer cartridges.

### **B1.2.4 Time**

Finally, the biggest of resources that was required in this project is time. The researcher has a full-time job and a family. Strict time management was employed in balancing work, home and university time requirements. An illness in the family did not help the situation as the researcher had to provide care to the wife after undergoing surgery.

## **B1.3 Risk Management**

During the execution of the project there was exposure to some hazards and risks. These are outlined in the sections below.

### **B1.3.1 Personal Risk**

Preparing a research report involves a significant amount work especially activities that involve the use of a computer. While such work is considered light work, there are risks associated with spending long hours seated in front of a computer screen and having insufficient sleep. The hazardous activities associated with computer usage involve repetitive wrist movements, sitting posture and staring at the computer screen for long hours, among others. The mentioned activities can lead to wrist injuries, eye strain, muscle and joint problems and obesity.

Whenever a hazard is identified, control measures must be instituted to bring down the risk level and preserve good mental and physical well-being. Some of the controls that were implemented to either eliminate the risks or lower them to safe levels include, but are not limited to, the following:

- a) Ensuring that the computer monitor is at eye level
- b) Hands and wrists moving at the same time to operate mouse
- c) Feet resting flat on the floor
- d) Taking frequent breaks and drinking plenty of water
- e) Doing stretch exercises to warm up muscles.
- f) Avoiding driving after working late in the night

Fatigue is one of the risks associated with insufficient sleep. Working late into the night and going to work the following day exposed the researcher to road traffic hazards and electrical shock as the researcher's work activities involve live low voltage work. Discussions were carried out the work supervisor and work crew members to accommodate the researcher's fatigue situation and

plan for study leave where necessary. Table 3.5 below shows maximum safe working hours how fatigue was managed both at home and at work. The personal fatigue calculator helps to calculate fatigue score for each day.

**Table B1.3** Work Threshold Hours

Generally, we can work 12 hours in a day, 60 hours in a week and up to 7 days in a row safely, but as we increase the hours we work beyond 12 in a day and up to 16 or beyond 60 hours in a week and up to 84, the **likelihood of fatigue increases exponentially**.

Fatigue Likelihood Rating			
1 day max	8	12	16
3 days max	24	36	42
7 days max	40	60	84
00-06hrs	0	>0	24
Days/Reset	5	8	12

*Above: This table shows the science behind the Fatigue Likelihood Rating.*

The Personal Fatigue Calculator (PFC) is a fatigue risk assessment tool that **must be used whenever the Safe Work Hours are reached** (e.g. 12 hrs in 24 hr period; any work between midnight and 06.00am; consecutive days in excess of 7 days). It is also a requirement of the National Heavy Vehicle Regulator Work and Rest Hours Exemption Notice.

Answer the questions below to calculate your Personal Fatigue Score (PFS). Use your PFS with the Fatigue Action Matrix for actions to take. Document your score and implemented controls on the DTRMP.

Question		Answer
Are you about to work past any of the Safe Work Hour thresholds?		Yes / No
If No you are not required to complete the assessment If Yes, please continue with the following questions:		
A	How many hours have you slept in the 24 hrs prior to commencing work?	A =
B	How many hours did you sleep in the 24 hrs before that?	B =
C	Total of A + B = C	C =
D	How many hours have you been awake today? (i.e. time woke from sleep to current time)	D =
	<b>Hours</b>	<b>Score</b>
If your answer to A is:	≥ 5 hrs	0 points
	4 hrs	4 points
	3 hrs	8 points
	2 hrs	12 points
	1 hr	16 points
If your answer to C is:	≥ 12 hrs	0 points
	11 hrs	2 points
	10 hrs	4 points
	9 hrs	6 points
	8 hrs	8 points
	7 hrs	10 points
	6 hrs	12 points
≤ 5 hrs	14 points	
Add 1 point for every hour D is more than C e.g. if D = 14 and C = 10 add 4 points If D is less than or equal to C, score 0		G =
<b>Personal Fatigue Score (E + F + G)</b>		

Personal Fatigue Score	Fatigue Likelihood	Action matrix
0	Low	Document on DTRMP. Continue to monitor fatigue. Do not exceed maximum work hours.
1-7	Medium	Notify co-workers and implement controls with crew. Document on DTRMP. Inform Supervisor or WGL. Controls may include self/peer monitoring, task rotation, increased breaks, pacing work load. Consider whether high risk tasks should occur.
8-12	High	Stop Work. Discuss controls with Supervisor or WGL. Document on DTRMP. Controls may include increased supervision, task re-assignment, buddy check. High risk tasks (e.g. driving / operating heavy vehicles) should not be performed.
13+	Extreme	Stop Work (or do not commence). Discuss contingency with WGL/ Supervisor. Controls are unlikely to be sufficient. Continuing with any work requires GM approval.

Figure B1.1 Fatigue Score Calculator (Source – Ergon Energy)

Table B1.4 Hazard Identification and control

Activity	Hazards Identified	Controls Applied	Residual Risk	Allocation
Sitting and using computer For long hours	Issues with ergonomics. Repetitive movement of wrist. Eye Strain and muscle aches.	Apply Personal Fatigue Score, Take frequent breaks. Rest wrist on desk. Avoid getting too close to monitor.	Low	MM
Going to work after spending long hours on computer and sleeping late	Micro sleep. Exposure to electrical risks and road traffic hazards while at work	Inform supervisor when not fully fit for duty. Ask for study leave. Share with crew members	Low	MM

The table above shows a list of identified hazards and how controls were implemented to reduce the residual risk to low. A similar hazard hunt exercise was carried out at the workplace in conjunction with personal fatigue calculated to determine if the researcher had enough sleep in the previous 24 hours. A fatigue score of medium and high warranted work stoppage and rescheduling of work.

		Consequence			
		Minor	Moderate	Major	Catastrophic
Likelihood	Unlikely	Low	Low	Low	Low
	Less Likely	Low	Low	Medium	High
	Likely	Medium	High	High	High
	Most Likely	High	High	High	High

**Figure B1.2:** Likelihood and Consequence Matrix

#### B1.3.4 Project Risk

The research project was exposed to risks. One of the major imminent risks was loss of a soft copy of the project through computer software crashes. The risk was mitigated by periodically backing up the project file into external drives and in external servers.

There was a risk of failing to progress well with the project due to a major illness in the family where a member of the family had surgery and was incapacitated for three months. Progress on the research was greatly impacted.

#### B1.4 Limitations

Some of the resources that were meant to be used in implementing the methodology could not be sourced for the project. The limitations are outlined in the next sections below.

##### B1.4.1 Modelling Software

He original plan was to source the model and simulation software from the organisation that the researcher works for. Due to limited licences within the organisation, the researcher could not be accorded extra financial resources to obtain the licence as the organisation felt the researcher’s current job activities did not involve use of the relevant software package (PowerFactory).

The university of Southern Queensland have an alternative software package but unfortunately the software package is not yet available online for students. The researcher used Simscape/Simulink in MATLAB. However, the student licence has

limitations on the number of blocks that can be contained in a single simulation model. Due to these limitations, a complete network model could not be simulated as a complete assembly but had to be split into two halves.

One half comprises of the solar panels with irradiance and temperature control, DC-DC Converter with MPPT control using Perturb and Observe algorithm, Inverter with active and reactive power control, parallel load, power transformer, Point of Common Coupling, utility grid comprising of two sections of a 25kV transmission line, two load totalling 32MW a power transformer and a three phase source. The other half comprises of the utility grid and synchronous generator equipped with excitation system control and turbine and governor control. The two systems are simulated separately, and their outcomes are compared to establish how the network behaves under different PV penetration levels. The second half of the model has zero PV penetration.

#### **B1.4.2 Data Collection**

Data from specific solar farms and respective energy meter and transmission line parameters could not be used in this research as such data is protected by relevant data agents under the overall control of AEMO. The Power of Choice has brought up ring fencing rules on data transfer between regulated and unregulated distribution and transmission utility companies making it difficult to obtain solar farm data.

## Appendix C

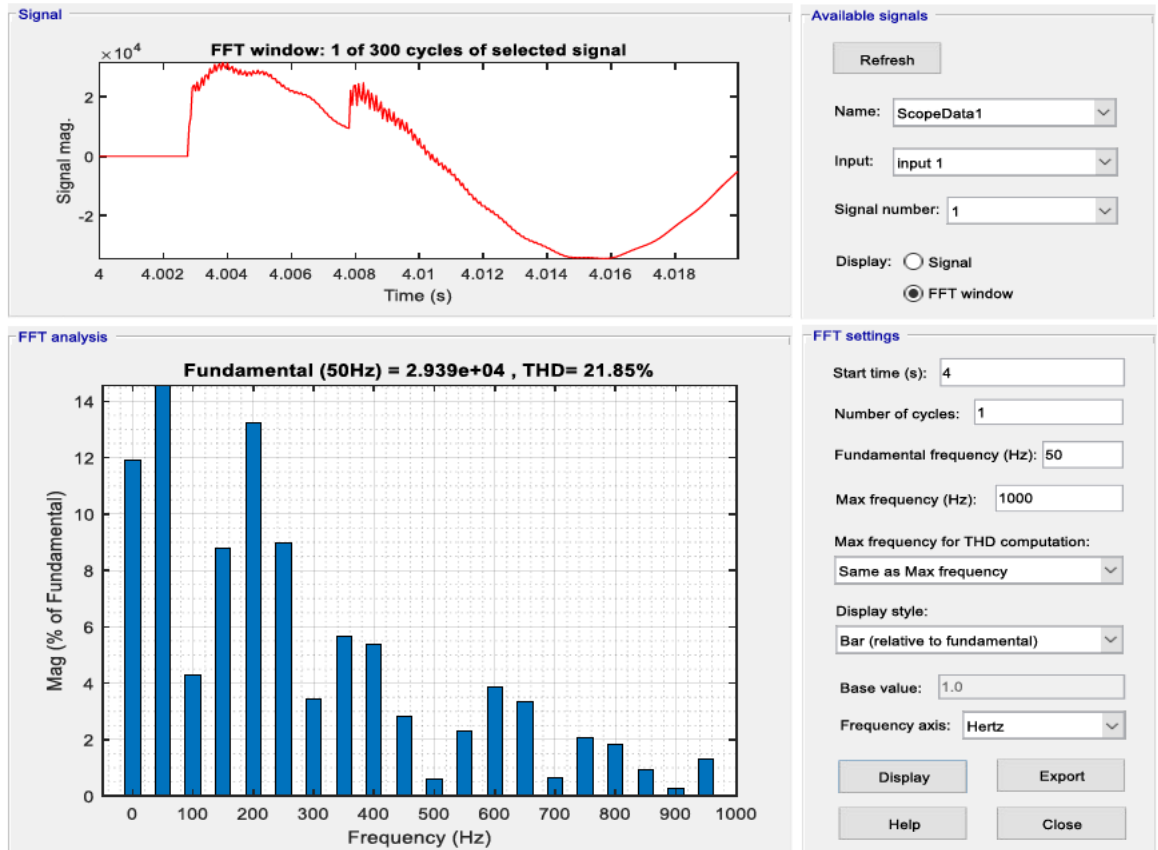


**Figure C.1: Harmonic content for PV system supplying 0.35% of Load - 3 Phase Symmetrical Fault**